ENDOPLASMIC RETICULUM TRANSLOCON FUNCTION IS REQUIRED FOR

DORSAL DIENCEPHALIC NEUROGENESIS IN THE ZEBRAFISH

By

Caleb Andrew Doll

Dissertation

Submitted to the Faculty of the

Graduate School of Vanderbilt University

in partial fulfillment of the requirements

for the degree of

DOCTOR OF PHILOSOPHY

in

NEUROSCIENCE

December 2012

Nashville, Tennessee

Approved:

David Miller

Lila Solnica-Krezel

Todd Graham

Joshua Gamse

For my parents,

Rick and Gayle,

For unbounded development of the mind

And the bliss that ensues

provided an open door for the past six years. His ongoing assistance through manuscript drafting and troubleshooting sustained me in graduate school. I must also thank the other members of my committee, Lila Solnica-Krezel, Todd Graham, and David Miller. Collectively, this group is a powerhouse of cell and developmental biology, and I could not be blessed with a more helpful and engaged group. I must stress my gratitude toward Lila Solnica-Krezel, as she mentored me for nearly a decade, even from afar in St. Louis. Her scientific mind is expansive and profoundly creative and has thereby thoroughly shaped my scientific endeavors.

Thanks also go out to the administrative staff of both the Department of Biological Sciences and the Brain Institute. Roz Johnson, who has been a part of both departments, has taken care of me for many years; Leslie Maxwell made sure that money was in my pocket; Carol Wiley helped procure my NIH funding; Mary Michael-Woolman took care of my Neuroscience stipends. I must also thank the chair of Biological Sciences, Charles Singleton, the Director of Graduate Studies Douglas McMahon, and the Director of the Brain Institute, Mark Wallace for their ongoing support and leadership.

The members of the Gamse laboratory are a cohesive group, always ready to tackle new issues in lab meetings and troubleshoot experimental design. Thanks go to Corey Snelson, the Gamse lab graduate student pioneer; Robert Taylor, an incredible friend with a mind like Ray Bradbury; Josh Clanton, whose witticisms know no end; Sataree Khuansuan, the lab enforcer; Simon Wu, an expansive knowledge base; Benjamin Dean, a friend in neuroscience and a

iv

TABLE OF CONTENTS

LIST OF FIGURES

x

LIST OF ABBREVIATIONS

CNS	central nervous system
cxcr4b	chemokine receptor 4b
Dh	dorsal habenula
Dpf	days post-fertilization
FR	fasciculus retroflexus
Hpf	hours post-fertilization
HuC	Hu antigen C
Kctd	K+ channel tetramerization domain-containing protein
IPN	interpeduncular nucleus
LPM	lateral plate mesoderm
L/R	left-right
LsDh	lateral subnucleus of the dorsal habenula
MsDh	medial subnucleus of the dorsal habenula
MO-ATG	start-site blocking morpholino
MO-SP	splice-site blocking morpholino
nrp1a	neuropilin1a
Sec61al1	Sec61 alpha-like1, the alpha subunit of the Sec61 translocon
RT	room temperature
RT-PCR	reverse transcription polymerase chain reaction
Tg	transgenic line
ulk2	*unc-51-like kinase 2*

CHAPTER I

INTRODUCTION

Modeling neural development

The human nervous system is the most complex network known to man. Astronomers can map distant galaxies with more precision than anatomists can describe the neurological pathways that govern our capacity for empathy, compassion, or the creation of long-term memory. Since the medieval assertion that the mind exists in the brain and not the heart, this remarkable organ has captivated the scientific community. With advancements in dissection, magnification, and classification, neuroscientists are confronted with further gradations of intricacy. Despite centuries of characterization, explorations into the neural systems that govern our conscious and unconscious behaviors remain rudimentary. Our understanding of human brain function must begin with detailed descriptions of brain development in model organisms, for the sake of simplification and amenability to genetic manipulation. In describing the genetic contributions to neurodevelopment in alternative models we will arrive at a greater comprehension of our own minds.

Neurons are polarized cells that communicate to create neural networks of remarkable diversity. One pole of the neuron consists of a dendritic field, which serves to receive signals from surrounding neurons. These signals can be either excitatory or inhibitory, effectually amplifying or dampening a given neuron's

likelihood to generate an axon potential at the other pole of the cell (the axon). This action potential refers to the propagation of an electric current down the length of an axon to communicate with dendritic fields of other neurons through synaptic connectivity. The language of neuronal communication is based in the molecules released in the synaptic cleft, referred to as neurotransmitters. Therefore, neurons use both electrical (action potential) and chemical (neurotransmitters) mechanisms to facilitate communication. In anatomical terms, a neuron receives information by way of afferent processes (afferents), and propagates signal to other neurons by way of efferent connectivity (efferents).

Neurons are highly organized in discrete domains in the brain, which are referred to as nuclei. Medical observations of patients with localized brain lesions have produced brain maps in which specific nuclei perform specialized behavioral functions. This medical history dates back to the ancient Greeks (Changeux, 1997). More recent studies have mapped areas such as the somatosensory region of the cerebral cortex, which contains carefully arranged neurons that are activated upon touch to a given area of the body (often pictorially depicted as a homunculus). Some regions of cortex, such as the hands, are given much more cortical representation, despite occupying a very small relative portion of epidermis (Marieb and Hoehn, 2007). However, most brain functions are far more complex than somatosensation. A combination of approaches including systems, behavioral, genetic, cellular, and molecular neuroscience is necessary to study more complex brain functions, and it is increasingly evident that developmental studies are paramount in the study of

brain disease, as proper organization, connectivity, and function underlie the formation of a properly formed brain.

This introduction is tailored toward asymmetric (left-right; L/R) brain development. As such, it covers models of lateralized brain anatomy and function as well as the embryological models that form our representation of how the brain forms. The ultimate goal is to understand human brain function, and I will begin with an introduction on asymmetry in the human cerebral cortex. Next, I will discuss the formation of the nervous system, including the induction of neural tissue, formation of the neural tube, and the cell biology of neurogenesis. Finally, I will discuss the zebrafish lateralized brain model, which builds upon cell, developmental, and genetic hypotheses in an effort to characterize the roots of the lateralized brain.

Advantages of a lateralized vertebrate brain

In vertebrates, external body plans possess a remarkable degree of bilateral symmetry, though internal organs often develop with a left-right (L/R) bias (Corballis, 2009). Vertebrate anatomy exhibits L/R asymmetry in the placement and coiling of the heart (Fishman and Chien, 1997; Hoyle et al., 1992; Schier and Shen, 2000), liver (Emery, 1963), and lobation of the lungs (Horsfield and Cumming, 1968), for example. The vertebrate lineage contains a conserved mechanism for the generation of asymmetry. This evolutionary event may correlate with the vertebrate requirement for more complex organ systems; body plans became more complex to facilitate the metabolic demand of an "active

searching lifestyle" (Cooke, 2004). For instance, the evolution of the heart from a simple tube into an asymmetric, multi-chambered structure provides greater efficiency and better adaptation to a terrestrial lifestyle (Olson, 2006). For a time, scientists believed that asymmetric adaptations were specific to the chordate lineage. The phylum Chordata, of the Deuterostomia superphylum includes the subphyla Vertebrata: fish, amphibians, reptiles, birds, mammals; Tunicatata: sea squirts; and Cephalochordatata: lancelets. However, investigation of protochordate species has pushed the asymmetric innovation to a more ancient common ancestor, as asymmetric gene orthologues are found in Amphioxus and Ciona (Boorman and Shimeld, 2002a, b), as well as mollusks (Grande and Patel, 2009). Although we do not know the precise origin(s) of asymmetry during evolution, its abundance in nature signifies the importance of asymmetry in the animal kingdom.

Left-right asymmetry is evident in human cortical anatomy and may be associated with hemispheric-specific brain function. The first example refers to the circumference of the brain, which is slightly rotated counterclockwise on the bilateral axis, a phenomenon referred to as Yakovlevian Torque. The result of this slight rotation is minor increases in the right frontal and left occipital lobes of the brain (Galaburda et al., 1978a; Geschwind and Levitsky, 1968). A second example of anatomical asymmetry resides in the planum temporale (PT), the famous region associated with the production and comprehension of speech (speech representation), as described by the mid-19th century work of Broca and Wernicke, respectively (Damasio and Geschwind, 1984). Humans are

predominantly right-handed, and right-handed individuals show a population bias toward left-hemisphere speech representation (Halpern et al., 2005). This representation correlates with size, as the left PT is larger in the majority of individuals (Kimura, 1983; Rasmussen and Milner, 1977). Ultimately, these findings contribute to the hemispheric specialization hypothesis: lateralized brain functions correlate with anatomical asymmetries (Boller, 1988; Galaburda et al., 1978a; Galaburda et al., 1978b). In other words, asymmetric brain activity such as speech representation is rooted in differences in neuroanatomy. However, this hypothesis remains controversial as individuals with right hemisphere speech representation (a minority) do not consistently display PT asymmetry in magnetic resonance imaging (MRI) studies (Moffat et al., 1998), and only a minority of left-handed individuals correlate with reversed (right-sided) speech representation (Kimura, 1983; Rasmussen and Milner, 1977). In considering handedness, these results effectively challenge the lateralized anatomical representation of speech model (Moffat et al., 1998), despite the fact that most right-handed individuals fit the stereotype (Beaumont, 2008).

The theory of hemispheric specialization of brain function in humans - initially posited by Broca and Wernicke - has been further elaborated by modern psychological testing and imaging techniques. For example, research on patients with unilateral lesions or resection of the corpus callosum have revealed that the left hemisphere is dominant in mathematics and logical reasoning; in contrast, the right hemisphere specializes in shape recognition, spatial attention, emotion processing, and artistic functions (Borod et al., 2002; Gazzaniga, 2005). This

lateralization theoretically allows hemispheric-specific functionality, and thus a potential increase of neural coding potential. For instance, both hemispheres are involved with the processing of a given sentence, but accomplish the task by different mechanisms, thereby leading to greater comprehension: the left hemisphere analyzes grammar and syntax while the right hemisphere processes the nonliteral aspects of discourse, metaphor and analogy (Whitaker, 2010). Advancements in functional magnetic resonance imaging (fMRI) have allowed scientists to view brain function in real time, utilizing blood flow as an indirect proxy. For instance, fMRI has implicated a reduction of asymmetry in a group of developmental brain disorders, including schizophrenia (Rossi et al., 1991; Yurgelun-Todd et al., 1996), dyslexia (Leonard and Eckert, 2008) and autism (Herbert et al., 2005); in which patients display reduced or reversed activation of particular brain regions upon stimulation (Sun and Walsh, 2006). These data suggest that asymmetric cortical activity correlates with proper cognitive function. They also imply that asymmetric aspects of brain anatomy and functionality are in place prior to the onset of environmental cues and cognitive development (Sun and Walsh, 2006). Therefore, a better understanding of the genetic pathways leading to the development of asymmetries in brain anatomy, and ultimately function, may eventually contribute to neurodevelopmental therapeutics.

The search for anatomically encoded brain asymmetries has led to substantial research in model organisms, including non-human primates and a variety of vertebrate species. Left-hemisphere asymmetries have been noted in the language homologues of chimpanzees (PT and inferior frontal gyrus) using

MRI (Cantalupo and Hopkins, 2001; Gannon et al., 1998). To date, the only direct link between neuroanatomy and behavior has been demonstrated in avian visual systems (Rogers and Andrew, 2002). An elegant model of visual asymmetry has been developed using chicks, as exposure to light in pre-hatched chicks leads to the development of lateralized visual pathway development. Chicks exposed to light before hatching were compared with chicks that were reared in darkness. The chicks were then tested on their capacity to pick out food grains from a background of small pebbles, a task that engages the right eye and the left hemisphere (Deng and Rogers, 1997), or alternatively to respond to the presence of a predator above the testing cage (left eye and right hemisphere)(Rogers, 2000). Chicks reared in darkness were able to locate food particles but were unable to respond to predators (Rogers et al., 2004). Further testing on monocularly deprived chicks (one eye deprived of light during rearing) revealed that specific exposure of the right eye to light spurs a developmental program that specializes the right eye/left hemisphere for foraging and the left eye/right hemisphere for predator detection (Dharmaretnam and Rogers, 2005). This data provides strong evidence for the hemispheric specialization model, but also calls into question the utility of lateralized behavior in social organisms. For example, population-level behaviors with given biases could prove disadvantageous as predators learn to predict movements (Lippolis et al., 2002; Rogers, 2000). However, the advantages of lateralized behaviors may prove more valuable, as lateralized chicks form more stable social communities (Rogers and Workman, 1989). In short, lateralized behaviors are not a unique

artifact of hominid evolution and likely evolved in earlier common ancestors, perhaps providing behavioral benefits and promoting overall fitness through the hemispheric specialization model.

Neural induction

The presence of asymmetric neuroanatomy in the adult organism is thought to arise from developmental events. Neurodevelopment is an extensive process that can be divided into four phases: neural induction, neurulation, neural patterning and neurogenesis. To describe neurodevelopment, we must begin with the totipotent single cell of a nascent fertilized embryo. This single cell will produce a remarkably diverse lineage, which will populate the vast majority of the tissues of the adult. Cell divisions in the embryo eventually give rise to distinct tissue classes, known as germ layers: mesoderm, endoderm, and ectoderm. These germ layers are segregated through the process of gastrulation; neural induction is initiated during gastrulation. Following gastrulation, tissues begin to undergo morphogenesis into mature organs: mesoderm (vertebrae, dermis, axial muscle, heart, kidneys), endoderm (gut, pancreas, liver, lungs), and ectoderm (skin and neural tissue)(Gilbert, 2000), at which point the early embryo begins to resemble its adult counterpart. The remainder of this review will focus on ectodermal (neural) development, though references to lateral plate mesoderm are necessary as this tissue directly influences neural development in the dorsal diencephalon of zebrafish.

In the 1920's, Spemann and Mangold posited a model for the induction of neural tissue from ectodermal progenitors. Using an amphibian model at gastrula stage, the authors grafted the blastopore lip (a mesodermal tissue) from a donor embryo to the ventral region of a second host embryo. The host embryo went on to develop a second, ventral neuraxis, composed of host-derived tissue and complete with a second notochord. The authors predicted that the blastopore lip, nicknamed the Gastrula Organizer, produced signals to bias the surrounding ectoderm toward a neural fate (Spemann and Mangold, 2001; Weinstein and Hemmati-Brivanlou, 1999). Molecular techniques in the early 1990s implicated antagonists of the Bone Morphogenetic Protein (BMP) signaling family, of the Transforming Growth Factor beta (TGF-β) superfamily in neural induction, and BMPs in epidermal induction. Importantly, BMP components were isolated in both the signaling tissue (mesoderm) and the receptive tissue (ectoderm). Research went forward on both fronts simultaneously, thus identifying BMP activators and inhibitors.

The first model of neural induction posited that neural tissue is the default state of ectoderm, as regulated by BMP pathway components. Bone morphogenetic protein signaling components have been isolated from both mesoderm and ectoderm, and act in concert for the proper specification of cells. Noggin is a secreted protein that fulfills the Organizer signal's criteria (Smith and Harland, 1992); Follistatin (Hemmati-Brivanlou et al., 1994; Nakamura et al., 1990) and Chordin (Sasai et al., 1994) are also involved, and all are expressed in mesodermal tissue. In addition, concentrated ectodermal supernatant is capable

of suppressing neural fate and maintaining ectoderm (Grunz and Tacke, 1990). Molecular screens of this ectodermal supernatant led to the discovery of BMP4 as an epidermal inducer (Fainsod et al., 1994; Wilson and Hemmati-Brivanlou, 1995). Expression of BMP4 is widespread in the ectoderm before gastrulation, but is importantly excluded from neural tissue in the neural plate (primitive nervous tissue, to be discussed subsequently)(Fainsod et al., 1994; Hemmati-Brivanlou and Thomsen, 1995). Furthermore, dissociating *Xenopus* ectoderm in culture leads to widespread neural induction, suggesting that neural fate is the "default" for ectoderm (Godsave and Slack, 1989; Grunz and Tacke, 1989; Sato and Sargent, 1989). Finally, the molecular function of the organizer came to light, as the Organizer's secreted molecules were identified as inhibitors of BMP activity. Noggin (Zimmerman et al., 1996) and Chordin (Piccolo et al., 1996) directly bind to BMP4 protein and prevent binding of the BMP4 ligand to its receptor protein. Follistatin inhibits BMP in a slightly different manner, allowing binding of BMP to receptor but forming a trimeric complex that inhibits the propagation of downstream signal (Fainsod et al., 1997; Iemura et al., 1998). The resultant model posits that ectodermal tissue is by default fated toward neural differentiation, but is initially held in check by BMP expression before segregation of the germ layers. Expression of BMP (in ventral mesoderm) and BMP inhibitors (in dorsal ectoderm) during gastrulation provides a molecular distinction between ectodermal tissues and facilitates the subsequent differentiation of neural progenitors from the dorsal ectoderm.

The neural induction model has been revised since these initial amphibian studies, as researchers questioned the application of the default hypothesis to amniotic (avian, reptilian, and mammalian) neural induction. However, murine embryonic stem cells (ES) cultured in media devoid of extrinsic cues express neural markers within hours (Smukler et al., 2006). Despite this encouraging result, the absence of extrinsic cues fails to reflect the larger *in vivo* environment of neurodevelopment, and it is now clear that amniote neural induction occurs through a more complex mechanism. This being said, inhibition of BMP signaling remains paramount in neuroectodermal specification and additional growth factors implicated in amniotic neural specification, including Wnt and Fgf, fulfill this inhibitory role (Wilson et al., 2000). Experiments on chick epiblast (as yet-unspecified neural and epidermal tissue), found that BMP inhibition through Noggin and Chordin-producing cells was not sufficient to induce neural tissue in non-neural epiblast cells, despite the fact that node (the orthologue to the organizer) grafts in non-neural epiblast induce neural tissue (Streit et al., 1998). These results hint at the presence of a second neural-inducing factor in epiblast cells. Pharmacological blockage of Fibroblast Growth Factor (FGF) signaling in cultured chick epiblast cells leads to a maintenance of BMP gene expression and the inhibition of neural fate (Wilson et al., 2000). This work built on previous findings in that FGF treatment of embryonic tissue induces expression of neural markers and suppresses epidermis (Kengaku and Okamoto, 1993, 1995; Lamb and Harland, 1995), and a dominant-negative FGF receptor effectively inhibits neural induction by Noggin overexpression (Launay et al., 1996). Ultimately,

activation of FGF is required in concert with BMP inhibition in the dorsal side of the embryo for neural fate induction (Delaune et al., 2005; Lamb and Harland, 1995; Londin et al., 2005; Wilson et al., 2000). In fact, FGF may be required prior to BMP, as neural plate is established through FGF activity, and subsequent suppression of BMP activity acts to maintain (and not initiate) neural differentiation (Linker et al., 2009). Furthermore, an ES functional screen identified a Wnt pathway antagonist, sFRP2 as a potent neural inducer (Aubert et al., 2002) and an *in vivo* model demonstrated that Wnts induce epidermis, acting through BMP-Smad signal transduction (Fuentealba et al., 2007). The default model is dependent on starting conditions and may therefore by variable by organism. In summary, the neural default model for ectoderm proved too simplistic as an explanation for amniotic neural induction, and the presence of FGF and Wnt signaling provides further fine-tuning of ectoderm during gastrulation.

This brief introduction to neural induction references experiments that include a developmental window in which neural cells are produced (experiments begin before/during gastrulation and end after neural progenitors or neurons are in place). Although there is no distinct temporal window between the processes of neural induction and neurulation, a discussion of the latter is now necessary to illustrate the formation of the neural tube. Induction continues to occur during neural tube formation, but following gastrulation, the dorsal organizer differentiates into prechordal mesoderm and the notochord. The latter is an

anteroposterior strip of mesoderm that signals to the overlying nervous tissue of the neural tube.

Neurulation

Neurulation refers to the formation of a neural tube (NT) from a flattened population of neuroectodermal cells, known as the neural plate. Two forms of neurulation have been described: primary (the bending and folding of the neural plate to form a hollow tube) and secondary (the formation of a solid rod of neural tissue, followed by cavitation of cells in the center of the rod, thus forming a tube) (Gilbert, 2000). Amniote neurulation generally occurs through the primary mechanism with some secondary occurring at the posterior end of the embryo (Harrington et al., 2009). Cells of the NT will contribute the majority of neurons that populate the CNS as well as neural crest cells (of which pigment cells of the skin and some neurons are derived). Neurulation effectively segregates the three components of the ectoderm: neural tube (neural progenitors; to be described below), the overlying epidermis, and the neural crest. In a broader context, neurulation occurs alongside somitogenesis; somites are paired mesodermal blocks of cells that will eventually form the vertebrae and muscles.

Primary neurulation has been modeled in detail in both *Xenopus* and chick, and comparative analysis with human neurulation suggests that all three make use of primary neurulation in anterior regions with limited secondary neurulation at the posterior pole (zebrafish neurulation occurs with slight deviations, as described subsequently)(Harrington et al., 2009). The first stage of

neurulation entails the formation of the neural plate, as neuroepithelial cells receive mesodermal signals to elongate and obtain columnar morphology (Keller et al., 1992; Smith and Schoenwolf, 1989). This neural plate lengthens along the AP axis and narrows along the mediolateral axis (Schoenwolf and Alvarez, 1989). These neuroepithelial cells divide every 8-10 hours (Smith and Schoenwolf, 1987), and roughly 50% of these divisions contribute to the length (rather than width) of the plate, thereby contributing to the larger extension process (Sausedo et al., 1997). Next, bilateral folds become evident at the lateral edges of the neural plate. Cells just anterior to the node (notochord), at the center of the neural plate are called medial hinge point cells (MHPs). MHPs undergo a morphological shift, decreasing their height and becoming wedge shaped, thereby forming a hinge. Two additional furrows form at the connecting site of the neural plate and the remainder of the ectoderm, thereby known as the dorsolateral hinge points (DLHPs)(Schoenwolf and Franks, 1984). Both MHPs and DLHPs utilize structural molecules to change shape, as cytochalasin B exposure, an inhibitor of microfilaments prevents wedge formation (Nagele and Lee, 1987) and application of colchicine, an inhibitor of microtubule polymerization, prevents apical constriction (Karfunkel, 1972). The neural plate bends on these hinge points, which act as pivots for the rotating cells of the presumptive neural tube (Smith and Schoenwolf, 1991).

When the two sides of the neural plate meet at the dorsal midline they adhere together to form a complete tube. This process is variable by organism and has important clinical implications due to the prevalence of NT closure

defects in humans. In chick, the process of NT closure begins at the level of the presumptive midbrain and then proceeds both anterior and posterior from this point, as detailed through scanning electron micrographs (Portch and Barson, 1974). In mammals, closure initiates at different points along the AP axis, dependent on the animal (e.g. mouse, human)(Golden and Chernoff, 1993). NT closure defects (NTDs) are common in humans, with an occurrence rate of 1 in 1000 live births (Detrait et al., 2005). NTDs include anencephaly (failed rostral closure) and myelomeningocele (failed closure in the vertebral column, also known as spina bifida). The former is uniformly lethal whereas spina bifida can now be surgically repaired *in utero*, a significant improvement from postnatal NT surgeries (Adzick, 2010). A gamut of genetic factors contribute to NT formation, including *pax3* (Epstein et al., 1991)*,* the dietary factors folate and Vitamin B$_{12}$ (Molloy et al., 2009), as well as cell adhesion molecules. However, the precise genetic mechanisms of NT closure are still poorly understood.

A variety of vertebrate models have implicated cell adhesion proteins as essential components of neural tube closure and subsequent neurogenesis. Indeed, cadherins have characterized roles in adhesion (Sano et al., 1993), cell migration (Nakagawa and Takeichi, 1995), protein transport (Dantzig et al., 1994), and the formation of epithelia (Gumbiner et al., 1988; Vestweber and Kemler, 1985). Classical cadherins - of particular note E-cadherin (*cdh1*) and N-Cadherin (*cdh2*) - are homophilic, calcium-dependent adhesion molecules that contain five extracellular cadherin-binding motifs interspersed by calcium binding sites. Intracellularly, cadherins possess a binding site for β-catenin (Tepass et al.,

2000) and domains that interact with α-catenin, β-catenin, and p120 (Reynolds et al., 1994). Cadherins are often thought of in the context of adherens junctions, as mediators of tissue integrity and cell polarity in epithelial sheets (D'Souza-Schorey, 2005). As the nervous system emerges from the ectodermal tissue class (epithelial progenitors), cadherins represent a prime area of focus in the study of neurogenesis.

The expression patterns of E- and N-cadherin predict their relative roles in neurulation. At neural plate stage, neuroectodermal cells express E-cadherin (epidermal), but transition to express N-cadherin (neural) and N-CAM as the NT forms (Detrick et al., 1990; Fujimori et al., 1990). Indeed the timing and location of N-cadherin expression patterns suggest the molecule is capable of mediating NT closure, as it is evident in the neural plate following induction in chick (Hatta and Takeichi, 1986), frog (Detrick et al., 1990) and mouse (Radice et al., 1997). Furthermore, in *Xenopus*, misexpression of N-Cadherin in non-neural ectoderm results in defects in NT size and organization (Detrick et al., 1990; Fujimori et al., 1990), and knockdown of N-cadherin in chick leads to disrupted neuroepithelial integrity and NT formation (Bronner-Fraser et al., 1992; Ganzler-Odenthal and Redies, 1998). Although the brain phenotype of the mouse N-cadherin knockout is relatively mild (Radice et al., 1997), the zebrafish mutant has notable NT formation defects (Lele et al., 2002), including defects in intercalation as examined *in vivo* (intercalation is a cell behavior that drives the morphogenetic processes of convergence and extension)(Hong and Brewster, 2006). Cadherins are integral for NT formation, and remain crucial components of the nascent

neuroepithelium, a highly polarized field of progenitors that generate much of the nervous system.

Neurulation in zebrafish occurs through a distinct mechanism, though many genetic factors are well conserved. Most notably, the neural grooves and folds evident in chick are not found in zebrafish development, which does not show evidence of neural plate bending. Instead, the apical surfaces on both sides of the midline become juxtaposed by a smooth fusion of bilateral epithelia, thus forming a neural rod, in which a lumen forms through cavitation (secondary neurulation)(Lowery and Sive, 2004). Cells of the zebrafish neural plate do not express junctional complexes (Geldmacher-Voss et al., 2003), but nevertheless retain epithelial characteristics throughout neurulation (Hong and Brewster, 2006). This process incorporates some aspects of primary neurulation as it does entail the folding of a pre-existing epithelial sheet (Lowery and Sive, 2004; Papan and Campos-Ortega, 1999).

Even as the neural tube closes the presumptive regions of the nervous system, called vesicles, can already be distinguished along the A-P axis. In the head region the prosencephalon (forebrain), mesencephalon (midbrain), and rhombencephalon (hindbrain) become distinct (Gilbert, 2000). Upon further development, the hindbrain becomes further subdivided into the metencephalon (pons and cerebellum) and myelencephalon (medulla). The forebrain is split into the rostral telencephalon and the caudal diencephalon. The telencephalon further differentiates into the neocortex and the basal ganglia, whereas the diencephalon (interbrain) develops largely as a mediator of forebrain limbic system and

neocortical signals to the rest of the CNS, thereby modulating sensory, motor, and cognitive functions (Chatterjee and Li, 2012). The diencephalon contains the thalamus, epithalamus, pretectum, and hypothalamus. The forebrain, midbrain, and hindbrain, along with the spinal cord, cranial nerves, and the ventricular system represent the principal components of the early central nervous system.

Of special interest to our research, the development of the diencephalon includes specification of both the habenulae and the pineal gland. As mentioned previously, the diencephalon mediates limbic and neocortical signals to the midbrain (Sutherland, 1982). In line with this role as intermediary between brain regions, the habenulae have recently emerged as an exciting area of study due to associations with emotive decision-making, ultimately providing a link to many psychiatric disorders including schizophrenia, depression, and drug-induced psychosis (Hikosaka et al., 2008). Fibers from the neocortex, basal ganglia, and limbic system innervate the habenulae by way of the stria medullaris (Hikosaka et al., 2008; Sutherland, 1982). Efferents from the habenula form the fasciculus retroflexus and terminate at dopaminergic and serotonergic nuclei in the midbrain and hindbrain (Sutherland, 1982). In addition, the pineal gland produces melatonin and is involved in regulation of circadian activity (Collin et al., 1989). The development of dorsal diencephalon will be described in detail in subsequent sections.

This differentiation of the nascent brain occurs alongside a rapid expansion of total brain volume, and is tightly linked with the development of the ventricular system. Pressure from the accumulation of cerebrospinal fluid (CSF)

within the ventricles causes a dramatic expansion of brain volume (Desmond and Levitan, 2002; Desmond and Schoenwolf, 1985). The ventricular system of amniotes contains four ventricles, all of which issue from the central canal of the nascent neural tube. These cavities are filled with CSF, which provides protection, nutrition, pressure equilibrium, and removal of waste (Engelhardt and Sorokin, 2009). Neurons are born from neuroepithelial progenitors that exist in a periventricular domain (beside the ventricle). The right and left lateral ventricles (1st and 2nd ventricles) are bilaterally paired structures bounded by the fornix and thalamus in human anatomy. The lateral ventricles connect with the third ventricle at the midline of the brain. The 3rd ventricle is a cleft between the thalami of each hemisphere. Finally the 4th ventricle mediates CSF flow in the pons and upper medulla. Diencephalic neurons are specified from the progenitors residing proximal to the 3rd ventricle (Altman and Bayer, 1978).

Axial gradients of neuronal specification in the diencephalon

Several signaling gradients act upon the principal axes of a developing embryo, and relative exposure to these signals facilitates the production of unique subsets of neurons, organized into regions referred to as nuclei (McConnell, 1995). Tissue surrounding the NT provides signals that restrict the fate of neural progenitors, generally by spurring production of transcription factors in these progenitor cells (Bang and Goulding, 1996). Transcription factors spur the production of specific cell surface receptors and signal transduction components, ultimately facilitating the precise connectivity of a given neuron,

through the axonal growth cone and dendritic elaboration (Tessier-Lavigne and Goodman, 1996)

Much of the data supporting dorsoventral patterning has been gleaned from the spinal cord. Neurons of the spinal cord mediate motor output and relay pain response from the periphery. A group of glial cells form the floor plate, which lies at the ventral region of the spinal cord. Cells of the floor plate and the underlying mesodermal notochord secrete Sonic hedgehog (*Shh*). Progenitor cells within the ventral neural tube are fated by their reception of the Shh signaling gradient (Gilbert, 2000). For instance, cells of the ventral NT are fated to be motor neurons, and various classes of interneurons arise from a region just dorsal to the motor neuron (pMN) domain. Genetic ablation of Shh signaling components leads to a loss of ventral cells types, including motor neurons, interneurons, and even the floor plate (Chiang et al., 1996; Ericson et al., 1997; Ericson et al., 1996; Orentas et al., 1999). The Shh gradient provides specification of given neuronal classes by activating specific transcription factor expression in progenitor cells (Jessell, 2000).

A similar organizing center exists at the dorsal region of the spinal cord, referred to as the roof plate (Lee et al., 2000; Millonig et al., 2000). The roof plate controls specification of dorsal neural types by secretion of BMP (Lee et al., 1998; Liem et al., 1997; Timmer et al., 2002) and Wnt proteins (Megason and McMahon, 2002; Muroyama et al., 2002). Neural crest cells also originate at the dorsal region of the cord, and share progenitor cells with the roof plate (Bronner-Fraser and Fraser, 1989; Bronner-Fraser and Fraser, 1988; Selleck and Bronner-

Fraser, 1995). Following an initial wave of neural crest specification, these progenitors lose their neural crest potential (and migratory potential). Next, the roof plate specifies dI1 interneuron progenitors by way of BMP signaling (Chizhikov and Millen, 2004; Liem et al., 1997; Liu et al., 1997; Timmer et al., 2002). Ectopic expression of activated β-catenin leads to complete dorsalization of the neural tube; in contrast, inhibition of Wnt signaling with a dominant negative (inactive) form of TCF (the transcription factor activated by the Wnt/β-catenin pathway) shifts ventral gene expression to the dorsal neural tube (Alvarez-Medina et al., 2008)

Dorsoventral patterning of the diencephalon appears to be well conserved with the spinal cord (Bach et al., 2003; Lim and Golden, 2007). The Sox14 and Gbx2 transcription factors are expressed in discrete DV domains and respond to Shh activity, utilizing specific Gli molecules to initiate a transcriptional response (Hashimoto-Torii et al., 2003). The patterning program becomes more complex in the diencephalon due to the expression of additional factors in the floor plate, including epidermal growth factor (EGF)(Colas and Schoenwolf, 2000), BMP (Dale and Wardle, 1999; Furuta et al., 1997), and FGF molecules (Karabagli et al., 2002).

Anteroposterior (A-P) patterning of the nervous system has also been well established through a variety of vertebrate models. The initiation phase of A-P patterning begins prior to gastrulation, as demonstrated through fate maps of blastula stage embryos. The mesoderm of the head is specified through organizer activity at the dorsal midline (Saude et al., 2000). This dorsal organizer

is generated through overlapping expression of Wnt/B-catenin, Nodal, and BMP (Schier and Talbot, 2005). The organizer expresses inhibitors of Wnt and BMP to facilitate development of anterior structures (Niehrs, 2004; Schier and Talbot, 2005). Loss of BMP signaling results in an expansion of anterior structures (dorsalization); in contrast, loss of BMP inhibitors leads to ventralization (Agathon et al., 2003; Szeto and Kimelman, 2006).

Following gastrulation, the A-P axis of the head is marked by the emergence of segmented structures, a series of bulges including the rhombomeres of the hindbrain (Schilling, 2008). These hindbrain rhombomeres form individual compartments in which cell lineages are restricted by distinct boundaries (Fraser et al., 1990), and defined by a combinatorial code of transcription factors, including the Hox family (Moens and Prince, 2002). Initially, Wnt signals serve to repress anterior gene expression; subsequently posterior regional patterning is achieved through concentration dependent reception of Wnt, FGF, and retinoic acid signals (Cho and De Robertis, 1990; Sive et al., 1990).

A rich history of A-P forebrain modeling has led to the prosomere model, which describes six distinct domains within the forebrain. Under this model, the diencephalon emerges from the P2 prosomere (Rubenstein et al., 1994). The boundary between P1 and P2 prosomeres (telencephalon and diencephalon) is largely morphological, and is only evident in the dorsal domain (Trujillo et al., 2005). Prosomeric divisions are based in anatomy and gene expression and may not represent physical boundaries, as retroviral clones disperse widely upon

insertion into a given prosomere, regardless of prosomeric boundary (Arnold-Aldea and Cepko, 1996). However, the P2/P3 boundary (prethalamus and thalamus) does appear to be more sharply divided, and responds to signals secreted by the zona limitans intrathalamica (ZLI) at neural tube stage (Zeltser et al., 2001). The ZLI is a crucial organizer of the diencephalon, forming a morphogenetic gradient through Shh secretion that patterns the P2 domain (Hashimoto-Torii et al., 2003), in combination with the floor plate, which also secretes Shh (Echelard et al., 1993). *shh* null mice possess severely retarded diencephalic growth, due to decreased proliferation and increased cell death (Ishibashi and McMahon, 2002), likely due to loss of Shh secretion by the ZLI (Chiang et al., 1996). The cell death is likely caused by disruption of dorsal Wnt/BMP/FGF signaling due to increased Gli3 repressor function in the absence of Shh (Ishibashi and McMahon, 2002; Litingtung and Chiang, 2000; Ulloa et al., 2007). Finally, Wnt signaling is also necessary for ZLI organizer function. Canonical Wnt acts to induce dorsal thalamic tissue, while application of the Wnt antagonist Dkk results in prethalamic (ventral thalamus) differentiation (Braun et al., 2003).

The posterior boundary of the diencephalon, the di-mesencephalic boundary (DMB) is defined and marked by expression of Pax6, Pax2, and Engrailed (En). Pax6 is a diencephalic marker that terminates at the DMB (Mastick et al., 1997; Puschel et al., 1992; Warren and Price, 1997). In contrast, Pax2 and En are midbrain markers with an anterior extent at the DMB (Araki and Nakamura, 1999). Ultimately Pax6 represses Pax2 and En to define the DMB

(Matsunaga et al., 2000), and En acts to repress diencephalic fate; ectopic En expressed in the diencephalon leads to a rostral shift of the DMB and the presence of mesencephalic features in the diencephalon (Araki and Nakamura, 1999). Finally, both En and FGF are required to maintain the DMB (Scholpp et al., 2003).

Neurons are generated from a polarized neuroepithelium

Neurons arise from precursor cells that reside in a specialized microenvironment, or niche, that provides control over specification, differentiation, and critically, self-renewal (Fuchs et al., 2004). The vertebrate neural niche is located along the ventricles of the brain, and is therefore known as the ventricular zone (VZ). Cells of the ventricular zone display epithelial characteristics, and are thereby named neuroepithelial cells (NECs). NECs display apical-basal polarity (apical = proximal to ventricle; basal = distal from ventricle) and display a variety of polarized elements.

NECs display apical-basal polarity in both intracellular and extracellular composition. First, NEC centrosomes are localized beneath the apical surface (Chenn et al., 1998), facilitating cell division that occurs within this apical domain prior to interkinetic nuclear migration (a phenomenon of neurogenesis in which cell divisions occur at specific locations within the ventricular zone)(Murciano et al., 2002). Tight junction (TJ) and adherens junction (AJ) complexes serve to tightly adhere cells to one another at the ventricular (apical) surface (Fishell and Kriegstein, 2003; Huttner and Brand, 1997). AJs serve to maintain radial
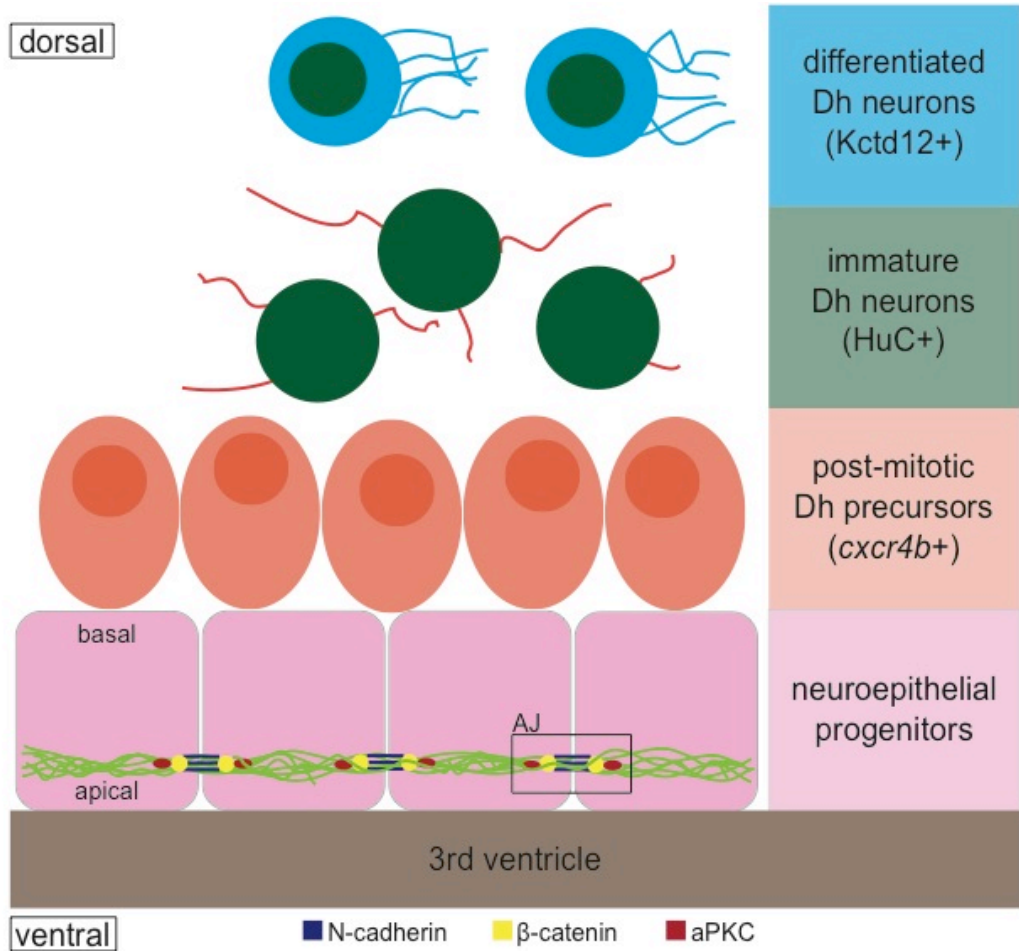
Figure 1. Schematic of habenular neurogenesis. Mature neurons of the dorsal habenula (blue, Kctd12^{+}) originate from progenitor cells lining the 3rd ventricle (pink). Progenitors exist as a neuroepithelium, remaining in tight contact with neighbors using adherens junctions (AJ). Progenitors divide and eventually give rise to post-mitotic habenular precursors, marked by *cxcr4b*. Upon further differentiation, these cells express HuC/D, a pan-neuronal marker.

morphology (bipolar cellular morphology) and proliferative capacity through recruitment of the cytoplasmic Par family/atypical protein kinase C (aPKC)/Cdc42 (Aaku-Saraste et al., 1996; Manabe et al., 2002; Zhadanov et al., 1999), members of the catenin/armadillo protein family (Farkas and Huttner, 2008; Meng and Takeichi, 2009; Stepniak et al., 2009), and Numb, a Notch pathway factor involved in neuronal differentiation (Cayouette and Raff, 2002; Rasin et al., 2007). Additionally, the apical plasma membrane contains several exclusive transmembrane components, including prominin-1 (Weigmann et al., 1997), N-cadherin (Aaku-Saraste et al., 1996) and ephrin B1 (Stuckmann et al., 2001). The basal end of NECs contacts the basal lamina via receptors known as integrins (Meng and Takeichi, 2009; Wodarz and Huttner, 2003). Integrins are alpha-beta heterodimers that bind specific ligands of the extracellular matrix (ECM) such as fibronectin, laminin or collagen (Weigmann et al., 1997). Ultimately, these adhesive interactions between neural precursors and the ECM membrane are key for the process of neuronal migration (Sarkisian et al., 2008; Schmid and Anton, 2003).

Adherens junctions are crucial for NEC maintenance as blocking AJ component function leads to precursor delamination, malformation of the neural tube and widespread disruption of the neuroepithelium. These neural tube phenotypes are witnessed upon knockdown of the Rho-GTPase cdc42 (Cappello et al., 2006), aPKC ζ (Ghosh et al., 2008), aPKC λ (Imai et al., 2006), N-cadherin (Kadowaki et al., 2007), and Numb (Rasin et al., 2007). NECs (neural progenitors) surrounding the ventricle can hyperproliferate, giving rise to excess

precursors when adherens junctions are disrupted. This is true for several AJ factors, including N-cadherin (Chalasani and Brewster, 2011), RhoA (Katayama et al., 2011), αE-catenin (Lien et al., 2006), and Numb (Rasin et al., 2007). This hyperproliferation is accompanied by a prominent shift in morphology. For example, periventricular cells (NECs) become multilayered and variable in size and shape upon disruption of αE-catenin (an AJ component) in murine neural progenitors (Lien et al., 2006).

Self-renewal is perhaps the most critical component of progenitor cells in development. The retention of self-renewal allows the production of distinct cellular classes over an extended temporal scale. Disrupting the balance of self-renewal and neurogenesis can lead to neurodevelopmental defects in brain size and organization (Pang et al., 2008), and affect cognition or motor function (Courchesne et al., 2007). A role for N-cadherin has been described in a variety of neural progenitors. For instance, motor neurons of the spinal cord express reduced levels of N-cadherin and are some of the first cells to differentiate in the spinal cord (Rousso et al., 2012). In line with this argument, cultured pMN cells rapidly lose their stem cell characteristics as compared to other progenitor cell types (Mukouyama et al., 2006). As stated previously, N-cadherin is required for neural tube formation, and *cdh2* mutants also display reduced NEC adhesion, displacement of neurons along the dorsoventral and anteroposterior axes, and importantly, increased mitoses and ectopic neurogenesis in the dorsal midbrain and hindbrain (Lele et al., 2002).

Control of cell division is a crucial toward the maintenance of neural stem cells. More specifically, the plane of cell division determines whether daughter cells retain neuroepithelial precursor fate or begin to differentiate as immature neural progenitors (Huttner and Brand, 1997). This is thought to be due to the unequal distribution of cell fate determinants in apical and basal domains of the mother cell, as extrapolated from extensive work in the fruit fly (Jan and Jan, 2001; Knoblich, 2001; Wodarz and Huttner, 2003). Symmetric divisions within the plane of the ventricle generally lead to the production of two NEC daughters that remain proliferative (Miyata et al., 2004; Noctor et al., 2004), thereby expanding the surface of the neural tube laterally (Rakic, 1988). These proliferative divisions are not limited to NECs, however, as radial glia-like cells in the SVZ (that lack epithelial morphology) also undergo symmetric and asymmetric proliferative divisions, greatly expanding the depth of the SVZ (Hansen et al., 2010). Asymmetric divisions (perpendicular to the ventricle) produce one NEC and one neural progenitor, as daughter cells would inherit either apical or basal constituents (Chenn and McConnell, 1995), a process that increases as more NECs switch over to generate neurons (Haydar et al., 2003).

Finally, the length of the cell cycle affects neurogenesis (Calegari and Huttner, 2003). In the absence of the cell cycle inhibitor p27Kip1, mice develop enlarged brains (Fero et al., 1996; Nakayama et al., 1996). Interestingly, some cell cycle components are expressed in spatially restricted domains in the brain, as cyclin D1 and cyclin D2 are restricted to distinct rhombomeres in the hindbrain (Wianny et al., 1998). Brain size is also affected by the fraction of progenitors

that exit the cycle (become neurons)(Caviness et al., 2000). Shortening the cell cycle (G1) in murine neuroepithelial cells by IGF-1 shifts the balance toward proliferative cell divisions (Hodge et al., 2004), and progenitors undergoing neurogenic divisions have longer cell cycles than proliferative cycling neighbors (Calegari et al., 2005). The control of cell division polarity may be mediated by the transcriptional activity of β-catenin, acting downstream of Wnt signaling (Bellaiche et al., 2001), as constitutively active β-catenin transgenic mice develop enlarged brains (Zechner et al., 2003). Importantly, these transgenics have a 2-fold increase in precursors re-entering the cell cycle during cortical neurogenesis (Chenn and Walsh, 2002), suggesting that β-catenin activity spurs proliferation.

A role for protein secretion in neurogenesis

Development of any tissue is highly dependent on timely and abundant production of extracellular and transmembrane proteins. For instance, chondrocytic cells of the neurocranium and jaw are especially secretory in nature, and produce a large amount of extracellular matrix material in order to form cartilage. Upon loss of secretory pathway components such as Sec23 or Sec24, cartilaginous elements are greatly reduced in zebrafish (Boyadjiev et al., 2006; Lang et al., 2006; Sarmah et al., 2010). In the developing choroid plexus (CP) of the brain, choroidal epithelial cells (CECs) display a higher secretory capacity than other CP cells or cultured astrocytes, producing transport proteins, collagen subunits, ECM proteins, proteases, and neurotrophic factors (Thouvenot et al., 2006)(See Figure 2).
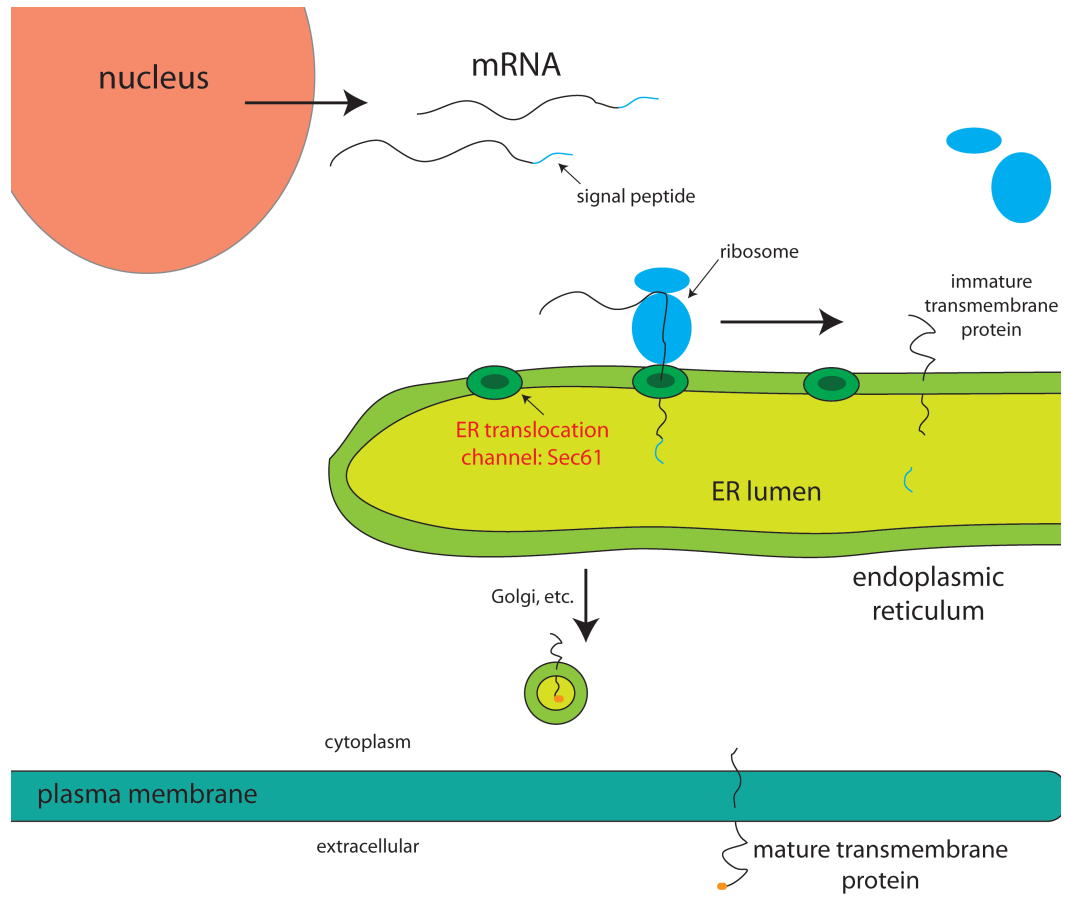
Figure 2. Translocation of newly translated peptides at the endoplasmic reticulum (ER). Following transcription in the nucleus, transmembrane proteins are co-translationally inserted into the ER membrane. After subsequent processing, mature proteins are trafficked to the surface of the plasma membrane. Translocon channels illustrated as dark green disks.

Affecting the final step of protein secretion, the *hydrocephalus with hopping gait* (*hyh*) mutation in mouse has provided crucial evidence on the impact of protein trafficking on neurogenesis. This hypomorphic mutation in the *Alpha-snap* gene results in a disruption of SNARE-mediated vesicle fusion at the plasma membrane, ultimately leading to hydrocephalic brain development in mice (Bronson and Lane, 1990; Chae et al., 2004). Further examination found that *hyh* mice produce excess early born, deep-layer cortical neurons and fewer later born neurons via depletion of the progenitor pool (Chae et al., 2004). In addition, human mutations causing an autosomal recessive condition with microcephaly (small brain) and periventricular heterotopia (migration-impaired neurons clustered near the ventricle) have been mapped to mutations in ADP-ribosylation nucleotide-exchange factor-2 (*ARFGEF2*)(Sheen et al., 2004). This gene codes for brefeldin A-inhibited GEF2 protein (BIG2), required for vesicle and membrane trafficking from the trans-Golgi network (Shinotsuka et al., 2002a; Shinotsuka et al., 2002b). Finally, *hemorrhagic hydrocephalus* (*hhy*) mutant mice display subcortical heterotopia (displaced neurons in subcortical regions), with some cells in direct contact with ventricular fluid. Late-born Satb2+ neurons are dramatically displaced in the subcortical zone of *hhy* mice, which also show premature depletion of neural progenitors and a shift toward neurogenesis rather than self-renewal of NECs (Mori et al., 2012). The *hhy* mutation maps to *Ccdc85c*, which is expressed at apical adherens junctions of radial glia (Mori et al., 2012). Although the function of the protein is not yet known, it is predicted to

contain several modified features in its mature form and would therefore need to traverse the secretory pathway.

The generation of asymmetric vertebrate organs

Although vertebrates display considerable divergence after the tailbud stage of embryogenesis, most achieve L/R asymmetry using a conserved genetic mechanism, via the Nodal signaling family (Shiratori and Hamada, 2006). A role for Nodal was first noted in studies of visceral laterality. During somitogenesis, components of this family are expressed in the left lateral plate mesoderm, including Nodal (Collignon et al., 1996; Levin et al., 1995; Lowe et al., 1996; Lustig et al., 1996; Sampath et al., 1997), the Nodal antagonist Lefty (Cheng et al., 2000; Ishimaru et al., 2000; Kosaki et al., 1999; Meno et al., 1999; Meno et al., 1997; Meno et al., 1996; Rodriguez Esteban et al., 1999; Thisse et al., 2000) and Pitx2, a downstream transcriptional effector of Nodal signaling (Campione et al., 1999; Gage et al., 1999; Kitamura et al., 1999; Lin et al., 1999; Logan et al., 1998; Lu et al., 1999; Patel et al., 1999; Piedra et al., 1998; Ryan et al., 1998; Schweickert et al., 2000; Yoshioka et al., 1998). Lefty is also expressed in the ventral midline where it prevents right-sided Nodal signaling (Ohi and Wright, 2007). Subsequent organogenesis results in the production of rudimentary organs and systems, and ultimately, Nodal signaling cassette influences the morphology of the visceral organs (Capdevila et al., 2000).

Mutations affecting Nodal expression lead to disruptions in asymmetric organ development. If Nodal is expressed in the right LPM instead of the left, the

result is a condition known as *situs inversus*, in which all organ lateralities are coordinately reversed; if Nodal is bilateral or absent in the LPM, heterotaxia is the result, in which the laterality of each individual organ is randomized independently of other organs (Lowe et al., 1996). Therefore, precise control over Nodal expression is crucial. The spatial control of Nodal expression is mediated through the activity of a monociliated endodermal organ, called the node in mouse, Hensen's node in chick, gastrocoel roof plate in frog, and Kupffer's vesicle in fish (Essner et al., 2002). It is thought that the counterclockwise movement of these monocilia restricts Nodal expression to the left LPM (Nonaka et al., 1998), though the precise mechanism is not fully understood and may also involve ionic transport (Levin, 2004).

Most vertebrates utilize Nodal signaling to generate asymmetry in visceral organs; however, teleost fish also utilize the signaling cassette to influence asymmetric features of the brain. Indeed, Nodal expression has not been detected in the brains of other vertebrates, suggesting that this mechanism is a derived feature of teleosts (Concha and Wilson, 2001). In teleosts, Nodal signals are secreted from cells of the anterior lateral plate mesoderm, inducing a transient pulse of Nodal expression (20 to 24 hpf) in the left epithalamus (Bisgrove et al., 2000; Concha et al., 2000; Halpern et al., 2003; Liang et al., 2000; Soroldoni et al., 2007). Mutants that lack Kupffer's vesicle, the ventral midline, or components of Nodal pathway can cause right sided, bilateral, or absent Nodal in the LPM, which is in turn reflected in the epithalamus (Bisgrove

et al., 2000). The precise effects of Nodal signaling on epithalamic development will be outlined in the subsequent section.

The zebrafish dorsal diencephalon as model for asymmetric neural development

The zebrafish, *Danio rerio* has emerged as a premier model system for documenting vertebrate neurodevelopment. A single mating pair produces a large number of embryos, and embryos develop into fertile adults in the matter of three months. This in turn facilitates another major advantage, the ability to perform large-scale forward genetic screens. In addition, the *Danio rerio* genome contains highly conserved homologs of most mammalian genes. The genome is amenable to transgenesis via a variety of methods. In addition, zebrafish embryos are transparent, which allows real-time imaging of neurodevelopment in vivo.

Zebrafish are now utilized for research in nearly every facet of development. As with many vertebrate animals, their brains develop with asymmetric (lateralized) features. The dorsal diencephalon (or epithalamus) of the zebrafish is especially asymmetric (Figure 3). In regard to the dorsoventral axis, it exists at the dorsal-most pole of the brain and lies between the telencephalon and midbrain on the anteroposterior axis. At the center of the epithalamus is the pineal organ, a photoreceptive nucleus that contains cone and rod photoreceptors, glia, and projection neurons. The pineal organ is positioned at the dorsal surface of the brain, which allows direct light illumination and serves
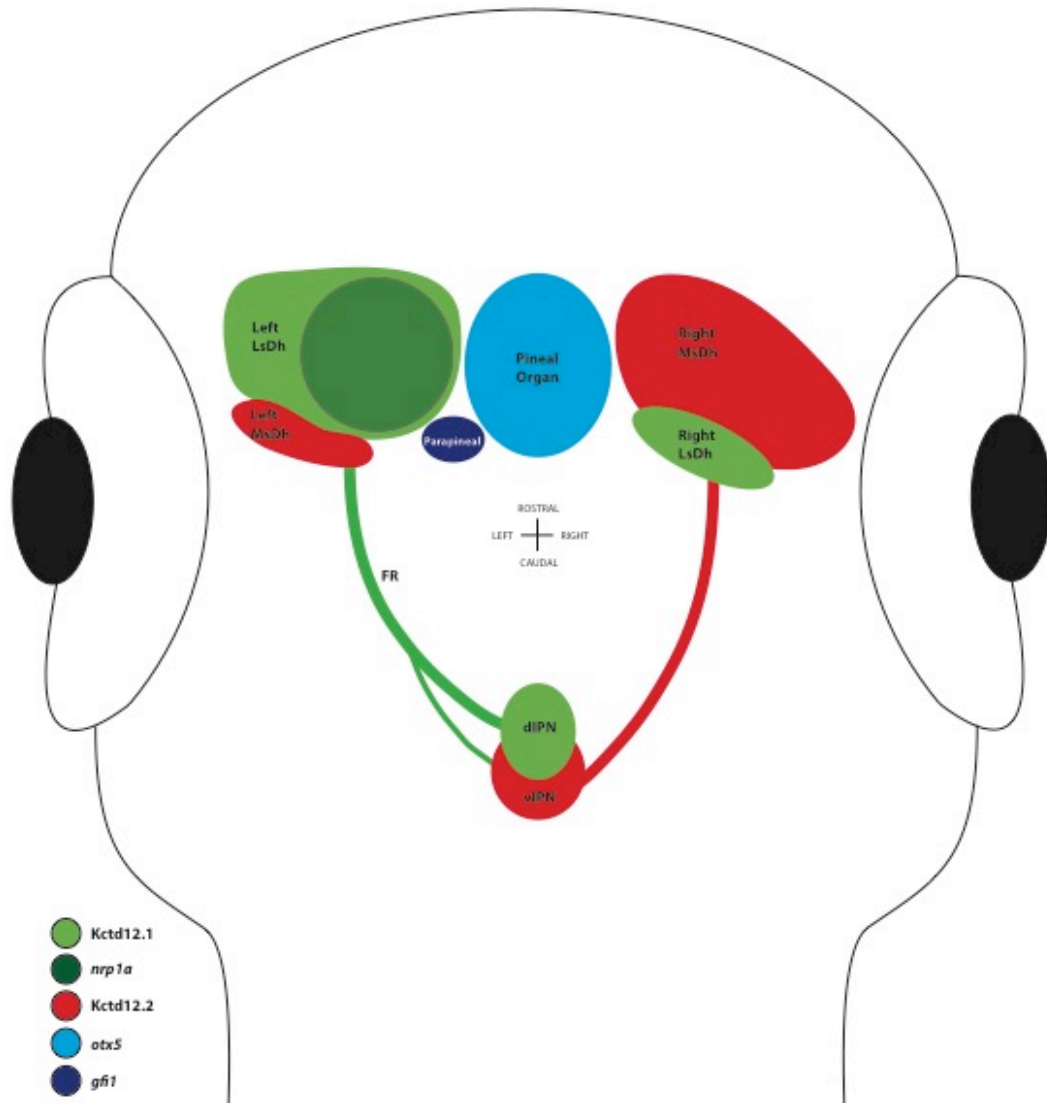
Figure 3. Asymmetric gene expression in the dorsal diencephalon of the larval zebrafish. The accessory parapineal organ develops near the left dorsal habenula (*gfi*-1). The dorsal habenula are subdivided into the medial and lateral subnuclei (MsDh, LsDh). LsDh neurons express Kctd12.1 and *nrp1a*, while MsDh neurons express Kctd12.2. Molecular asymmetries are manifest in differential midbrain targeting, as left habenular neurons innervate the dorsal and ventral interpeduncular nucleus (IPN) and right habenular neurons exclusively target the ventral IPN.

as the primary transduction pathway for sensing day length and controlling melatonin release (Allwardt et al., 2001; Doyle and Menaker, 2007; Falcon, 1999; Falcon et al., 2009; Kazimi and Cahill, 1999). The parapineal is an accessory nucleus that emerges from the left side of the pineal complex early in embryogenesis (Aizawa et al., 2005; Concha et al., 2000). The parapineal lacks photoreceptors but is neural in nature, as cells in this small nucleus produce axons that innervate their immediate lateral neighbor, the habenula (Concha and Wilson, 2001). Outside of a role for elaboration of subnuclear habenula asymmetries, the precise role of the parapineal is not known, though it expresses AANAT2, the melatonin biosynthetic enzyme (Gamse et al., 2002; Gothilf et al., 1999).

The habenular nuclei are bilateral and can be subdivided into dorsoventral and latero-medial subnuclei through anatomy and gene expression (Figure 3). The dorsal habenula, considered the zebrafish equivalent of the medial habenula in humans (Diaz et al., 2011), is divided into lateral and medial subnuclei (LsDh, MsDh), which are populated by neurons that are born along the third ventricle of the brain (Aizawa et al., 2007; Concha et al., 2003). A single neuroepithelial cell can contribute to both lateral and medial subnuclei (Aizawa et al., 2007), suggesting at least bipotential capacity in habenular progenitors (the progenitor can produce at least two distinct neuronal subtypes). These progenitors undergo their final mitoses (become precursors), migrate to the dorsal surface, and express subnucleus-specific genes.

Nodal signaling regulates pineal complex asymmetry, including the left-biased placement of the pineal stalk (Liang et al., 2000) and leftward migration of the parapineal organ (Concha et al., 2000; Liang et al., 2000; Snelson et al., 2008). In addition, Nodals spur asymmetric initiation of neurogenesis in the flanking habenulae (Roussigne et al., 2009). Remarkably, embryos deficient for Nodal or express Nodal genes bilaterally still possess single, asymmetrically located parapineals and habenulae with asymmetric subnuclei, though asymmetries are L-R reversed in 50% of mutant larvae (Aizawa et al., 2007; Concha et al., 2000; Concha et al., 2003; Gamse et al., 2005; Gamse et al., 2003; Kuan et al., 2007b).

The parapineal acts to reinforce the elaboration of habenular asymmetries. Ablation of the parapineal results in a dramatic reduction in the left lateral subnucleus (LsDh) and an expansion of the medial subnucleus (MsDh), such that the left and right habenula are roughly symmetrical (Gamse et al., 2005; Gamse et al., 2003). Similarly, when embryos are depleted for *tbx2b,* a transcription factor required for parapineal formation and migration, habenulae resemble those of parapineal-ablated embryos (Snelson et al., 2008). Conversely, rare embryos are found with bilateral parapineals on either side of the pineal organ; these individuals develop both habenulae with left-sided characteristics (Gamse et al., 2003). Thus a convergence of secreted signal (Nodal), transcription factor activation (*tbx2b*) and parapineal innervation are required for left-right asymmetry in habenular development. The precise interplay of these components has not yet been determined.

Gene expression in the zebrafish habenulae is distinctly asymmetric and corresponds with the subnuclear boundaries (Figure 3). Neurons of the lateral subnucleus of the dorsal habenula (LsDh) express the gene *potassium channel tetramerization domain-containing 12.1* (*kctd12.1*). The medial subnucleus (MsDh) is composed of neurons expressing the related *kctd12.2* gene. The protein products from these genes help govern asymmetric neuropil formation in the habenular nuclei via interaction with Unc-51-like kinase 2 (Ulk2), a kinase that promotes neuronal process extension (Zhou et al., 2007). Both Kctd12 proteins negatively regulate Ulk2, such that overexpression of Kctd protein or knockdown of Ulk2 results in reduced habenular neuropil. Conversely, overexpression of Ulk2 or knockdown of Kctd leads to enhanced neuropil (Taylor et al., 2010; Taylor et al., 2011). In addition, an axon guidance co-receptor *neuropilin 1a* (*nrp1a*) is expressed exclusively in the LsDh and functions to guide habenular efferent axons to the dorsal domain of the interpeduncular nucleus (IPN). Disruption of *nrp1a* or its ligand, *semaphorin 3a* (*sema3a*) disrupts dorsal targeting and efferent axons ectopically innervate the ventral IPN (Kuan et al., 2007b).

Asymmetric dorsal habenulae develop through an asymmetric program of neurogenesis, through the production of precursor cells and the assignment of precursors to subnuclei. The earliest asymmetry in the habenular nuclei is observed at 28 hpf. Neurons arise from mitotically active neuroepithelial cells lining the 3rd ventricle, referred to henceforth as progenitors. Cells fated for the Dh lose their neuroepithelial characteristics (columnar, epithelial morphology)

and become habenular precursor cells, which are post-mitotic, yet undifferentiated. Habenular precursor cells, marked by expression of *chemokine receptor 4b (cxcr4b)* gene are observed at 28 hpf in the left Dh but not the right Dh (Roussigne et al., 2009). Neurons expressing *huC:gfp+*, a transgenic reporter of post-mitotic neurons (Marusich et al., 1994), are evident in the left Dh as early as 32 hpf, and in the right Dh *huC:gfp+* cells are evident at 36 hpf. Asymmetry in precursor production persists until 48 hpf. Importantly, initial expression of *huC* and *cxcr4b* remains asymmetric following ablation of the parapineal (Roussigne et al., 2009), suggesting that asymmetric habenular neurogenesis begins independently of the parapineal, despite the parapineal's profound impact on subsequent differentiation into mature neurons (*kctd12.1*, *kctd12.2, brn3a*) and axon targeting (*nrp1a*)(Bianco et al., 2008; Concha et al., 2003; Gamse et al., 2005; Gamse et al., 2003). In addition, precursors are asymmetrically assigned to Dh subnuclei. Using BrdU incorporation and subsequent immunostaining for LsDh and MsDh neurons, the Okamoto laboratory illustrated this asymmetric process (Aizawa et al., 2007). On average, lateral subnucleus neurons are born before their medial subnucleus neighbors, with a peak of LsDh neurogenesis at 32 hpf, of which a greater proportion are born on the left side of the brain. The medial subnucleus undergoes neurogenesis later, peaking at 48 hpf, and largely contributing to the right side of the brain (Aizawa et al., 2007). The mechanism for this transition from LsDh to MsDh neurogenesis has not been described, though it is clear that the parapineal is essential for LsDh expansion and MsDh repression through ablation experiments.

Importantly, the development of habenular asymmetries has been linked to behavioral outcomes. Because zebrafish eyes are positioned laterally, each eye is exposed to a separate visual landscape. Interestingly, adult zebrafish show a right eye preference when viewing novel objects (Miklosi and Andrew, 2006; Miklosi et al., 2001), while the left eye is equipped for comprehensive assessment of familiarity (Miklosi and Andrew, 2006; Miklosi et al., 1997). Morpholino depletion of the *spaw* gene results in a higher proportion of zebrafish with randomized parapineal placement (right sided), and an associated reversal of habenula subnuclear asymmetries (Long et al., 2003). In behavioral tasks, although these L/R reversed morphants show no differences in motor response to stimuli, they did show a significant delay in navigation (the time between introduction into the testing chamber and its swimming a distance roughly twice its body length), cover less distance in exploration, and show a reduced average speed as compared to controls (Facchin et al., 2009). In addition, genetic inactivation of the LsDh of zebrafish causes freezing behavior instead of the normal flight response to a conditioned fear stimulus (Agetsuma et al., 2010). These altered behavioral responses may implicate the habenula as a player in the dopaminergic pathway, a neurotransmission system with entrenched roles in learning, reward seeking (Arias-Carrion and Poppel, 2007), and fear conditioning (Fadok et al., 2009). In line with this hypothesis, lesion studies in mammals indicate that the habenula mediates fear, motivation and reward (Heldt and Ressler, 2006; Morissette and Boye, 2008), and the medial habenula and IPN

are involved in dopaminergic pathway modulation (Taraschenko et al., 2007a; Taraschenko et al., 2007b).

In summary, asymmetric Dh development begins with embryonic left-sided cues (Nodal), which spurs neurogenesis in the left Dh before the right, as best visualized by the asymmetric expression of the habenular precursor gene *cxcr4b*. Habenular progenitors are bipotential, yet generate subnucleus-specific neurons in temporally distinct domains: LsDh neurons are first produced, and MsDh neurons follow. Overlaid upon the asymmetric program of neurogenesis, subsequent differentiation affects the relative size of the dorsal habenular subnuclei. This differentiation requires input from the left-sided parapineal. By roughly 56 hpf, the composite program results in a large left LsDh paired with a smaller MsDh and the large right MsDh paired with a smaller LsDh.

Discussion

Despite centuries of neurological history and decades of molecular research on neurodevelopment, the functional brain atlas remains in infancy. Left-right asymmetry is evident in human brain anatomy, and hemispheric-specific activation is common in many behavioral tasks. The correlations between reduced lateralized brain activity and neurodevelopmental disorders such as schizophrenia, dyslexia, and autism lends considerable weight toward developmental studies on L/R brain development in model organisms.

The transition from a single fertilized cell to a fully elaborated brain requires a genetic program with utmost precision in temporal and spatial regulation. Some of these genes are recurring players in neurogenesis, such as the cell adhesion protein N-cadherin, which has defined roles in neurulation and neurogenesis.

CHAPTER II

MUTATION OF SEC61AL1 REVEALS A ROLE FOR PROTEIN PRODUCTION IN NEUROEPITHELIAL PROGENITOR CELLS

Preface

An ENU mutagenesis screen was utilized in the search for genetic components involved in the generation of brain asymmetry. The isolated mutants were processed for the expression of the gene *kctd12.1*, a marker specific for the lateral subnucleus of the dorsal habenulae in zebrafish. One mutant isolated from this screen was mapped to *sec61alpha-like1*, the major component of the translocon localized at the endoplasmic reticulum. This mutant, nicknamed *big time*, has an expanded LsDh in the right hemisphere, and a concomitant reduction in the MsDh.

Methods

Zebrafish wild-type and transgenic lines

Zebrafish were raised at 28.5 °C on a 14/10 light/dark cycle. Embryos and larvae were staged according to hours or days post-fertilization as previously described (Kimmel et al., 1995). The wild-type stain AB (Walker, 1999), the newly

identified ethylnitrosourea induced mutation *sec61al1*^{c163}, and the retroviral insertion mutation *sec61al1*^{hi1058} (Golling et al., 2002) were used.

Mutagenesis and screening

Mutagenesis was performed by placing male zebrafish in 3 mM ENU for three 1-hour treatments with 48 h between treatments. F1 fish were generated by mating ENU-mutagenized males to AB females. Their progeny were raised to adulthood and intercrossed to produce F2 families. At least 6 matings were performed to screen each F2 family and the resultant F3 larvae were collected at 4 days post fertilization (dpf) and fixed in 4% paraformaldehyde (PFA) for *in situ* hybridization with the *kctd12.1* probe. Putative mutants showing reversed or bilaterally symmetric expression of *kctd12.1* in the habenular nuclei were re-identified in the progeny of F2 heterozygotes and lines were established through outcrosses to AB fish. The *sec61al1*^{c163} mutation was identified by increased expression of *kctd12.1* in the right habenular nucleus of homozygous mutant embryos.

Positional cloning of *sec61al1*^{c163}

Heterozygous fish (AB) carrying the *sec61al1*^{c163} allele were mated with wild-type fish of the WIK strain (Rauch, 1997). F2 heterozygote larvae were used for meiotic mapping with simple sequence length polymorphism (SSLP) markers, as previously described (Bahary et al., 2004). There were no recombination events between the microsatellite marker z7248 and the *c163* mutation in 375

meioses. From examination of the zebrafish genome (Zv8, Ensembl)(Hubbard et al., 2009), we found that z7248 was only 5 kilobases away from the *sec61al1* locus. To identify the lesion in *sec61al1*, cDNA was prepared using Superscript II reverse transcriptase (Invitrogen). For DNA sequencing, cDNA was amplified with Pfu DNA polymerase and primers flanking the *sec61al1* open reading frame, and then subcloned into the pCRII-Topo vector (Invitrogen). The clones were sequenced using an ABI 3730xl sequencer and data was analyzed with Sequencher software (GeneTools).

Genotyping of *sec61al1^{c163}* mutants

For genotyping of homozygous mutant larvae, DNA was extracted by boiling larvae for 10 minutes in 25 µL of embryo lysis buffer (Bahary et al., 2004), then proteinase K (Roche Applied Bioscience) was added to a final concentration of 0.5 mg/mL. Samples were incubated at 55 °C for 1 h, then boiled for 10 min to deactivate the proteinase K. The *sec61al1^{c163}* mutation is located at nucleotide 92 of 100 in exon 6, introducing a premature stop codon (TGT to TGA). Mutant embryos were genotyped using a nested PCR method, with the outer set of primers amplifying ~400 bp of genomic sequence: forward: 5′-CCCTGAGCTTAAAGCCACAT-3′, reverse: 5′-TTCCATTGAATTTCAGTTTTCC-3′. We designed primers flanking the mutation site that introduce a Hinf1 recognition sequence in the inner PCR product from the mutant allele: forward: 5′-TCTCACCTGAAGATGATCAGGAGGAGCATGG-3′, reverse: 5′-ATGAAACCATTTGAGGGTGAT-3′ (product size ~ 350 bp). The inner PCR

product was digested with Hinf1 (NEB) at 37 °C overnight, then electrophoresed on a 3% agarose gel. sec61a1[hi1058] mutants were genotyped as previously described (Golling et al., 2002; Nissen et al., 2006).

Morpholino injections

An antisense morpholino oligonucleotide (MO) complementary to the translation initiation site was used to deplete *tbx2b* function (Gross and Dowling, 2005; Snelson et al., 2008). Antisense MOs for *sec61al1* were designed against the translation initiation site (sec61al1ATG-MO) (5′-GCCATGATGACGGTCCCCTGAAATC-3′) or corresponding to the intron 7/exon 8 boundary (sec61al1SP-MO) (5′-GCTGTGTGCAATGTTTTACCTTTCG-3′). For each morpholino, the stock solution (10 mg/mL) was diluted in distilled water, and embryos (1–2 cell stage) were pressure injected with ~ 1 nL of MO per embryo. The *tbx2b*[ATG-MO] was used at 8 ng/embryo, the *sec61al1*[ATG-MO] at 500pg/embryo, and the *sec61al1*[SP-MO] at 4 ng/embryo.

in situ hybridization

Whole mount in situ hybridization was performed as described previously (Gamse et al., 2003; Thisse and Thisse, 2008) using reagents from Roche Applied Bioscience. RNA probes were labeled using fluorescein-UTP or digoxygenin-UTP. To synthesize antisense RNA probes, the following templates and enzymes were used:

Plasmid name	Reference	Enzyme used to linearize plasmid	RNA Polymerase
pBS-otx5	(Gamse et al., 2002)	EcoRI	T7
pBK-CMV-kctd12.1	(Gamse et al., 2003)	EcoRI	T7
pBK-CMV-kctd12.2	(Gamse et al., 2005)	BamHI	T7
pCRII-kctd8	(Gamse et al., 2005)	BamHI	T7
pBS-gfi1	(Dufourcq et al., 2004)	SacII	T3
pCR4-nrp1a	(Kuan et al., 2007b)	NotI	T3
pSPORT1-sst1.1	(Argenton et al., 1999)	SalI	SP6

Embryos were incubated at 70 °C with the antisense probe in hybridization solution containing 50% formamide. Hybridized probes were detected using alkaline phosphatase-conjugated antibodies and visualized by 4-nitro blue tetrazolium (NBT) and 5-bromo-4-chloro-3-indolyl-phosphate (BCIP) staining for single labeling, or NBT/BCIP followed by iodonitrotetrazolium (INT) and BCIP staining for double labeling (Thisse and Thisse, 2008).

BrdU labeling

Bromodeoxyuridine (BrdU)(5 mL of 10 mm solution with 10% dimethyl sulfoxide [DMSO] in embryo medium) was added to dechorionated embryos at 32 or 48 h post fertilization (hpf). Embryos were incubated on ice for 30 min, then removed to a new dish and washed 4 x 5 min in embryo media. Embryos were allowed to grow until 4 dpf in embryo media containing 0.003% phenylthiouracil

(PTU). At 4 dpf, embryos were fixed in 4% PFA overnight at 4 °C. Immunolabeling was performed on embryos with mouse-anti-BrdU and rabbit-anti-Kctd12.1 antibodies, as described below.

Immunofluorescent labeling

2-4 dpf embryos were fixed for at least 36 h in Prefer fixative (Anatech) at room temperature. Embryos were stored in 0.1% Tween in PBS at 4°C for up to two weeks. Embryos were blocked in PBS with 0.1% Triton X-100, 10% BSA, 1% DMSO and 2% sheep serum (PBSTrS). For antibody labeling, rabbit anti-Kctd12.1 (1/500)(Gamse et al., 2005), chicken anti-Kctd12.1 (1:500)(Snelson et al., 2008), rabbit anti-Kctd12.2 (1:500)(Gamse et al., 2005), mouse anti-HuC/D (1:500), Invitrogen A21271), mouse anti-acetylated alpha-Tubulin (1:500, Invitrogen 32-2700), and mouse anti-BrdU (1:500, Developmental Studies Hybridoma Bank, University of Iowa) were used. Larvae were incubated overnight in primary antibody diluted in PBSTrS, and primary was detected using goat anti-rabbit, goat anti-chicken, or goat anti-mouse secondary antibodies conjugated to Alexa 488 or Alexa 568 fluorophores (1:350, Molecular Probes). Cell nuclei were detected with ToPro3 (1:3000, Invitrogen).

For cryosectioned zebrafish tissue, embryos were fixed in BT fix (4% paraformaldehyde, 0.15 mM $CaCl_2$, 4% sucrose in 0.1 M PO_4 buffer) overnight on rocker. Subsequently embryos were embedded in 2% agarose/5% sucrose, and sunk overnight in 5% sucrose. Next, blocks were frozen in 2-methyl butane/liquid N_2, and sectioned at 10 µm thickness on a Leica CM1850 cryostat.

Sections were then rehydrated for 1 h in 1x PBS, blocked for 1 h in 2% sheep serum/BSA in 1x PBS (AB Block), then incubated with rabbit anti-aPKC (1:200, Santa Cruz Biotechnology) for 2 h at room temperature. Sections were then washed 6 x 5 min in 1x PBS, incubated with goat anti-rabbit Alexa 568 (1:200, Invitrogen) and Alexa 488-phalloidin (1:100, Invitrogen) in AB Block for 2 h. Sections were washed 5 x 5 min in PBS, and cell nuclei were stained with Hoechst (1:1000 in PBS, Invitrogen), via room temperature incubation for 15 min. Sections were washed 5 x 5 min in 1x PBS, cleared with glycerol and imaged on a Leica 6000M compound microscope.

For fluorescent in situ (FISH)/Immunofluorescent double labeling, larvae were treated in accordance to the in situ hybridization protocol described above with the following alterations. Both anti-DIG and rabbit anti-Kctd12.1 antibodies were applied simultaneously to samples on the first day of labeling. Next, embryos were washed 5 x 1 h in PBSTr, incubated overnight in PI Buffer (1x PBT, 2% sheep serum, 2 mg/mL BSA) with goat anti-mouse Alexa 488 antibody. Next, embryos were washed 4 x 20 min with PBSTr, 3x 5 min in Fast Red Buffer (0.1 M Tris pH 8.2, 0.4 M NaCl, 0.1% Tween-20), and developed in Fast Red Substrate (1 mL Fast Red Buffer + 1 Fast Red TR/Napthol AS-MX tablet [4-Chloro-2-methylbenzenediazonium/3-Hydroxy-2-napthoic acid 2,4-dimethylanilide phosphate; Sigma F4648]).

TUNEL labeling

4 d embryos were fixed and permeabilized as for in situ hybridization including Proteinase K treatment and 5 x 5 min washes in PBT. Next, the ApopTag Plus Fluorescein in situ Apoptosis Detection Kit (Chemicon) was utilized as follows. Embryos were immersed in 150 uL Equilibrium Buffer (EB) for 10 min at room temperature. EB was removed at 50 uL Terminal Deoxynucleotidyl Transferase (TdT) was added (77 uL Reaction Buffer + 33 uL TdT enzyme) and incubated overnight. The reaction was stopped with Stop Buffer (1 mL Stop/Wash Buffer + 34 mL ddH20), then embryos were blocked in PI Buffer for 1 h at RT, followed by overnight incubation at 4 °C in POD conjugated anti-DIG antibody (Roche) diluted 1:1000 in PI Buffer. Embryos were then washed 4 x 10 min in MABT (5 mL 1M Maleic Acid pH 7.5, 1.5 mL 5M NaCl, 500 uL 10% Tween-20, 43 mL ddH20). For color precipitation, embryos were incubated for 30 min at RT in TSA-Alexa 555, diluted 1:1000 in PBS.

Quantification of neurons

To quantify the number of neurons in the medial and lateral dorsal habenulae, embryos were labeled with Kctd12.1, Kctd12.2, or HuC/D antibodies and co-stained with ToPro3 nuclear dye. Using a Zeiss LSM510 Meta upright confocal microscope, 1 μm optical slices were obtained through the dorsal diencephalon, starting dorsally at the pineal organ and continuing ventrally through Kctd12 expression in the habenulae. The number of Kctd12+ neurons in either habenula was counted manually in each slice, using ToPro3 expression to

distinguish individual nuclei within the field. This allowed the separation of neurons with large dendritic fields or with large soma filling several optical sections. Two criteria were used to qualify as Kctd12+: 1) the fluorescent signal must be present throughout the entire cytoplasm and surround the nucleus. 2) The intensity of Kctd expression must measure 100 arbitrary units or higher (out of 4096) using the Quantification tool in Volocity software (Improvision). Differences between mutant and sibling embryos were calculated using a Student's T-Test. A measure of asymmetry was generated using an asymmetry index (AI), calculated as the difference between the left and right medial or lateral subnucleus divided by the total number of neurons: [AI = (#L - #R) / (#L + #R)]. An AI score between 0 and 1 indicates the left subnucleus contains more neurons and a value between -1 and 0 indicates a larger right subnucleus (Roussigne et al., 2009).

For quantification or cerebellar neurons, we captured confocal Z-stack images of whole larval brains labeled with HuC/D antibody at 72 hpf. The area quantified was anteriorly bounded by the optic tectum (TeO) and posteriorly bounded by the medulla (MO). The medial boundaries were defined by the most medial HuC+ cell on either the left or right side. Lateral boundaries were confined to 80 µm away from the medial boundaries to control for the variability in roof plate width. The dorsal boundaries were confined by the dorsal-most HuC/D+ neuron on either the left or right side of the embryo, and the ventral boundary was 5 µm below the dorsal boundary.

To quantify spinal cord neurons, embryos were labeled with antibodies against HuC/D and acetylated alpha-tubulin. Tails were removed and mounted laterally, and imaged at the level of the posterior border of the yolk sac (1 µm optical sections in confocal Z-stacks). Neurons were counted in a given hemisegment, and Rohon-Beard neurons were quantified separately, as distinguished by the latter's large soma and location at the dorsal-most position in the spinal cord (Park et al., 2000; Roberts and Appel, 2009).

Electron microscopy

Larvae at 54 hpf were fixed in 2.5% gluteraldehyde and post-fixed in 1% osmium tetroxide. They were then stained en bloc with 0.5% uranyl acetate. Samples were next dehydrated in an ethanol series and embedded in epoxy resin. Samples were then sectioned with a Recheirt ultramicrotome, stained with lead citrate and then imaged on an FEI Techai 12 transmission electron microscope.

Results

Enlarged lateral subnucleus of the dorsal habenula in *c163* mutants

A forward ENU mutagenesis screen generated mutants with altered expression of the *kctd12.1* gene in zebrafish. One such mutation, *c163*, caused symmetric expression of *kctd12.1* in the lateral subnuclei (LsDh) at early larval stages. In wild-type embryos, Kctd12.1 protein is expressed in approximately

three times as many cells in the left habenula as the right (Figure 4A). Kctd12.1 expression is more extensive in *c163* mutants, with particular expansion in the right habenula (Figure 4A'). An examination of habenular anatomy via ToPro3 nuclear expression reveals a morphological change in *c163* larvae, signifying a considerable expansion of the right LsDh along with an expansion of the soma-free core of the right LsDh (Figure 4B).

The *c163* mutation also has a profound effect on the development of the medial subnuclei (MsDh). In wild-type, larvae develop bilateral MsDh with the opposite directionality to the LsDh, such that the MsDh in the right habenula is larger (dashed line in Figure 4B') and contains more Kctd12.2 neurons (Figure 4C). In *c163* larvae the MsDh are bilaterally reduced and remaining cells occupy the lateral edges of the habenulae (Figure 4C'). In addition, in *c163* mutants the relatively few Kctd12.2+ neurons are found in small clusters or exist as individual cells. In wild-type, Kctd12+ neurons organize into a single coherent nucleus.

Neurons from the dorsal habenula project efferent processes that terminate in the interpeduncular nucleus (IPN), traveling through the dorsal diencephalon to the midbrain by way of the fasciculus retroflexus (FR)(Sutherland, 1982). In zebrafish, neurons from the left Dh innervate both dorsal and ventral regions of the IPN, whereas right Dh axons only innervate the ventral IPN (Agetsuma et al., 2010; Gamse et al., 2005; Kuan et al., 2007a). The axon guidance gene (semaphorin receptor) *neuropilin1a* (*nrp1a*) is expressed in the left Dh of wild-type larvae, and largely excluded from the right Dh (Figure 4D). Morpholino depletion of Nrp1a protein production disrupts targeting of left Dh
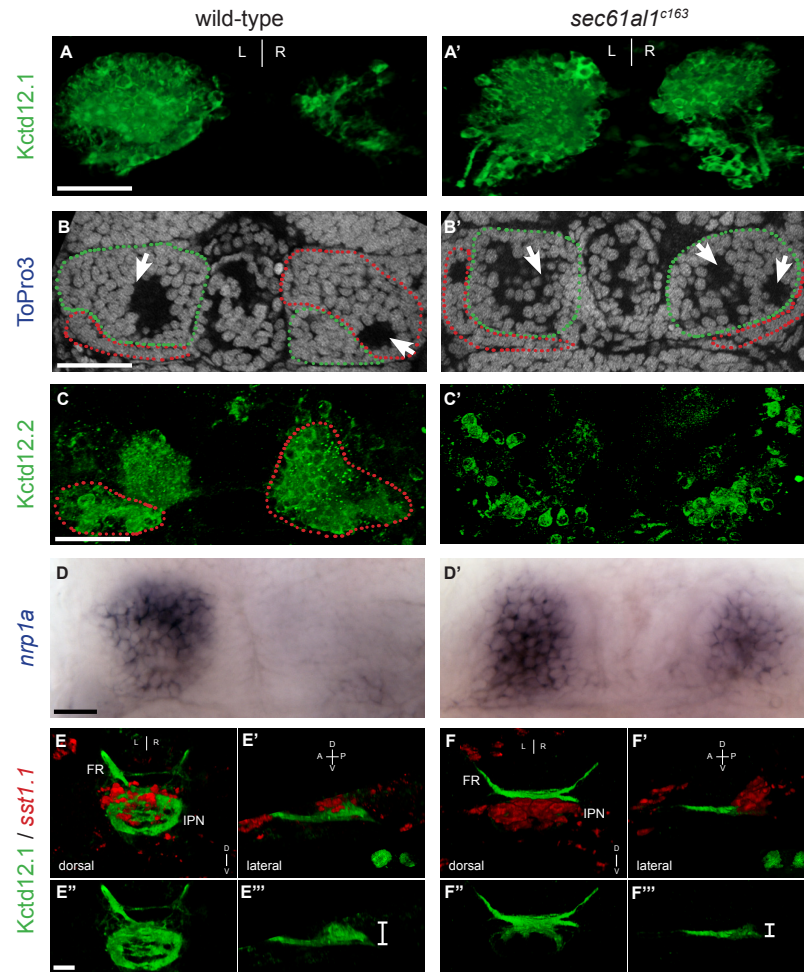
Figure 4. The lateral subnuclei of the dorsal habenulae are enlarged in *sec61al1^{c163}* mutants. (A) Kctd12.1 protein is detected in more cells of the left LsDh of the dorsal habenula than the right. (A') By contrast, *sec61al1^{c163}* mutants exhibit more Kctd12.1 neurons in both habenulae, particularly the right. (B) In wild-type larvae, the LsDh (green dashed line) includes a large, round soma-free area on the left but a smaller soma-free area on the right (white arrows). (B') In *sec61al1^{c163}* mutants, both the left and right habenula contain large cell-free areas. (C) In wild-type larvae, neurons of the MsDh express Kctd12.2, and are more abundant in the right dorsal habenula than the left. (C') In the dorsal habenulae of *sec61al1^{c163}* mutants, the number of cells expressing Kctd12.2 is reduced. (D) *nrp1a* is expressed in a lateral portion of the LsDh of wild type embryos. (E–E''') Axons from neurons expressing Kctd12.1 (green) target neurons of the dorsal and ventral IPN, which express *somatostatin1.1* (*sst1.1*; red in E,E') in WT embryos. (F–F''') In *sec61al1^{c163}* mutants, Kctd12.1-expressing projections are confined to the ventral domain of the IPN (white bracket: F'''). All images are dorsal views at 4 dpf, except E', E''',F' and F''', which are lateral views. FR: fasciculus retroflexus. IPN: interpeduncular nucleus. Scale bars: (A–C = 30 µm; D = 10 µm; E'' = 20 µm).

neurons in the dorsal IPN (Kuan et al., 2007b). In *c163* mutants, *nrp1a* transcript is ectopically present in the right Dh (Figure 4D'). We anticipated that increased *nrp1a* expression in the right Dh of *c163* would correlate with increased bilateral dorsal IPN innervation by Dh neurons, but in fact found the opposite. Wild-type Dh Kctd12.1+ neurons project efferents that cross the midline multiple times, in turn innervating both ventral and dorsal IPN domains, as marked by expression of *somatostatin1.1* (Figure 4E). In *c163* mutants, Kctd12.1+ neurons display reduced midline crossing and innervate only the ventral IPN (Figure 4E'). Thus despite the ectopic expression of the *nrp1a* axon guidance receptor in the right habenula, *c163* mutants project axons that innervate the IPN in a pattern similar to wild-type right habenula neurons.

Altered distribution of habenular neurons in the lateral and medial subnuclei in *c163* mutants

To precisely describe the changes in habenular subnuclei morphology in *c163* mutants, we counted the number of cells expressing Kctd12.1 in the lateral subnucleus and Kctd12.2 in the medial subnucleus. We used these data to create an asymmetry index (AI; see Materials and Methods) to reflect the degree of difference between subnuclei in the left and right habenulae. At 48 hours post fertilization (hpf), Dh neurons have already begun to elaborate dendrites and axons (Concha et al., 2003; Kuan et al., 2007b). Subnuclear Dh asymmetry is already evident in wild-type embryos at this stage (Figure 5A,B,C)($AI^{lateral} = 0.36$; $AI^{medial} = -0.13$), but *c163* embryos show reduced Dh subnuclear asymmetry

Figure 5. Kctd12.1 expression is significantly expanded and Kctd12.2 expression significantly decreased throughout larval development in *sec61al1^{c163}* mutants. (A, B, C) In wild-type larvae at 48 hpf, there are 2.1 times as many Kctd12.1-expressing neurons (green) in the left LsDh of the dorsal habenula as in the right. In the MsDh, there are 1.3 times as many Kctd12.2- expressing neurons (red) in the right side as the left. (A', B', C') In *sec61al1^{c163}* mutants, more Kctd12.1+ and fewer Kctd12.2+ neurons are found in the right habenula. (D–F') At 72 hpf, a similar situation to 48 hpf is observed. Images are 3D reconstructions of 50 µm-thick confocal Z-stacks through the epithalamus. Scale bars represent 10 µm. Significance determined by Student's T-test (*p<0.05, **p<0.01); n=6. Insets in A–B', D–E' show ToPro3 labeling in a single confocal section of the Z-stack.

(Figure 5A',B',C')(AI^{lateral} = 0.21; AI^{medial} = 0.04). *c163* mutants have a significant increase in Kctd12.1 neurons in both habenulae (p<0.05) and fewer Kctd12.2 neurons in the right habenula as compared to siblings (p<0.01; unpaired two-tailed T-tests). At 72 hpf, wild-type embryos have even more pronounced asymmetry (Figure 5D,E,F; AI^{lateral} = 0.51; AI^{medial} = -0.35), whereas the lateral and medial Dh are nearly symmetrical in *c163* mutants (Figure 5D',E',F'; AI^{lateral} = 0.16; AI^{medial} = -0.20). In total, *c163* embryos generate ~47 extra Kctd12+ neurons as compared to controls (MsDh + LsDh). The most dramatic difference is seen in the right LsDh, in which *c163* larvae form nearly twice the number of Kctd12.1+ neurons as siblings (Figure 5F,F').

The *c163* dorsal habenula phenotype is independent of the parapineal organ

In wild-type zebrafish, the left-positioned parapineal organ influences the relative size of the left habenular subnuclei. Parapineal ablation leads to larvae with reduced left LsDh and an enlarged left MsDh. In contrast, when the parapineal is reversed (right-sided), the right LsDh is larger and the right MsDh is smaller (Concha et al., 2000; Gamse et al., 2005; Gamse et al., 2003). Since *c163* mutants display an expansion of *kctd12.1* expression in the right habenula, we examined the possibility that mutants possess a second parapineal in the right hemisphere. However, the enlarged right LsDh in *c163* is not the result of a duplicated or enlarged parapineal: mutants possess a single parapineal, marked
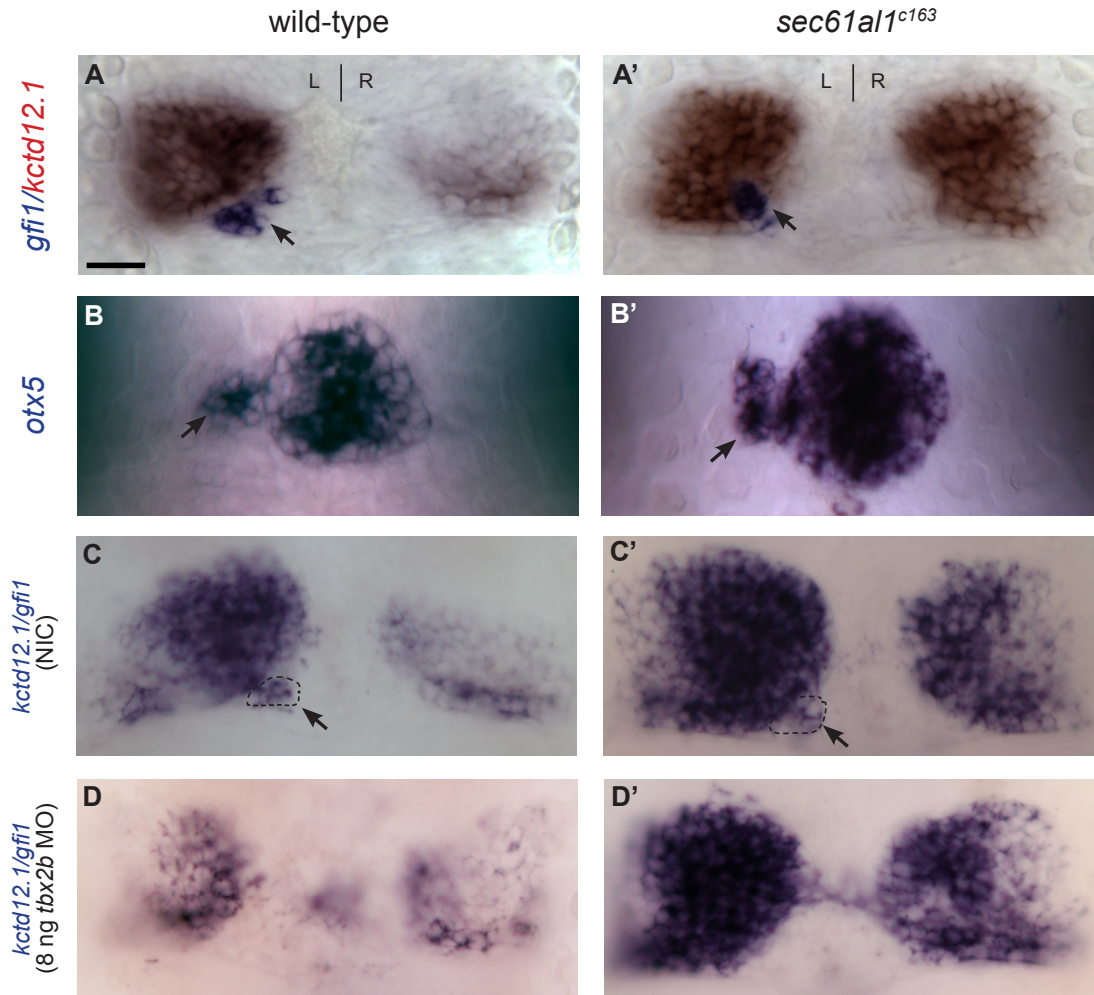
Figure 6. The enlarged LsDh phenotype of *sec61al1^{c163}* is independent of the parapineal organ. (A) In wild-type larvae, the parapineal organ (*gfi-1*, blue) is found adjacent to the left LsDh (*kctd12.1*, red). (A') Likewise, *sec61al1^{c163}* mutants possess a single parapineal organ on the left side of the brain. (B) The pineal complex (consisting of the pineal and parapineal, labeled by *otx5*) is similar in WT and (B') *sec61al1^{c163}* mutant larvae. (C) Compared to an non-injected control (NIC), with a parapineal organ on the left side of the brain (dashed oval), (D) disruption of parapineal organ formation using a *tbx2b* antisense morpholino causes a reduction in the size of the left LsDh (*kctd12.1*). (C', D') However, in *sec61al1^{c163}* mutants, reduction of the parapineal organ has no effect on the size of the LsDh on either the left or right side. All views are dorsal. Panels A, C, D = 96 hpf; B = 72 hpf. Parapineal indicated by black arrowheads A–C'. Scale bar = 10 μm.

by expression of *gfi-1*, closely abutting the left habenula as in wild-type (Figure 6A-B').

To examine whether the enlarged right LsDh phenotype is dependent on the parapineal organ, we prevented parapineal formation by injecting morpholino to deplete the T-box transcription factor *tbx2b* (Snelson et al., 2008). Tbx2b depletion in embryos wild-type for *c163* led to a great reduction of parapineal cells, with the few remaining *gfi*-1+ cells scattered at the midline. The left LsDh is reduced in size (Figure 6D) and resembles the right LsDh of untreated wild-type embryos (Figure 6C). In contrast, *c163* larvae with Tbx2b depletion lack parapineal but possess LsDh that are similar to untreated *c163* mutants (Figures 6C',D'). Importantly, this result demonstrates that a left LsDh develops in *c163* larvae despite the lack of a parapineal. This indicates that the formation of a large LsDh in each hemisphere occurs independently of parapineal influence and that the *c163* habenular phenotype is not specific to the right side of the brain.

c163 represents a nonsense mutation in *sec61a-like-1*

The *c163* mutation shows full penetrance and recessive heritability (182/728; 25.0%). The mutation is embryonic lethal by 5 days post fertilization (dpf). Homozygous mutants are shorter than siblings, a phenotype evident at 36 hpf. By 56 hpf, *c163* mutants exhibit a dorsally curved axis, have smaller cartilaginous jaw elements, and smaller eyes as compared to wild-type (Figure 7B).
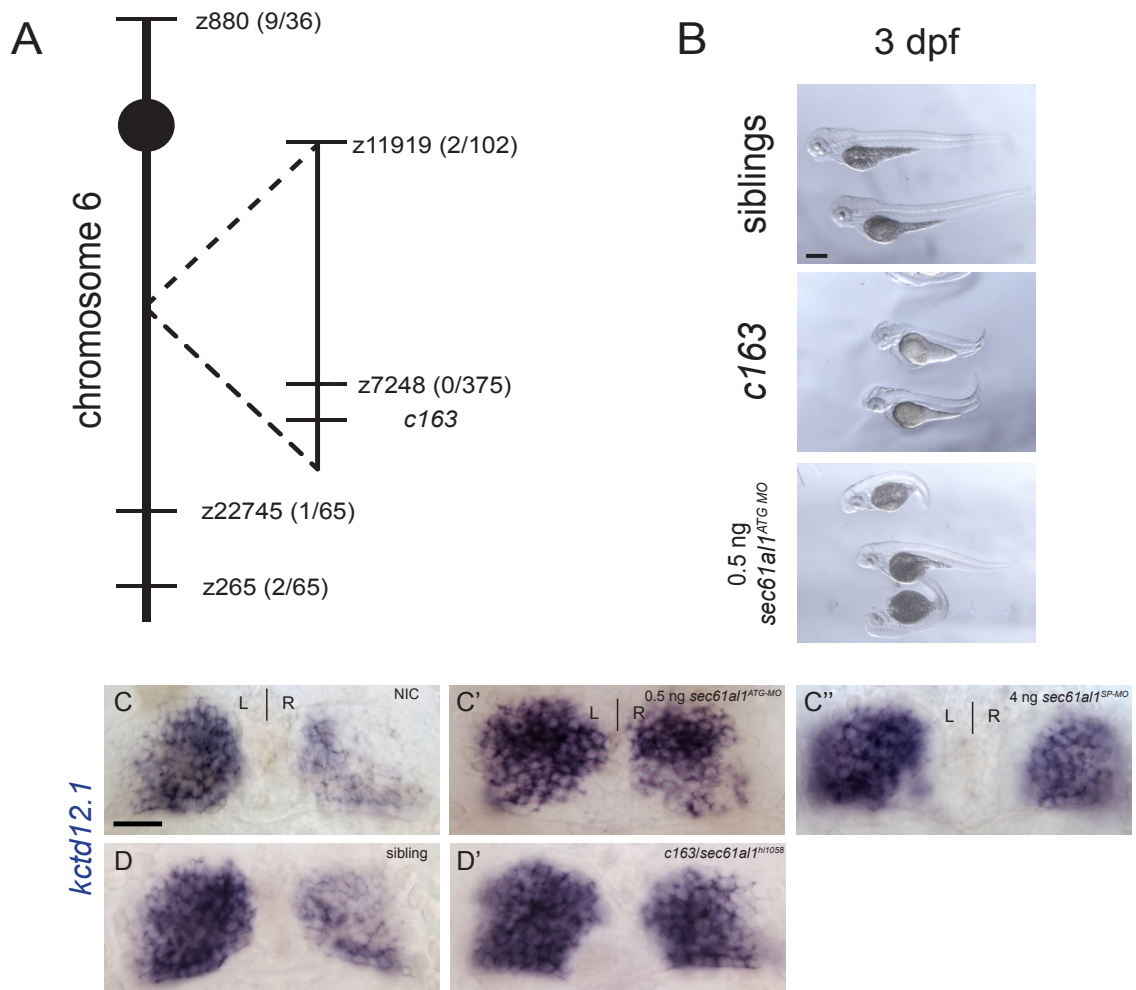
Figure 7. The *c163* lesion is a nonsense mutation in *sec61al1*. (A) Linkage to microsatellite markers were used to map *c163* close to z7248, near the *sec61al1* locus. (B) *c163* mutants are characterized by a reduction in jaw and head volume, and a short, dorsally curved axis. (C) Compared to a non-injected control, (C') treatment with a morpholino complementary to the start site or (C'') to a splice acceptor site in the *sec61al1* transcript results in excess *kctd12.1*-expressing neurons in the right habenula. (D, D') The retroviral insertion mutant, *sec61al1*[hi1058] fails to complement *c163*. Transheterozygotes for *hi1058* and *c163* have increased numbers of *kctd12.1*+ cells in the dorsal habenulae. Scale bars: B-D' = 20 µm.

Using microsatellite linkage mapping in a WIK/AB hybrid strain, the *c163* mutation was positioned close to the *sec61a-like-1* (*sec61al1*) locus. This gene encodes a major pore-forming subunit of the eukaryotic endoplasmic reticulum (ER) translocon channel (Figure 7A). Sec61al1 mediates polypeptide trafficking across the ER membrane as well as introduction of nascent transmembrane proteins into the ER membrane (Rapoport, 2007). cDNA isolated from *c163* mutants revealed a premature stop codon in exon 6, which encodes a portion of the 4th transmembrane domain of the alpha subunit. This premature stop codon is predicted to truncate more than half of the protein, including 6 of 10 transmembrane domains (Van den Berg et al., 2004) as well as the L6 and L8 cytosolic loops mediating ribosomal interaction (Raden et al., 2000). We therefore conclude that the *c163* mutation produces a non-functional Sec61 alpha subunit.

We confirmed the *sec61al1* locus by two methods. First, *sec61al1*[c163] failed to complement a previously identified retroviral insertion mutation, *sec61al1*[hi1058Tg] (Golling et al., 2002)(Figures 7D,D'). Second, two different antisense morpholino oligonucleotides targeting the *sec61al1* transcript caused enlargement of the right LsDh, similar to the phenotype observed in *c163* homozygous larvae (Figures 7C',C'').

Since *sec61al1* mediates the trafficking of a variety of transmembrane and secreted proteins through the ER, we expected to see a reduction in ER volume and reduced extracellular matrix (ECM) in *sec61al1*[c163] mutants. Chondrocytes are a highly secretory cell type of the developing jaw. Chondrocytic nuclei are

| wild-type | *sec61al1*[c163] |
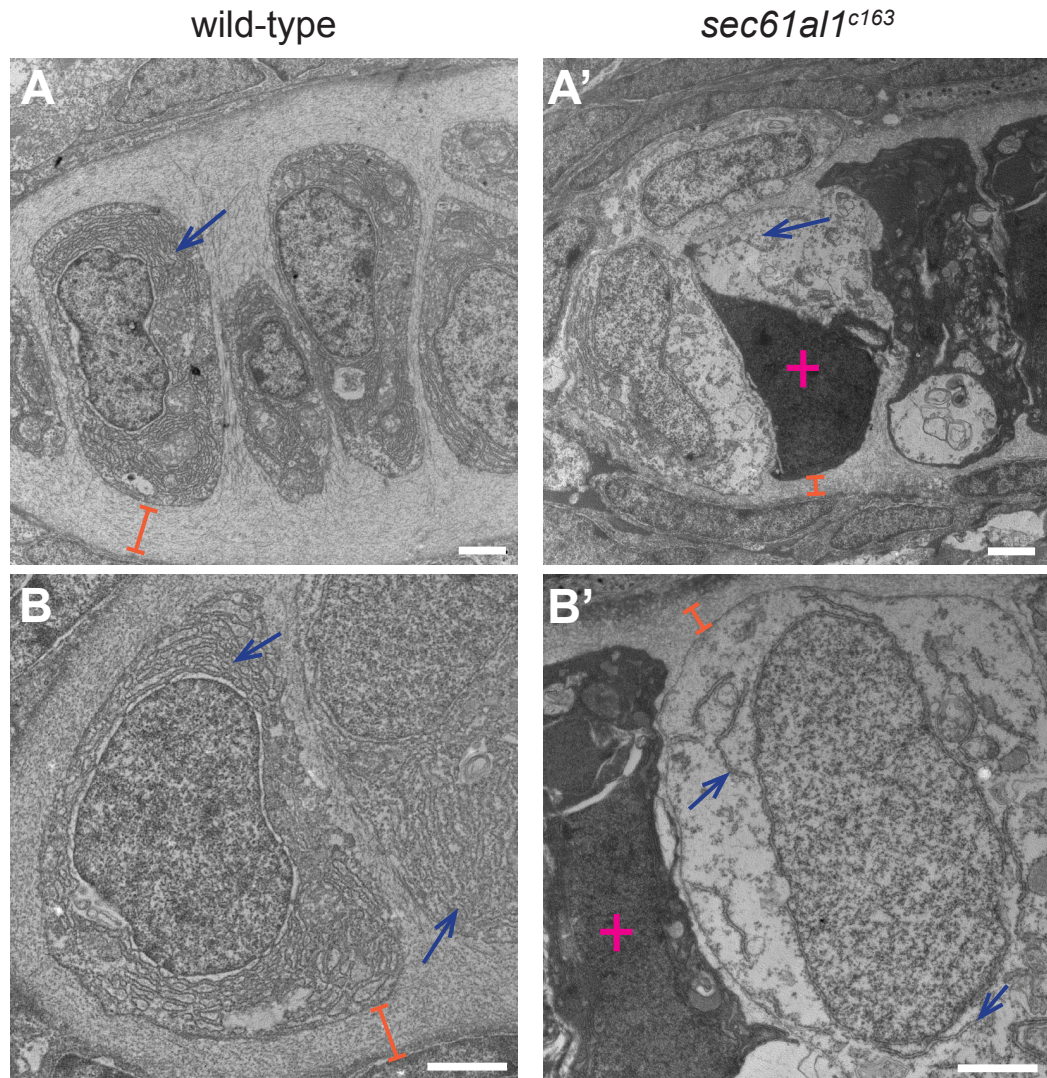
Figure 8. Transmission electron micrographs of jaw chondrocytes document endoplasmic reticulum (ER) and extracellular matrix (ECM) deficits in *sec61al1*[c163] mutants. (A, B) Chondrocytes of wild-type controls have dense ER throughout the cytoplasm (blue arrows) and extensive ECM surrounding chondrocytes (orange brackets). (A', B') Endoplasmic reticuli are sparse and discontinuous in *sec61al1*[c163] mutants and the ECM is reduced in thickness. Dead cells are common in *sec61al1*[c163] mutant micrographs (pink cross). All scale bars = 2 µm.

surrounded by an extensive network of ER, and are enmeshed in an ECM that is easily visible in electron micrographs of wild-type larvae (Figures 8A,B)(Lang et al., 2006). The chondrocytes of *sec61al1^{c163}* mutants have dramatically reduced ER volume and sparse ECM (Figures 8A',B'). These results are consistent with impairment of the exocytic pathway in *sec61al1^{c163}* mutants.

sec61al1 transcript is maternally provided (Figure 9A). At later stages, expression is extensive in the embryo (Figure 9B), with increased expression in highly secretory tissues such as the exocrine pancreas and jaw chondrocytes (Figure 9C). In addition, expression is increased in the anterior hindbrain (8C, red arrow), but found at a lower abundance in the remainder of the brain.

Nodal expression is unaffected in *sec61al1^{c163}* mutants

In the larval zebrafish Nodal signaling spurs initiation of neurogenesis in the left dorsal habenula prior to the right (Roussigne et al., 2009). Expression of *southpaw/nodal-related 3* (*spaw/ndr3*) in the lateral plate mesoderm is the first molecular evidence of L/R asymmetry in the zebrafish embryo. This expression is a prerequisite for expression of Nodal genes in the pineal complex, including *lefty1* (Long 2003). Expression of *spaw* is confined to the left LPM in *sec61al1^{ATG-MO}* morphants at 22 hpf, similar to non-injected control embryos (NIC)(Figures 10A,A'). In addition, expression of the Nodal-responsive gene *lefty1* is confined to the left half of the epithalamus at 25 hpf in both morphants and controls (Figures 10B,B'). Therefore, depletion of Sec61al1 does not alter asymmetric expression of Nodal pathway genes during early development.

Figure 9. *sec61al1* is maternally provided and extensively expressed in the embryo and larva. (A) Maternally provided *sec61al1* mRNA (purple) in the blastoderm at 4 hpf. (B) Extensive expression of *sec61al1* at 22 hpf, throughout the head and trunk. (C) By 72 hpf, *sec61al1* transcript is expressed throughout the head, and more highly expressed in the jaw (blue arrow), midbrain/hindbrain boundary (red arrow), and exocrine pancreas (pink arrow). Scale bars = 10 μm.
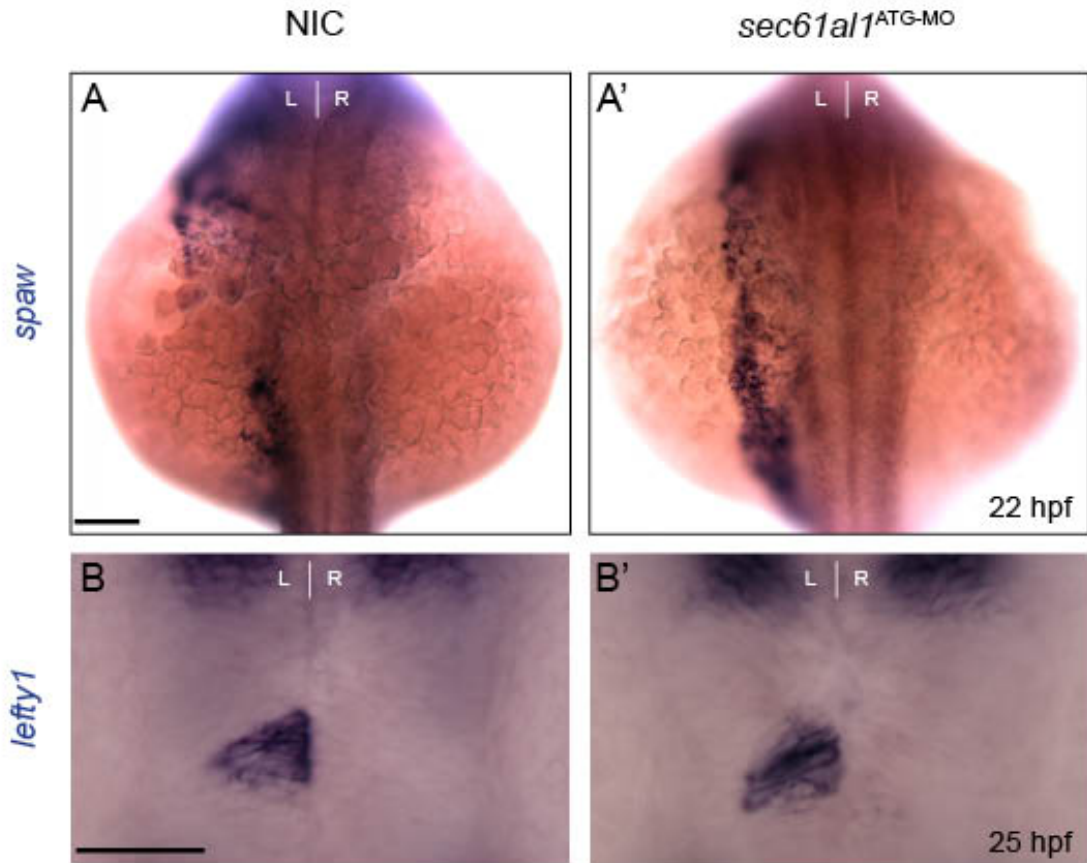
Figure 10. Depletion of *sec61al1* does not affect expression of Nodal pathway genes in the left lateral plate mesoderm and epithalamus. (A) *southpaw* (*spaw*) is expressed in the left lateral plate mesoderm at 22 hpf in non-injected controls (NIC) (A') as well as in *sec61al1* morphants injected with 500 pg *sec61al1*[ATG-MO] (morphant: 15/16 left- side, 1/16 bilateral versus NIC: 9/11 left-side, 2/11 bilateral). (B) *lefty1* expression is confined to the left side of the epithalamus at 25 hpf in NIC and (B') *sec61al1* morphants (NIC: 19/22 left-sided, 3/22 absent; morphant: 27/29 left-sided, 2/29 absent). All views are dorsal. Scale bar = 10 µm.

The *sec61al1^{c163}* mutation increases habenular neurogenesis

The alterations in the size of the habenular subnuclei in *sec61al1^{c163}* mutants suggest an alteration in epithalamic neurogenesis. We hypothesized that excess Dh neurons could arise through two mechanisms. The first possibility is that mutant habenular progenitor cells undergo neurogenesis at a faster rate than siblings, thereby producing excess habenular neurons. This can be tested by examining the production of neurons over a given time scale. Secondly, excess neurons could result from decreased apoptosis, i.e. neurons that are programmed to die in wild-type embryos survive in mutant embryos (See Figure 13).

We examined the first possibility by examining expression of HuC and D, neuron-specific RNA binding proteins, which are expressed in neural precursors after they exit the cell cycle (Marusich et al., 1994). We used expression of HuC/D in *sec61al1^{c163}* and siblings across several developmental time points to provide temporal clues as to when neurogenesis is disrupted. At both 40 and 48 hpf, *sec61al1^{c163}* mutants possess similar numbers of HuC/D^{+} neurons as compared to controls (p^{RHb} = 0.19; unpaired two-tailed *T*-test)(Figures 11A",B"). However, by 56 hpf, these mutants have a significant increase in RHb neurons as compared to wild-type, indicating an excess of neurogenesis relative to wild-type between 48 and 56 hpf (Figure 11C").

Increased neurogenesis was also notable in the left habenula of *sec61al1^{c163}* mutants and is notable prior to the defects seen in the right
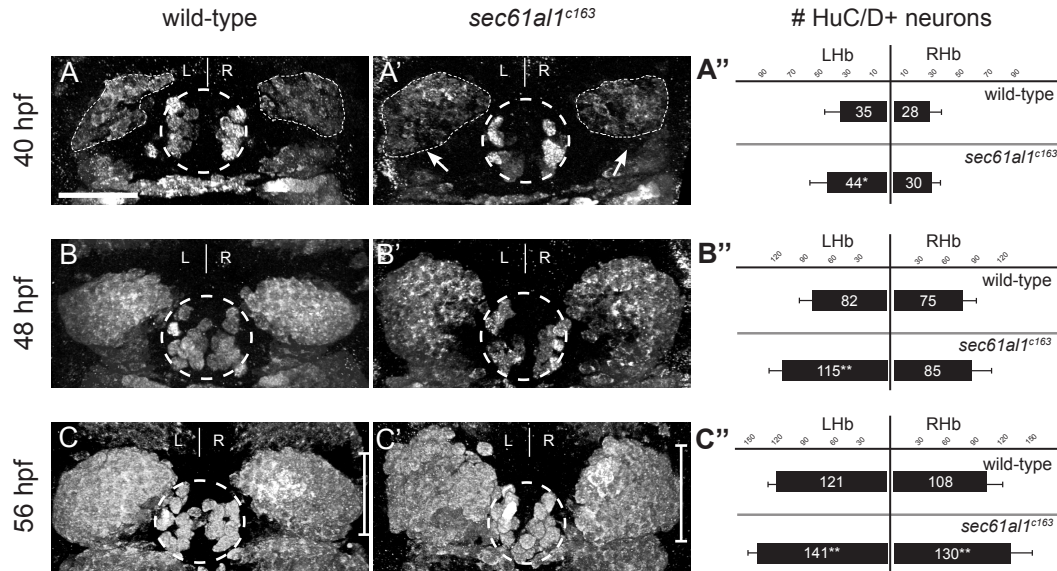
Fig. 11. Excess habenular neurons form in *sec61al1^{c163}* mutant habenulae. (A–C') Post-mitotic neurons in wild-type or *sec61al1^{c163}* mutant embryos as detected by HuC/D antibody labeling. (A) A representative wild-type embryo has fewer HuC/D+ habenular neurons at 40 hpf as compared to (A') a *sec61al1^{c163}* mutant. (A") Quantification of data at 40 hpf. The number of left habenula neurons was significantly increased in homozygous mutants compared to wild-type siblings. (B–B") At 48 hpf, significantly more neurons were detected in the left habenula of mutants than in wild-type controls. (C–C") By 56 hpf, both the left and right habenulae of mutants contain more neurons than controls. In all panels, the pineal organ is outlined by a dashed circle. Scale bar = 30 μm. Significance determined by Student's T-Test (*p < 0.05, **p < 0.01); 40 hpf (n = 12), 48 hpf (n = 9), 56 hpf (n = 12). Images are extended focus projections of confocal Z-stacks through the dorsal diencephalon.

hemisphere. At 40 hpf, mutants have roughly 9 more HuC/D$^+$ cells in the left habenula, as compared to controls (Figure 11A"; p^{LHb} = 0.03). At 48 hpf, this imbalance increases to roughly 33 more HuC/D$^+$ cells (Figure 11B"; p^{LHb} = 0.00002). This imbalance is less severe at 56 hpf, with only 20 more neurons in mutant RHb as compared to siblings (p^{LHb} = 0.02)(Figure 11C").

Prolonged production of LsDh neurons in the right habenula of *sec61al1^{c163}* mutants

To further characterize the neurogenic program in *sec61al1^{c163}* mutants we used a proliferation assay to indicate when neurons of the lateral subnucleus are born. Neurogenesis peaks in the LsDh around 32 hpf in wild-type embryos (Aizawa et al., 2007). In *sec61al1^{c163}* mutants, most of the Kctd12.1+ neurons of the LsDh appear after 48 hpf (roughly 100 Kctd12.1+ neurons appear between48 and 72 hpf, Figures 5C',F'). We therefore tested whether *sec61al1^{c163}* mutants generate Kctd12.1+ neurons in the LsDh for a longer period of time than wild-type with a BrdU incorporation assay. Neurons are post-mitotic, therefore cells that retain substantial expression of BrdU along with the mature habenular marker Kctd12.1 at 96 hpf represent neurons that underwent their final mitotic division at the time of the initial BrdU pulse. Neurons that lack substantial BrdU expression were either born before or after the BrdU pulse, or underwent additional mitoses following the pulse, thereby diluting the BrdU label.

Embryos were pulsed with BrdU at 32 or 48 hpf, followed by a chase without BrdU until 96 hpf, at which point they were fixed and immunolabeled for

Kctd12.1 and BrdU. We found that roughly 7 more Kctd12.1-expressing neurons are born on the right side of *sec61al1*[c163] mutant embryos at 32 hpf (Figures 12B-B''') compared to wild-type siblings (Figures 12A-A'''). There is a small and non-significant increase in Kctd12.1$^+$ neurons born at 32 hpf (p^{right} = 0.0002; p^{left} = 0.14, nonpaired two-tailed *T*-test, n = 41). A similar trend is seen at 48 hpf, as roughly 7 more Kctd12.1$^+$ neurons are born on the right side of the brain as compared to siblings (Figures 12A''',B'''; p^{right} = 0.023, n = 5). These data indicate increased generation of Kctd12.1$^+$ neurons at 32 and 48 hpf on the right side of the brain.

The cell proliferation data suggest an increase in cell division of habenular progenitor cells in *sec61al1*[c163] mutant embryos. It is also possible that more precursor cells differentiate in mutants than in wild-type. If differentiation were enhanced in mutants we would note a depletion of precursor cells in the epithalamus. Therefore we examined expression of *chemokine receptor 4b* (*cxcr4b*), which is expressed in habenular precursor cells (Roussigne et al., 2009). At 46 hpf *sec61al1*[c163] mutants have similar numbers of cells expressing *cxcr4b* in the habenulae (Figure 13D), indicating that habenular precursors are not depleted by loss of Sec61al1.

The loss of Sec61al1 affects the rate of neuronal production in the dorsal habenula, a process that could also be affected by the rate of cell death. Therefore we examined apoptosis using TUNEL assays. Surprisingly we found an increase in apoptosis in *sec61al1*[c163] mutants. This increase was evident in a variety of tissues, including the retina, tail (data not shown), and diencephalon
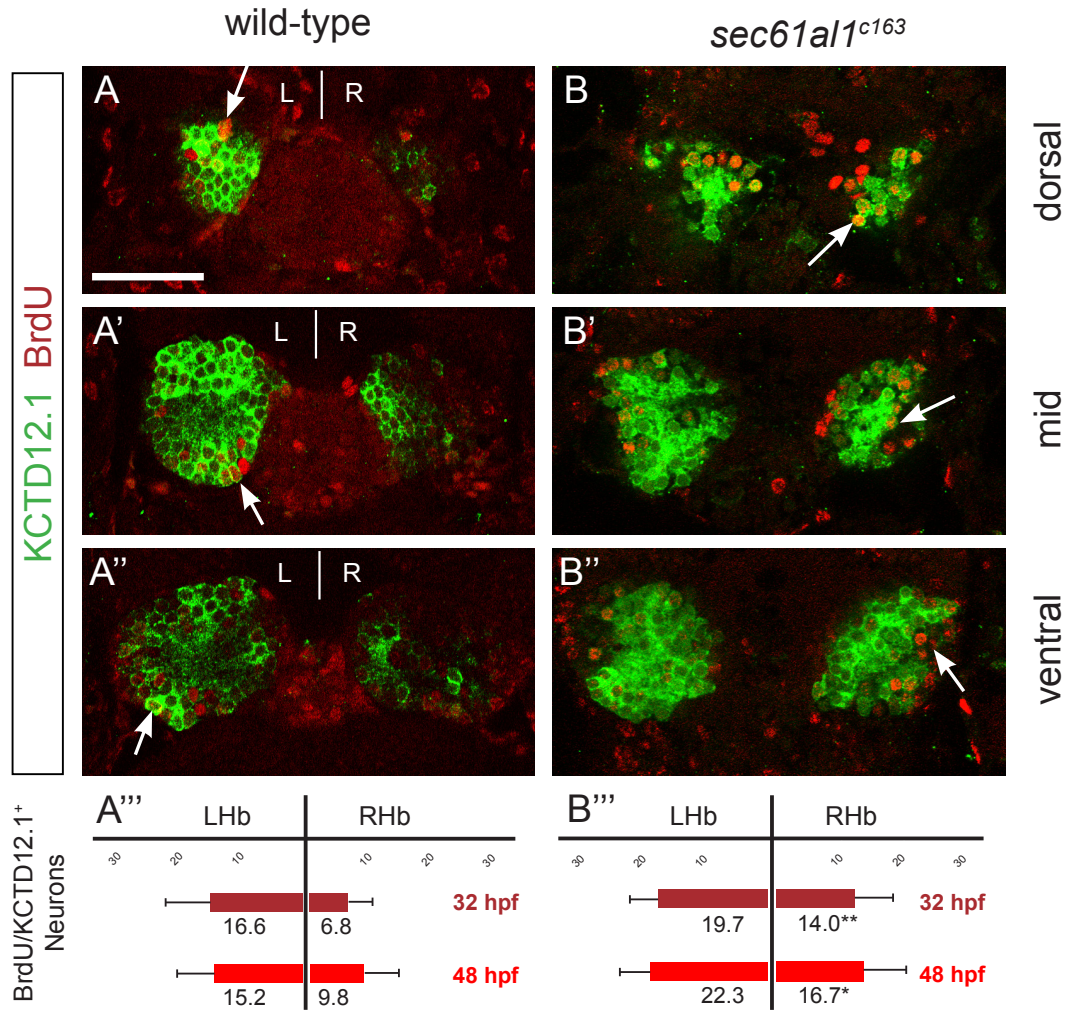
Figure 12. Increased cell division of LsDh progenitors in *sec61al1^c163* mutants. Embryos were briefly pulsed with BrdU at 32 hpf and chased until 4 dpf, when they were labeled for Kctd12.1 (green) and BrdU (red). As neurons are post-mitotic, brightly labeled BrdU+ cells are those that underwent a final mitosis during the BrdU pulse (white arrows); see text for further explanation of the labeling strategy. (A–A''') Compared to wild-type controls, (B–B''') significantly more neurons are born in the RHb of *sec61al1^c163* mutants at 32 hpf. This trend continues through 48 hpf (A''',B'''), as again there are significantly more neurons in the RHb of *sec61al1^c163* mutants (images not shown). Images are single z-plane images from confocal z-stacks. Dorsal (A,B), mid (A',B'), and ventral (A'',B'') sections are shown. Scale bar represents 30 μm. Significance determined by Student's T-test (*p<0.05; **p<0.01); n=41.
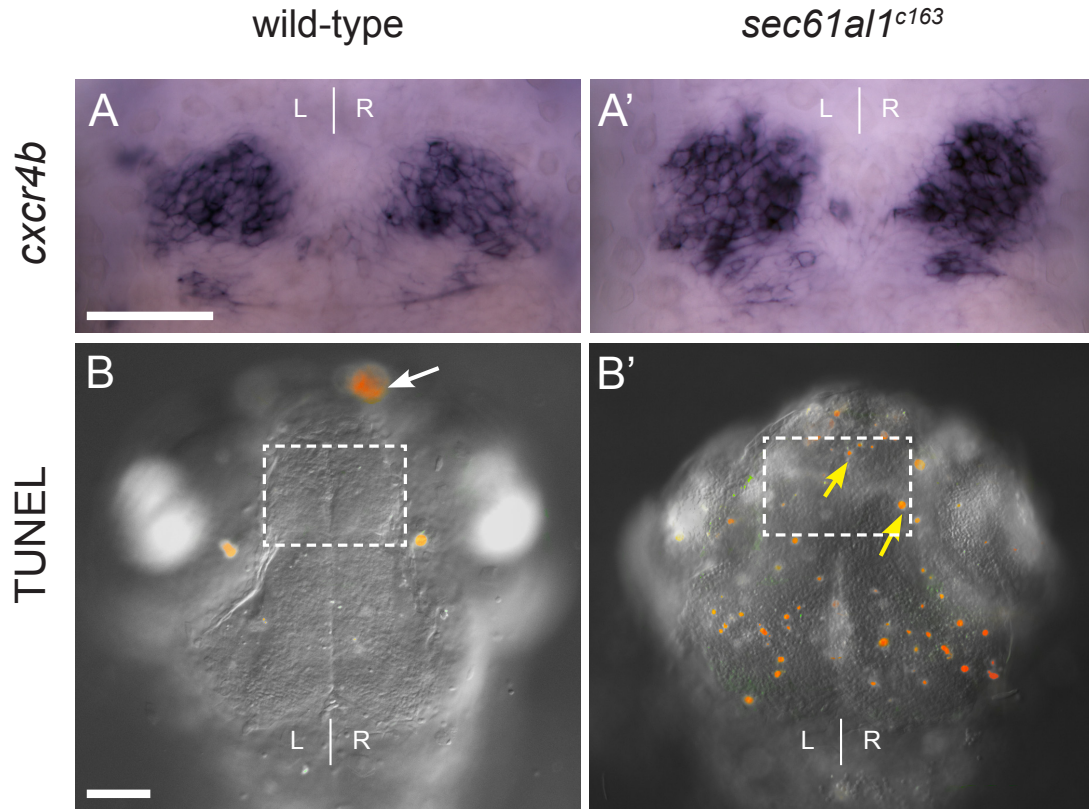
Figure 13. In the dorsal diencephalon of *sec61al1*[c163] mutant embryos, habenular precursor cells are retained and apoptosis is increased. (A) The number of habenular precursor cells expressing *cxcr4b* in wild-type embryos at 46 hpf (A') is similar to *sec61al1*[c163] mutants. (B) Apoptotic cells are rare in the dorsal diencephalon of wild-type embryos at 72 hpf (dorsal diencephalon in white bracket: 1.8 TUNEL^{+} cells per wild type diencephalon, n=4). The majority of apoptotic cells in wild-type heads are found in the olfactory placodes (white arrowhead). (B') Many apoptotic cells are detected in the dorsal diencephalon of *sec61al1*[c163] mutants (7.5 TUNEL^{+} cells per mutant diencephalon, n=4). Dorsal views, scale bars = 30 µm.

(Figure 13B'). More specifically, wild-type embryos had 1.8 TUNEL$^+$ cells in the diencephalon, as compared to 7.5 TUNEL+ cells in *sec61al1^{c163}* mutants (p<0.01; n=4).

Altered neurogenesis in *sec61al1^{c163}* mutants is not limited to the habenulae

Thus far we have characterized alterations in the development of the neurocranium and the dorsal diencephalon, but it is quite possible that the *sec61al1^{c163}* mutation affects other developmental programs. To investigate other regions of the nervous system, we looked at neuronal populations in the cerebellar plate and the spinal cord. The cerebellar plate is a symmetric paired structure in the zebrafish hindbrain that undergoes neurogenesis at roughly the same time as the habenular nuclei (Mueller and Wullimann, 2005). We counted the number of HuC/D+ neurons in the superficial layers of the developing cerebellar plate in *sec61al1^{c163}* mutants and their wild-type siblings. In wild-type, we find an average of 50 neurons in the dorsal-most 5 µm region of both the left and right cerebellar plate at 72 hpf (Figure 14A,B,C). In contrast, *sec61al1^{c163}* mutants have a significant increase of ~37 neurons in both the right and left sides of the brain (Figures 14A',B',C'; p^{left} = 0.0002, p^{right} = 0.002). These data indicate that mutation of *sec61al1* increases neurogenesis in the hindbrain as well as the dorsal diencephalon.

To examine the posterior CNS, we quantified neurons in the spinal cord. Interestingly, we found a reduction in spinal neurons in *sec61al1^{c163}* mutants at
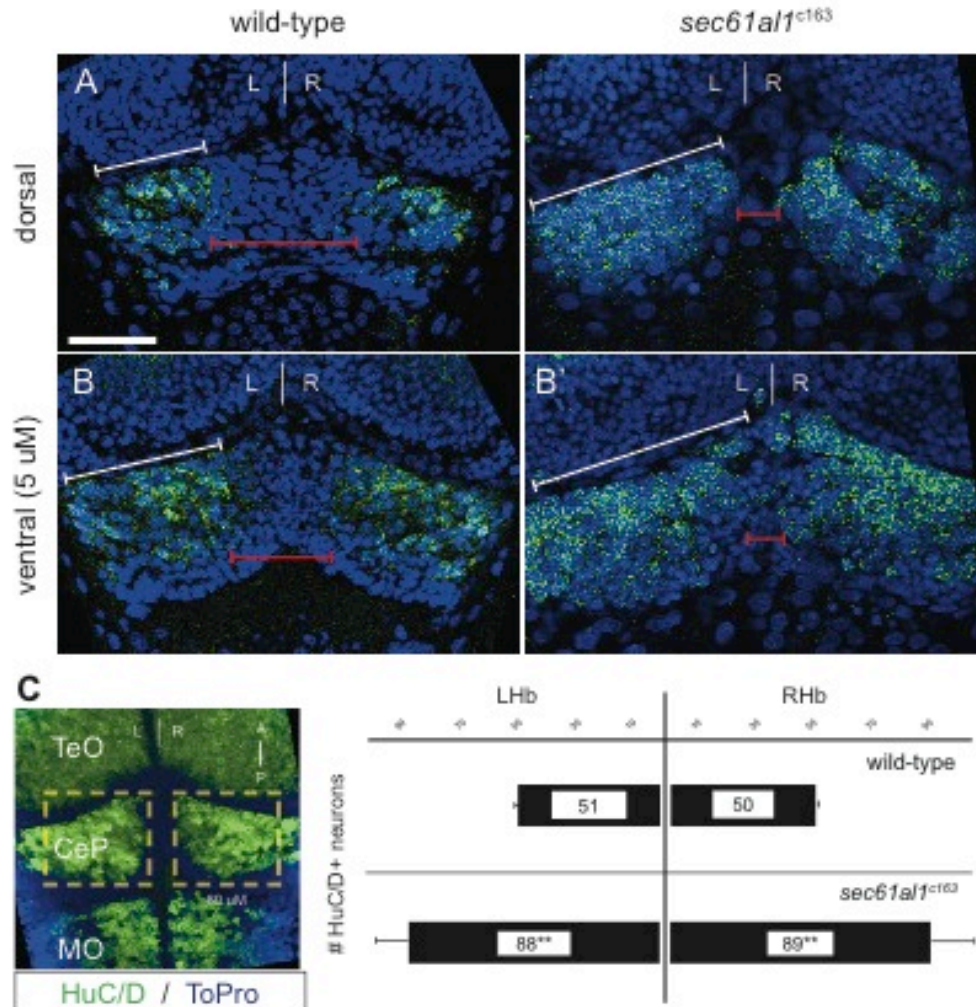
Figure 14. Excess neurons are found in the cerebellum of *sec61al1*[c163] mutants. We quantified neurons in the dorsal-most region of the cerebellum as a comparison to the development of the dorsally-located habenulae. HuC+ neurons are evident in optical sections from the (A) dorsal surface or (B) 5 µm below the dorsal surface of the cerebellar plate (white brackets) at 72 hpf. (A', B') More HuC+ cerebellar neurons are evident in *sec61al1*[c163] mutants, particularly in the medial region of the cerebellar plate (red brackets). (C) Representative extended focus image of the hindbrain for orientation; graphs represent data from 5 larvae. Images in A–B' are single plane images from confocal Z-stacks, with B,B' taken 5 µm ventral to A,A', respectively. Image C is an extended focus projection of a confocal Z-stack. Significance determined by Student's T-test, comparing the left, right, or total cerebellar neurons of *sec61al1*[c163] mutants with wild-type siblings (p<0.01, all T-tests); n=5. TeO = optic tectum; CeP = cerebellar plate; MO = medulla oblongata. Scale bars = 30 µm.

73

72 hpf. In each hemisegment, wild-type larvae have ~5 Rohon-Beard (RB) neurons, identified by their dorsal location, large cell body, and HuC/D immunofluorescence (Park et al., 2000)(Figure 15D, red arrows). Within the ventral spinal cord, many small, closely packed HuC/D+ neurons are found at the lateral edges of each segment (average of 102 per hemisegment, Figure 15B, white bracket). In contrast to wild-type, *sec61al1^{c163}* mutants lack almost all RB neurons (0.3 per hemisegment; p = 6.55 x 10-11)(Figure 15A') and have fewer neurons in the ventral cord (average of 79 per hemisegment; p = 0.013)(Figure 15B'). These data indicate that Sec61al1 may play different roles in neurogenesis at the rostral and caudal ends of the embryo.

Neuroepithelial cells are abnormal in the *sec61al1^{c163}* mutant diencephalon

Habenular neurons arise from periventricular neuroepithelial cells of the diencephalic (3rd) ventricle (Aizawa et al., 2007; Concha et al., 2003). The ratio of neurogenic to proliferative divisions by NECs depends on the inheritance of apical components by daughter cells (Bultje et al., 2009; Wodarz and Huttner, 2003). Adherens junctions (AJs) function to maintain separate apical and basolateral domains in epithelial cells. These AJs are protein complexes that include cadherin transmembrane proteins at their core (Harris and Tepass, 2010). Since Sec61al1 mediates the insertion of transmembrane proteins into the membrane (Heinrich et al., 2000; Schnell and Hebert, 2003), we hypothesized that apical-basal polarity would be disrupted in *sec61al1^{c163}* mutants. We addressed this question using transmission electron microscopy.
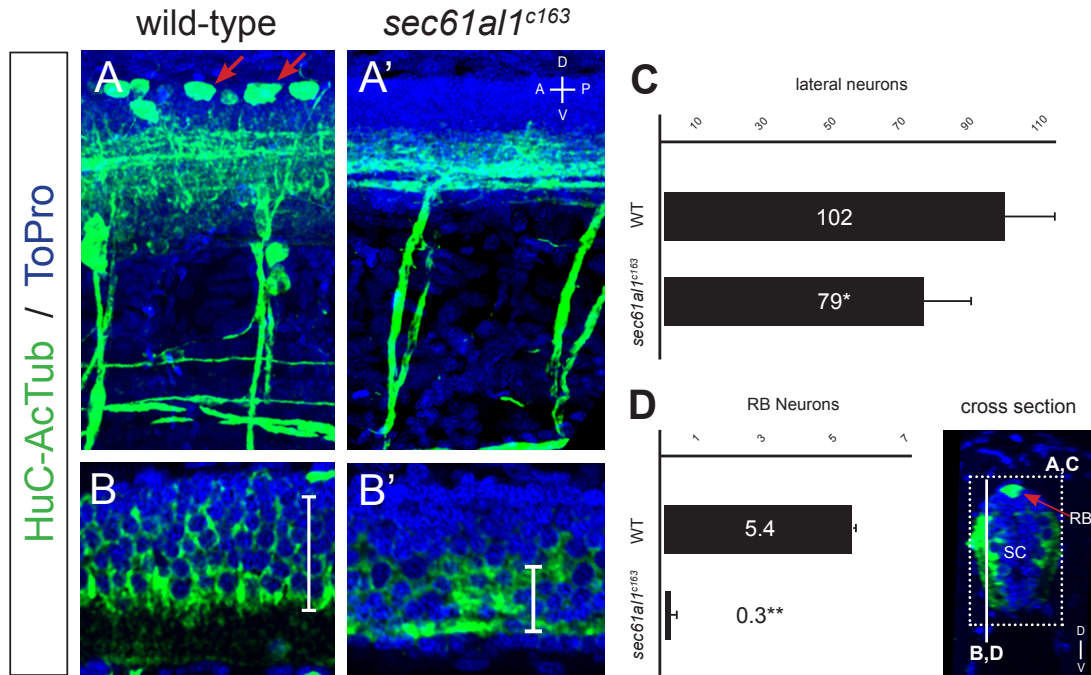
Figure 15. Fewer spinal neurons are present in *sec61al1*[c163] mutants. (A) At 72 hpf, large, dorsally positioned Rohon-Beard (RB) neurons expressing HuC/D and acetylated alpha-tubulin (AcTub; red arrows) are found in wild-type larvae. (B) In the ventral spinal cord, smaller, tightly packed neurons, also expressing HuC/D and AcTub, are found (white bracket). (A') *sec61al1*[c163] mutants lack Rohon-Beard neurons in the dorsal spinal cord and (B') develop fewer neurons in the ventral spinal cord as well. In addition, the ventral neurons are found in a more ventral location than wild-type (white bracket). (C) Quantification of HuC/AcTub+ neurons per hemisegment demonstrates fewer spinal neurons in *sec61al1*[c163] (p=0.013). (D) *sec61al1*[c163] mutants lack dorsal-most RB spinal neurons (p=6.55x10-11). Cells were counted in 1 µm sections from confocal Z-stacks. Inset beside D shows a coronal section through a wild-type spinal cord. RB neurons occupy dorso-medial positions, and the ventral cord neurons occupy both the left and right lateral sides. Scale bar = 20 µm. n=10 hemisegments, sibling and mutants. Images A,C are extended focus projections of a confocal Z-stack (projected region indicated by white box); B,D are single confocal planes (plane of focus indicated by white line). RB = Rohon-Beard; SC = spinal cord.

75

In wild-type larvae at 54 hpf, ventricular cells beneath the habenulae are evenly spaced and have columnar morphology with electron-dense junctions near the ventricular surface (Figure 16B). By contrast, NECs in $sec61al1^{c163}$ mutants have no obvious cell-cell junctions and are variable in size and shape (Figure 16B'). Nearly every ventricular cell exhibits apical blebbing in $sec61al1^{c163}$ mutants, consistent with the loss of cortical stability when apical-basal polarity is disrupted (Fehon et al., 2010).

To further investigate apical-basal polarity in the neuroepithelium, we labeled 56 hpf embryos with 488-conjugated phalloidin to reveal filamentous actin (F-actin), which is normally enriched in the cell cortex surrounding AJs (Harris and Tepass, 2010; Kuo et al., 2006). In wild-type, a thick band of actin filaments is found near the apical surface of NECs in the anterior 3rd ventricle. The most intense staining was found ~30 um from the dorsal surface (Figure 17C). In contrast, $sec61al1^{c163}$ mutants show discontinuous staining for apical F-actin in most ventricular cells (yellow arrowheads, Figure 17C'). In addition, wild-type embryos show apical localization of the Par complex component atypical protein kinase C (aPKC) in the columnar NECs abutting the ventricle (Figure 17D). aPKC staining appears irregular and intermittent in the NECs of $sec61al1^{c163}$ mutants (Figure 17D').
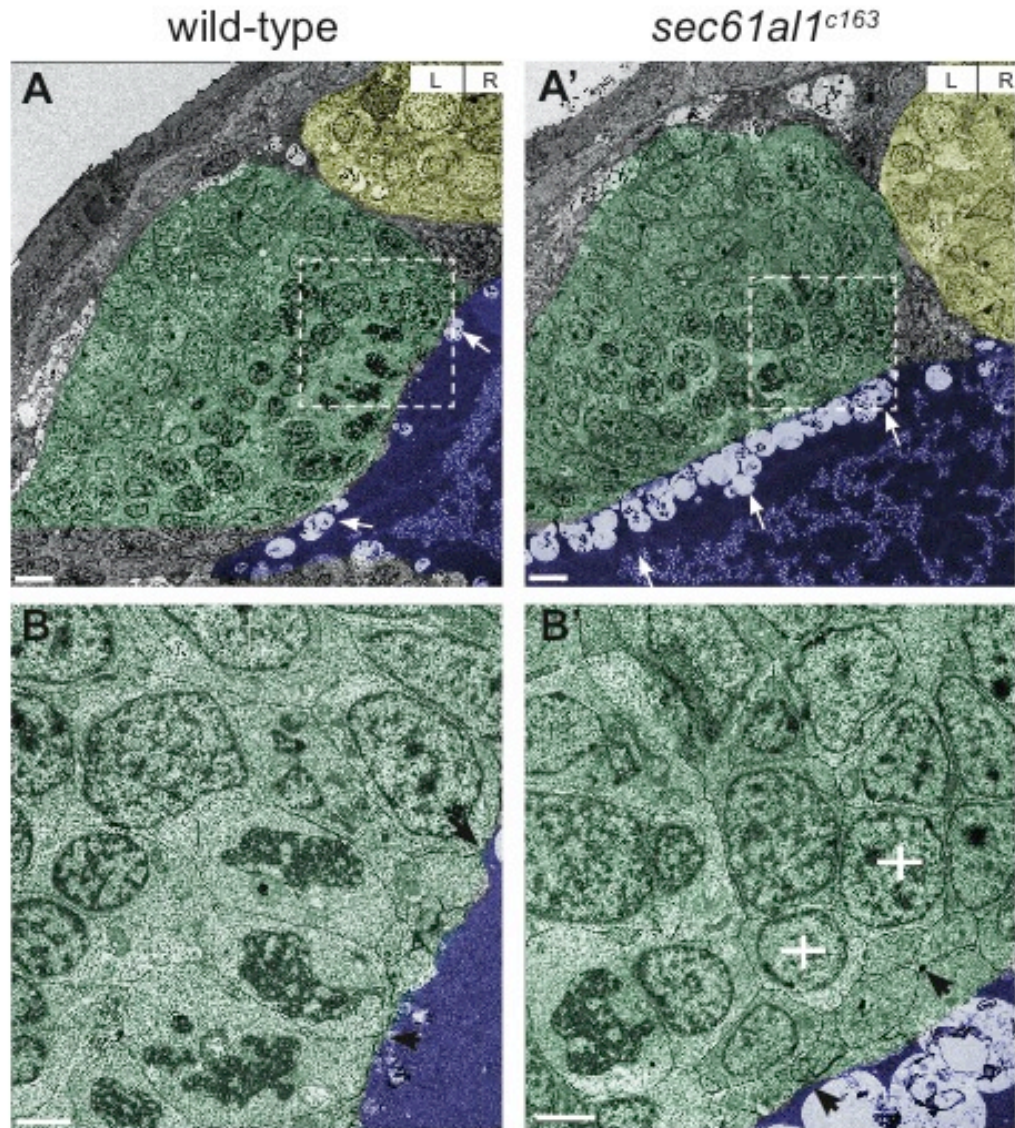
Figure 16. The ventricular epithelium is disrupted in *sec61al1^{c163}* mutants. (A) Transmission electron micrographs from coronal sections through the dorsal diencephalon of wild-type and (A') *sec61al1^{c163}* mutant larvae at 54 hpf, with the pineal organ (yellow), habenulae (green), and 3rd ventricle (purple) indicated by false coloring. (B, B') Higher magnification shows significantly more apical blebbing from cells lining the ventricle in mutants compared to wild-type siblings (arrows). (B) The well-defined columnar morphology and cell–cell junctions (black arrowheads) of wild-type ventricular cells are not found (B') in mutants. Rather, cells proximal to the ventricle are rounded (white crosses) and have few cell–cell junctions (black arrowheads). Dashed boxes in A, A' correspond to the region of higher magnification in the adjacent micrographs, B, B'. Scale bars: A,A'=20 μm; B,B'=5 μm.
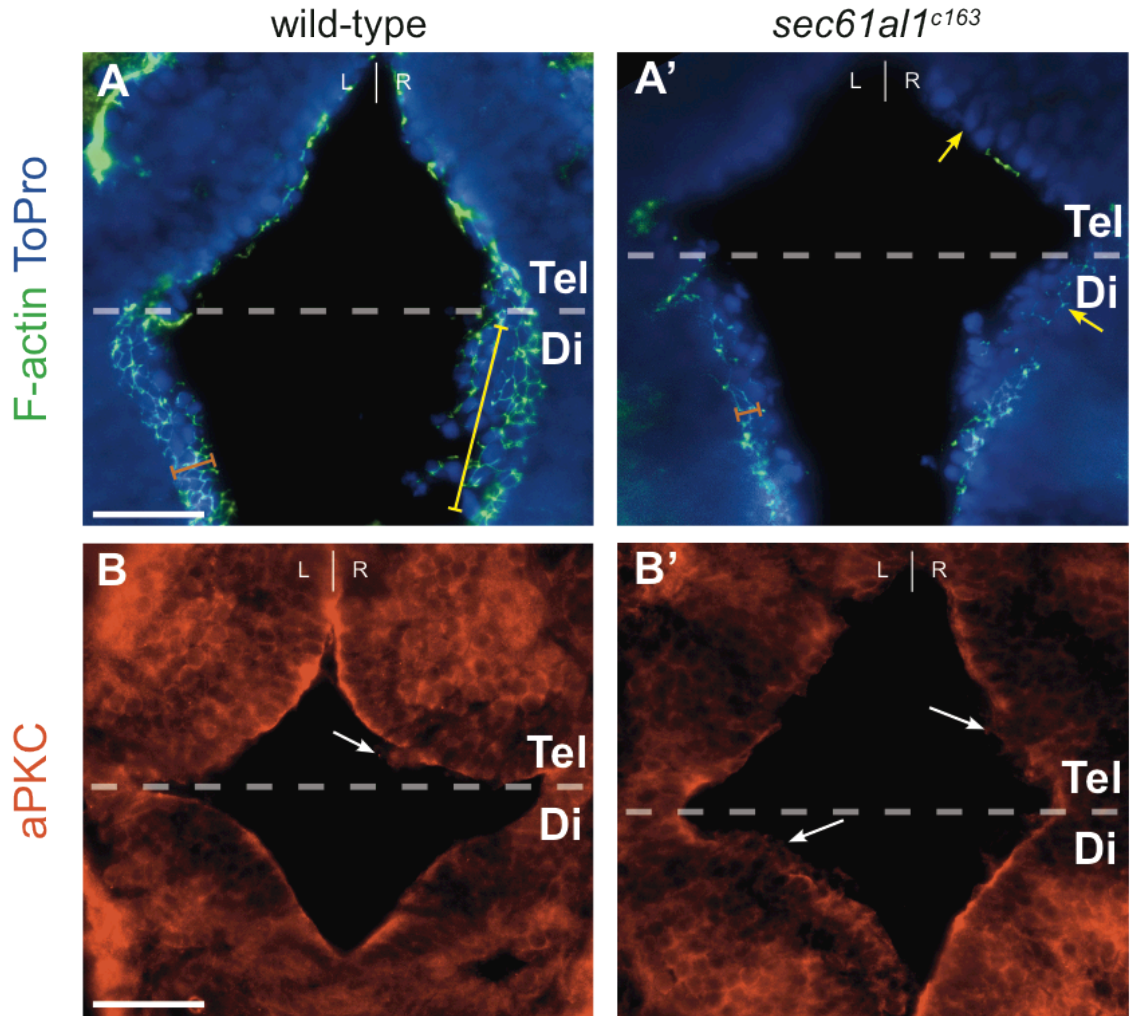
Figure 17. Loss of adherens junction apical localization in *sec61al1*[c163] mutants. (A) Filamentous actin (F-actin) in the ventricular neuroepithelium localizes to the apical membrane (orange bracket) in cells along the entire rostro-caudal axis of the anterior 3rd ventricle. (A') *sec61al1*[c163] mutants have reduced (orange bracket) F-actin in the caudal ventricular neuroepithelium (orange bracket) and many cells without apically-localized F-actin in the rostral ventricular neuroepithelium (yellow arrowheads). (B) aPKC localizes to the apical surface of the ventricular neuroepithelium in wild-type embryos, whereas (B') apical aPKC is reduced or absent in many cells of mutants. F-actin sections (A,A') are roughly 30 μm ventral from the dorsal surface, and aPKC sections (B,B') roughly 10 μm from the dorsal diencephalon. Tel, telencephalon; Di, diencephalon. Scale bars: A–B'=20 μm.

Discussion

The initial aim of a large forward genetic screen in zebrafish was to identify genes involved in asymmetric brain development. The *c163* mutation fulfilled this criterion in that mutants develop symmetric lateral subnuclei of the dorsal habenulae (LsDh), a profoundly asymmetric nucleus in wild-type embryos. Positional cloning revealed that the *c163* lesion maps to the *sec61alpha-like-1* gene, encoding a major component of the cytoplasm-to-ER protein translocation machinery, or translocon. *sec61al1^{c163}* mutants develop nearly symmetrical LsDh, with substantial ectopic Kctd12.1+ neurons in the right habenula. In addition, *sec61al1^{c163}* mutants develop markedly reduced medial subnuclei (MsDh). In the presumptive epithalamus, Nodal gene expression and the parapineal remain left-sided in *sec61al1^{c163}* mutants, indicating that the left-right axis is intact in these mutants. Despite these initial asymmetric cues, neurogenesis proceeds at a more rapid pace in mutants and is coupled with an extended period of LsDh proliferation. Neurogenic defects are not limited to the brain, as *sec61al1^{c163}* mutants possess excess neurons in the cerebellar plate and reduced neurons in the spinal cord. Finally, the neuroepithelial cells (NECs) of *sec61al1^{c163}* mutants, which represent habenular progenitors, show a profound loss of apical-basal polarity. Transmission electron micrographs document a loss of columnar morphology in NECs of mutant embryos, and these cells show extensive apical blebbing and overlapping membranes, indicative of polarity defects. Finally, *sec61al1^{c163}* mutants display reduced apical localization of both filamentous actin

(F-actin) and atypical protein kinase C (aPKC), both of which are canonical members of the adherens junction complex. We propose that Sec61al1 is necessary for trafficking of transmembrane adherens junction components that are vital toward the establishment of apical-basal polarity. In the absence of Sec61al1 function (and upon the gradual loss of maternal Sec61al1), adherens junctions are lost in neural progenitors, leading to expansion of the early-borne LsDh population at the expense of the later-born neurons of the MsDh.

Previous work in zebrafish has implicated the Nodal pathway – a canonical determinant of visceral asymmetry in all vertebrates – as a crucial factor in brain asymmetry. Indeed the dorsal diencephalon of zebrafish displays asymmetries in gene expression, anatomy, and connectivity. This may reflect an evolutionary measure to co-opt Nodal signaling in the brain of zebrafish, as other "lower" vertebrates such as reptiles and amphibians develop asymmetric dorsal diencephalic structures (Concha and Wilson, 2001) but do not express Nodal components in the brain. Nodal signaling is vital for zebrafish epithalamic development, as embryos depleted for the Nodal gene *spaw* generate equal numbers of neurons in the left and right sides of the brain between 34 and 38 hpf, in contrast to wild-type embryos, which produce more neurons in the left hemisphere (Roussigne et al., 2009). Embryos depleted for Sec61al1 exhibit asymmetric Nodal signaling and generate asymmetric pools of HuC/D+ neurons during early stages of habenular differentiation (40-48 hpf), similar to wild-type. However, *sec61al1^{c163}* mutants later form habenular subnuclei that are nearly symmetric, due to excess neurogenesis contributing to the LsDh on both sides of

the brain. In addition, parapineal development and migration appear normal in the absence of Sec61al1 function. Since the parapineal supplies a signal necessary for the differentiation of a large left LsDh in wild-type embryos (Concha et al., 2003; Gamse et al., 2003), we looked for the presence of an additional right-sided parapineal or a large, centrally located organ. However, in *sec61al1^{c163}* mutants, the parapineal remains unilateral and left-sided, and bilateral, large LsDh are formed even after disruption of parapineal formation. Together, this data indicates that early asymmetric cues for habenular differentiation are in place in *sec61al1^{c163}* mutants and that differentiation of excess LsDh neurons in the right habenula is independent of both Nodal signaling and parapineal-derived signals.

Expression of *sec61al1* is symmetric in the brain, but the effect of the *sec61al1^{c163}* mutation on the brain on production of LsDh neurons appears more dramatic in the right habenula. We resolved this paradox by disrupting the formation of the parapineal by injection of antisense morpholino targeting *tbx2b*. *tbx2b* knockdown in wild-type embryos leads to small LsDh development on both sides of the brain. However, *sec61al1^{c163}* mutants injected with *tbx2b* morpholino still developed large LsDh on both sides of the brain. We conclude from this result that there is symmetric suppression of LsDh neurogenesis on both sides of the brain that is relieved on the left half of the brain by parapineal influence. Without Sec61al1 function, neurogenesis remains asymmetric initially, but progenitors on both sides of the midline undergo an expanded period of proliferation and produce neurons of the LsDh at a much faster rate than siblings.

The ER-localized translocon is an essential component of the cell (Rapoport, 2007). Transcripts of *sec61al1* and the closely related *sec61al2* are maternally provided (Giraldez et al., 2006). Maternal loading of *sec61al1* transcript probably accounts for the survival of *sec61al1^{c163}* mutants until 4 dpf. However, there are tissues that are more profoundly impacted by loss of Sec61al1, indicating that some cell types are more sensitive to loss of proteins in the exocytic pathway. These include the chondrocytes of the jaw, which must secrete large quantities of extracellular matrix proteins (ECM) in order to form cartilage. In fact, cartilaginous components are reduced in mutants of the COPII genes *sec23* and *sec24*, which encode proteins necessary for the transport of vesicles from the ER to the Golgi (Boyadjiev et al., 2006; Lang et al., 2006; Sarmah et al., 2010). Similarly, we see a reduction in jaw elements in *sec61al1^{c163}* mutants.

The progenitor cells of the nervous system are also sensitive to the loss of exocytic pathway proteins. Mice homozygous for the *hyh* hypomorphic mutation of the *napa* gene display a dramatic increase in the number of cortical neurons. *napa* codes for the soluble N-ethylmaleimide-sensitive factor (NSF) attachment protein alpha (alpha-Snap) protein, which plays a role in fusion of exocytic vesicles at the plasma membrane (Clary et al., 1990). More specifically, alpha-Snap has a characterized role in targeting proteins for the apical surface of neuroepithelial cells (NECs). The *hyh* hypomorphic mutation is sufficient to disrupt adherens junctions, which in turn affects NEC polarization, ultimately

causing production of excess early-born deep layer cortical neurons (Chae et al., 2004; Hong et al., 2004).

Like *napa^hyh* mutants, the *sec61al1^c163* mutation leads to changes in apical-basal polarity in neuroepithelial progenitors and excess early-born Kctd12.1+ neurons of the LsDh. In wild-type zebrafish embryos, progenitor cells form an ordered epithelium with cell-cell junctions near the apical surface, features that are common to mammalian cortical progenitor cells (Cappello et al., 2006; Lien et al., 2006; Rasin et al., 2007). In *sec61al1^c163* we detect diminished expression of apical adherens junction components, including aPKC and F-actin. The ventricular and periventricular cells of *sec61al1^c163* mutants are multilayered and variable in size and shape, a phenotype reminiscent of the conditional removal of αE-catenin from neural progenitors in mice (Lien et al., 2006).

As an entry point for proteins destined for transmembrane or extracellular domains, Sec61 impacts the production of a multitude of proteins (Rapoport et al., 2004). Although it is apparent that Sec61 disruption affects the development of many, if not all tissues, we have focused primarily on neurogenesis. We propose that Sec61 is required to traffic components of the apical adherens junction within neuroepithelial progenitor cells of the central nervous system. With the loss of the translocon, progenitors are unable to maintain cell-cell junctions, or perhaps are unable to reestablish junctions following cell division, ultimately leading to a loss of polarity, delamination from the apical cortex, and ultimately, disruptions in neurogenesis. The cadherin family represents a crucial component of adherens junctions. Cadherins are transmembrane proteins that

mediate epithelial polarization and must be trafficked through Sec61. In line with this argument, loss of N-cadherin in zebrafish leads to increased proliferation of neural progenitors (Chalasani and Brewster, 2011). Furthermore, disruption of other adherens junction components, including RhoA, Cdc42, αE-catenin, or Numb/Numbl results in hyperproliferation of neural progenitors in the mouse cortex (Cappello et al., 2006; Farkas and Huttner, 2008; Katayama et al., 2011; Lien et al., 2006; Rasin et al., 2007). Collectively, this data contributes to our hypothesis that loss of Sec61 function affects adherens junctions, which in turn leads to increased proliferation of neural progenitors.

Disruption in apical-basal polarity in neural progenitors could also affect neurogenesis through inheritance of factors that determine the cell fate of daughter cells following mitoses. Adherens junctions generate polarity in epithelial tissues by localizing the Par3/Par6/aPKC signaling complex at the apical cortex of the cell (D'Souza-Schorey, 2005; Niessen and Gottardi, 2008; Wodarz and Nathke, 2007). Specifically, in neuroepithelial cells the proteins Par3, Par6, and aPKC all localize to the apical domain (Cappello et al., 2006; Costa et al., 2008; Imai et al., 2006). In the vertebrate neuroepithelium, inheritance of apically- and basally-located factors is correlated with symmetric versus asymmetric divisions (Geldmacher-Voss et al., 2003; Wodarz and Huttner, 2003; Zhong and Chia, 2008). When NECs divide, they generate one neuron and one progenitor cell. Some NECs delaminate from the apical surface and become basal progenitors, which give rise to two neurons when they divide (Farkas and Huttner, 2008). Importantly, loss of *cdc41* in the mouse

neuroepithelium leads to AJ disruption, a dramatic increase in basal progenitors, and the generation excess cortical neurons (Cappello et al., 2006). We hypothesize that the *sec61al1^c163* mutation leads to AJ disruption in NECs, whereby these progenitors delaminate and adopt a basal progenitor fate. In turn, these basal progenitors produce excess neurons in the dorsal diencephalon and the hindbrain. As anchor points for the actin bundles that traverse and link cells of the neuroepithelium, AJs are crucial for maintenance of cell polarity (Harris and Tepass, 2010). The extensive apical blebbing witnessed in cells of the *sec61al1^c163* mutant neuroepithelia could lead to the loss of apically localized factors and the increased production of basal progenitors. Use of a transgenic marker of cellular divisions, such as *Tg(h2av;egfp)*, in coordination with time lapse imaging may reveal the location of dividing progenitor cells (Pauls et al., 2001; Roberts and Appel, 2009) and reveal if more basal progenitors exist in the brains of *sec61al1^c163* mutant embryos.

CHAPTER III

ASYMMETRIC DEVELOPMENT OF THE LATERAL SUBNUCLEUS OF THE DORSAL HABENULA IS DEPENDENT ON TRANSLOCON-MEDIATED TRAFFICKING OF N-CADHERIN

Preface

We previously characterized a mutant harboring a nonsense mutation in *sec61a-like1*, a major component of the vertebrate cytoplasm-to-ER translocation machinery (Doll et al., 2011). *sec61al1* mutants develop symmetric, expanded lateral subnuclei of the dorsal habenula, and generate far fewer neurons of the medial subnucleus. This phenotype emerges from an altered program of habenular neurogenesis, in which progenitor cells proliferate for a longer period of time and generate neurons fated for the LsDh at a much faster rate than siblings. Ultrastructural analysis indicated a major disruption in the integrity of the ventricular neuroepithelium cells, and immunofluorescent labeling showed a loss of apical expression of atypical protein kinase C (aPKC) and filamentous actin (F-actin). Accordingly, we hypothesized that Sec61 function is necessary for the timely production of transmembrane protein components of the adherens junction, the apically located anchors that provide cortical integrity and promote renewal of neural progenitor populations.

We previously speculated that disrupted trafficking of N-cadherin to adherens junctions of the neuroepithelium lay at the heart of the *sec61al1*[c163] mutant phenotype. In fact, the work presented in this chapter indicates that disruption of N-cadherin function leads to epithalamic phenotypes that are reminiscent of *sec61al1*[c163] mutants. In particular, the null allele *cdh2*[vu125] (*cdh2* encodes the N-cadherin protein), and morpholino-mediated depletion of *cdh2* lead to symmetric development of the lateral subnucleus of the dorsal habenulae. However, *cdh2*[vu125] mutants generate fewer dorsal habenula neurons than wild-type or *sec61al1*[c163] mutants. Epistatic analyses indicate that Sec61al1 and N-cadherin function in the same pathway for habenular neurogenesis, but N-cadherin does not seem to be involved in the proliferation of habenular precursors. The data presented indicate that proper trafficking of N-cadherin through Sec61 is necessary for asymmetric development of the dorsal habenulae.

Methods

Zebrafish wild-type and transgenic lines

Zebrafish were raised at 28.5 °C on a 14/10 light/dark cycle. Embryos and larvae were staged according to hours or days post-fertilization as previously described (Kimmel et al., 1995). The wild-type stain AB (Walker, 1999) and the ENU induced mutations *sec61al1*[c163] (Doll et al 2011) and *cdh2*[vu125] (von der Hardt et al., 2007) were used.

Genotyping

For the *cdh2^vu125^* allele, a 484 bp PCR product was generated using the forward primer 5'- TGCAAGTGGGACTGGAACAC-3' and the reverse primer 5'-TGCCATGATGCGCTCCATGT-3'. The *cdh2^vu125^* lesion abolishes a BccI restriction site. Therefore, restriction digest with BccI of the wild-type allele generates bands of 377 and 107 bp, and the mutant product remains uncleaved (von der Hardt et al., 2007).

Morpholino injections

Antisense morpholino oligonucleotides (MO) complementary to translation initiation sites were used to deplete *cdh2* (Hong and Brewster, 2006; Lele et al., 2002) and *sec61al1* function (Doll et al., 2011). For each morpholino, the stock solution (10 mg/mL) was diluted in distilled water, and embryos (1–2 cell stage) were pressure injected with ~ 1 nL of MO per embryo. The *cdh2* MO was used at 1.9 ng/embryo, the *sec61al1^ATG-MO^* at 500 pg/embryo.

in situ hybridization

Whole mount in situ hybridization was performed as described previously (Gamse et al., 2003; Thisse and Thisse, 2008) using reagents from Roche Applied Bioscience. RNA probes were labeled using digoxygenin-UTP. To synthesize antisense RNA probes, the following templates and enzymes were used:

Plasmid name	Reference	Enzyme used to linearize plasmid	RNA Polymerase
pBK-CMV-kctd12.1	(Gamse et al., 2003)	EcoRI	T7
pBS-gfi1	(Dufourcq et al., 2004)	SacII	T3
pBS-otx5	(Gamse et al., 2002)	EcoRI	T7

Embryos were incubated at 70 °C with the antisense probe in hybridization solution containing 50% formamide. Hybridized probes were detected using alkaline phosphatase-conjugated antibodies and visualized by 4-nitro blue tetrazolium (NBT) and 5-bromo-4-chloro-3-indolyl-phosphate (BCIP) staining for single labeling, or NBT/BCIP followed by iodonitrotetrazolium (INT) and BCIP staining for double labeling (Thisse and Thisse, 2008).

Immunofluorescent labeling

2-4 dpf embryos were fixed for at least 36 h in Prefer fixative (Anatech) at room temperature. Embryos were stored in 0.1% Tween in PBS at 4°C for up to two weeks. Embryos were blocked in PBS with 0.1% Triton X-100, 10% BSA, 1% DMSO and 2% sheep serum (PBSTrS). For antibody labeling, rabbit anti-Kctd12.1 (1/500)(Gamse et al., 2005), and mouse anti-HuC/D (1:500, Invitrogen A21271) were used. Larvae were incubated overnight in primary antibody diluted in PBSTrS, and primary was detected using goat anti-rabbit, goat anti-chicken, or goat anti-mouse secondary antibodies conjugated to Alexa 488 or Alexa 568

fluorophores (1:350, Molecular Probes). Cell nuclei were detected with ToPro3 (1:3000, Invitrogen).

For cryosectioned zebrafish tissue, embryos were fixed in BT fix (4% paraformaldehyde, 0.15 mM $CaCl_2$, 4% sucrose in 0.1 M PO_4 buffer) overnight on rocker. Subsequently embryos were embedded in 2% agarose/5% sucrose, and sunk overnight in 5% sucrose. Next, blocks were frozen in 2-methyl butane/liquid N_2, and sectioned at 15 µm thickness on a Leica CM1850 cryostat. Sections were then rehydrated for 1 h in 1x PBS, blocked for 1 h in 2% sheep serum/BSA in 1x PBS (AB Block), then incubated with either rabbit anti-N-cadherin (1:200, Abcam) or rabbit anti-β-catenin (1:200, Sigma) for 2 h at room temperature. Sections were then washed 6 x 5 min in 1x PBS, incubated with goat anti-rabbit Alexa 568 (1:200, Invitrogen) and either Alexa 488-phalloidin (1:100, Invitrogen) or bodipy-ceramide (FL C5, Molecular Probes; dissolved in DMSO to a stock concentration of 5 mM, applied at 100 µm) in AB Block for 2 h. Sections were washed 5 x 5 min in PBS, and cell nuclei were stained with ToPro3 (1:3000 in PBS, Invitrogen), via room temperature incubation for 15 min. Sections were washed 5 x 5 min in 1x PBS, cleared with glycerol and imaged on a Leica 6000M compound microscope.

Quantification of neurons

To quantify the number of neurons in the medial and lateral dorsal habenulae, embryos were labeled with Kctd12.1, Kctd12.2, or HuC/D antibodies and co-stained with ToPro3 nuclear dye. Using a Zeiss LSM510 Meta upright

confocal microscope, 1 μm optical slices were obtained through the dorsal diencephalon, starting dorsally at the pineal organ and continuing ventrally through Kctd12 expression in the habenulae. The number of Kctd12+ neurons in either habenula was counted manually in each slice, using ToPro3 expression to distinguish individual nuclei within the field. This prevented double counting of neurons with large dendritic fields or with large soma filling several optical sections. Two criteria were used to qualify as Kctd12+: 1) The fluorescent signal must be present throughout the entire cytoplasm and surround the nucleus. 2) The intensity of Kctd expression must measure 100 arbitrary units or higher (out of 4096) using the Quantification tool in Volocity software (Improvision). Differences between mutant and sibling embryos were calculated using a Student's T-Test. A measure of asymmetry was generated using an asymmetry index (AI), calculated as the difference between the left and right medial or lateral subnucleus divided by the total number of neurons: [AI = (#L - #R) / (#L + #R)]. An AI score between 0 and 1 indicates the left subnucleus contains more neurons and a value between -1 and 0 indicates a larger right subnucleus (Roussigne et al., 2009).

Results

Loss of adherens junction components at the apical surface of diencephalic neuroepithelial progenitors in N-cadherin mutants

The loss of adherens junction (AJ) components in the neuroepithelium of the 3rd ventricle correlates with abnormal neurogenesis in the dorsal diencephalon (Doll et al., 2011). We previously reported the apical expression patterns of aPKC and F-actin in the diencephalic ventricle (Doll et al., 2011). To extend these results, 72 hpf wild-type embryos were sectioned coronally through the dorsal diencephalon, and stained for expression of additional AJ factors. In a similar pattern, both N-cadherin (Figure 18A,A''') and β-catenin (Figure 18C,C''') are tightly expressed along the apical surface of cells lining the 3rd ventricle. Furthermore, both N-cadherin and β-catenin show strong correlation with the membrane marker bodipy-ceramide (Figure 18A,C), indicating that these AJ components are correctly localized at or near the membrane.

We predicted that the ER translocation machinery is necessary to traffic AJ components to the apical surface of ventricular progenitors. In the absence of Sec61 function, we expect diminished AJ protein expression on cells surrounding the 3rd ventricle. Immunofluorescent labeling of sections through *sec61al1^{c163}* homozygous mutant embryos indicates that AJ protein deposition at the apical membrane is diminished. Expression of both N-cadherin (Figure 18B,B''') and β-catenin (Figure 18D,D''') is reduced in progenitor cells at the ventricular surface. Notably, although high levels of N-cadherin normally found in the ventricular
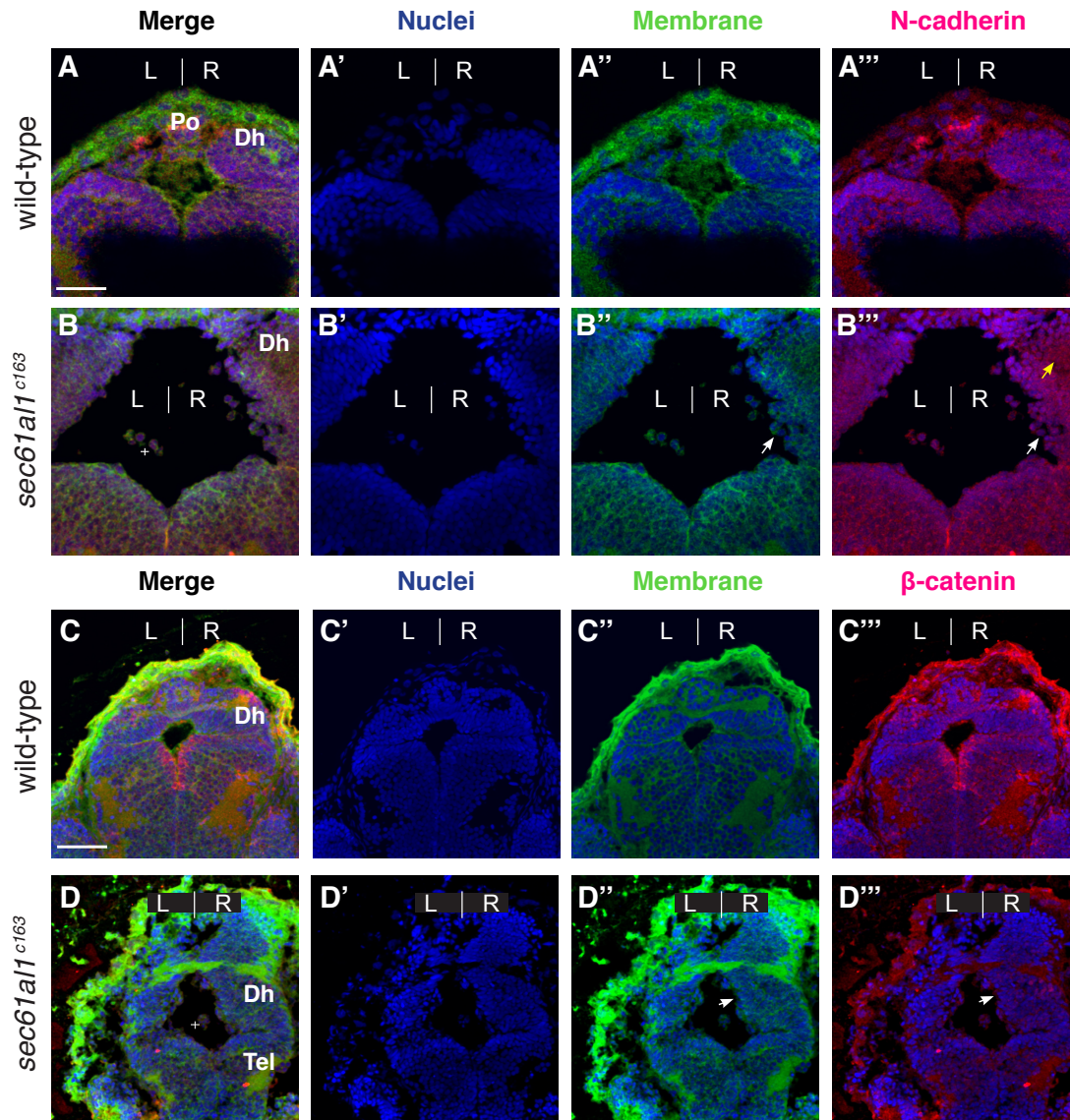
Figure 18. Diminished expression of N-cadherin and β-catenin at the apical surface of 3rd ventricle neuroepithelial cells in *sec61al1^c163* mutants. (A) Merge image showing expression of N-cadherin at the apical surface, tightly colocalized with the membrane marker bodipy-ceramide. (B) Reduced N-cadherin expression at the apical ventricular surface of *sec61al1^c163* mutant embryos. Note the presence of detached cells in the ventricle (white crosses, A,D). (C) Apical expression of beta-catenin. (D) Diminished beta-catenin expression in *sec61al1^c163* mutants. 72 hpf embryos sectioned coronally through the dorsal diencephalon (images in D s sectioned slightly more transverse). Scale bars = 20 um. n = 4 each genotype.

epithelium are reduced, not all N-cadherin expression is gone. For instance, cells distal from the ventricle located within the dorsal habenula still express some N-cadherin (yellow arrow, 18B''').

Disruption of N-cadherin function alters development of the dorsal habenulae

Since *sec61al1* mutants exhibit abnormal symmetric development of the habenular nuclei, and N-cadherin trafficking is disrupted in *sec61al1* mutants, we analyzed asymmetry of the dorsal habenulae in zebrafish embryos deficient for N-cadherin function. The *cdh2^{vu125}* mutation is pleiotropic; homozygotes develop with dorsal curvature of the trunk, a large expansion of forebrain volume (Bagatto et al., 2006; Lele et al., 2002), and cardiac edema (Bagatto et al., 2006). The penetrance of the *cdh2^{vu125}* allele is variable (see Figure 21), but all homozygotes develop with considerable brain malformations; mutants possess no obvious midbrain-hindbrain boundary, develop large ventricles, and an open neural tube, phenotypes similar to *cdh2^{fr7}* mutants (Lele et al., 2002). In fact, a 3D reconstruction of the dorsal diencephalon of a *cdh2^{vu125}* mutant reveals major malformations in neural architecture (Figure 23B). Despite these anatomical malformations, *cdh2^{vu125}* homozygotes survive until 4 dpf and develop dorsal diencephalic nuclei.

The habenular nuclei develop symmetrically in *cdh2* mutants. In wild-type larvae, the lateral subnucleus of the dorsal habenula (LsDh) is much larger in the left hemisphere of wild-type embryos than the right (Figure 19A). This left-right

asymmetry can be quantified using an Asymmetry Index (Methods); wild-type embryos possess an AI value of 0.41, indicating the left LsDh contains more Kctd12.1+ neurons than the right. In contrast, $cdh2^{vu125}$ mutants develop LsDh that are more symmetric than wild-type (AI = 0.15; n=9). $cdh2^{vu125}$ mutants generate fewer total neurons than wild-type, with significant reductions in the total number of Kctd12.1+ cells (bilateral sum), and in the left habenula (p<0.01) at 72 hpf (Images not shown).

We hypothesized that the reduction of habenular neurons may be an artifact of the severe neural malformations noted in the $cdh2^{vu125}$ allele. We therefore repeated these experiments but using a hypomorphic dose of a morpholino targeting the $cdh2$ gene (Lele et al., 2002). This treatment (1.9 ng of $cdh2^{ATG-MO}$) cause fewer effects on the overall development and the neural architecture of treated embryos as compared to $cdh2^{vu125}$ null embryos (Figure 20A''). In fact, $cdh2^{ATG-MO}$ larvae generated comparable numbers of total Kctd12.1+ neurons as untreated controls (Figure 19; wild-type = 204, $cdh2^{ATG-MO}$ = 190; n = 9).

$cdh2^{ATG-MO}$ larvae have a significant increase in Kctd12.1+ cells of the right LsDh (Figure 19; wild-type = 55, $cdh2^{ATG-MO}$ = 79; p<0.01). As a result, morpholino-treated embryos develop LsDh that are nearly symmetric (AI = 0.17), similar to $cdh2$ null mutants, providing further evidence that N-cadherin function is necessary for the generation of asymmetry in the habenular nuclei. We labeled embryos during earlier stages of habenular neurogenesis in an effort to further characterize the loss of LsDh asymmetry in $cdh2$ morphants. At both 48 and 56
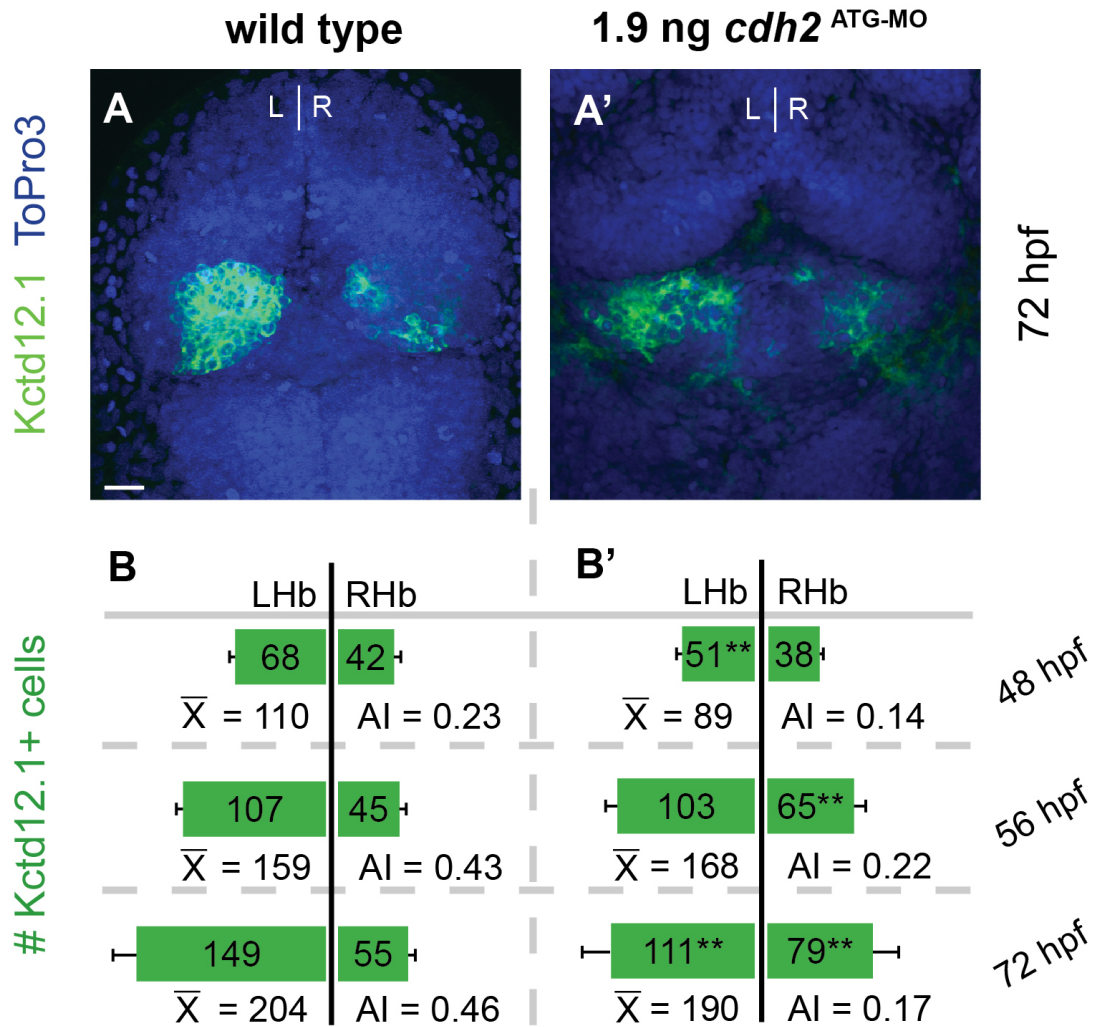
Figure 19. Progression of LsDh development is more symmetric upon *cdh2* depletion. Development of the LsDh in WT is profoundly asymmetric, starting at 48 hpf (B) and continuing through 72 hpf (A,B). Embryos depleted for *cdh2* generate LsDh that are more bilaterally symmetric than controls (A',B'). Morphant embryos generate comparable numbers of Kctd12.1+ cells at all time points, and significantly increased right LsDh at both 56 and 72 hpf (B'). **p<0.01, n = 4. AI = asymmetry index. Scale bar = 10 μm.

hpf, embryos depleted for *cdh2* developed comparable total Kctd12.1^{+} neurons (Figure 19B). However, at 48 hpf, morphants develop LsDh that are more symmetric than controls due to fewer neurons on the left side (AI[NIC] = 0.23; AI[cdh2ATG-MO] = 0.14). At 56 hpf, it is increased numbers of neurons in the right habenula that cause the *cdh2[ATG-MO]* habenulae to be more symmetric than wild-type controls. Roughly 15 neurons are added to the right LsDh of control embryos between 48 and 72 hpf, compared to the addition of 40 neurons in morphants (Figure 19). Conversely, only 60 neurons are added to the left LsDh of morphants compared to 81 in controls. We conclude that reduction in N-cad activity causes neurogenesis to become more symmetric between 48 and 72 hpf in the LsDh.

Loss of N-cadherin function alters habenular morphology

In our analyses of Kctd12.1 expression in *cdh2* mutants and morphants, we noted profound changes in the relative size and shape of the habenulae. wild-type embryos develop two distinct, coherent LsDh nuclei, with each Kctd12.1+ neuron closely abutting other cells of the nucleus (Figure 20). In contrast, islands of Kctd12.1+ neurons form in *cdh2[vu125]* mutants, resulting in LsDh that display a lesser degree of cohesion (Figure 20').

We quantified these observations by measuring the relative depth and volume of LsDh in wild-type and *cdh2[vu125]* mutants. Although *cdh2* mutants have established deficits in neural tube closure (Lele et al., 2002), we find that *cdh2[vu125]* develop LsDh with an insignificant increase in total width (Figure 20C).
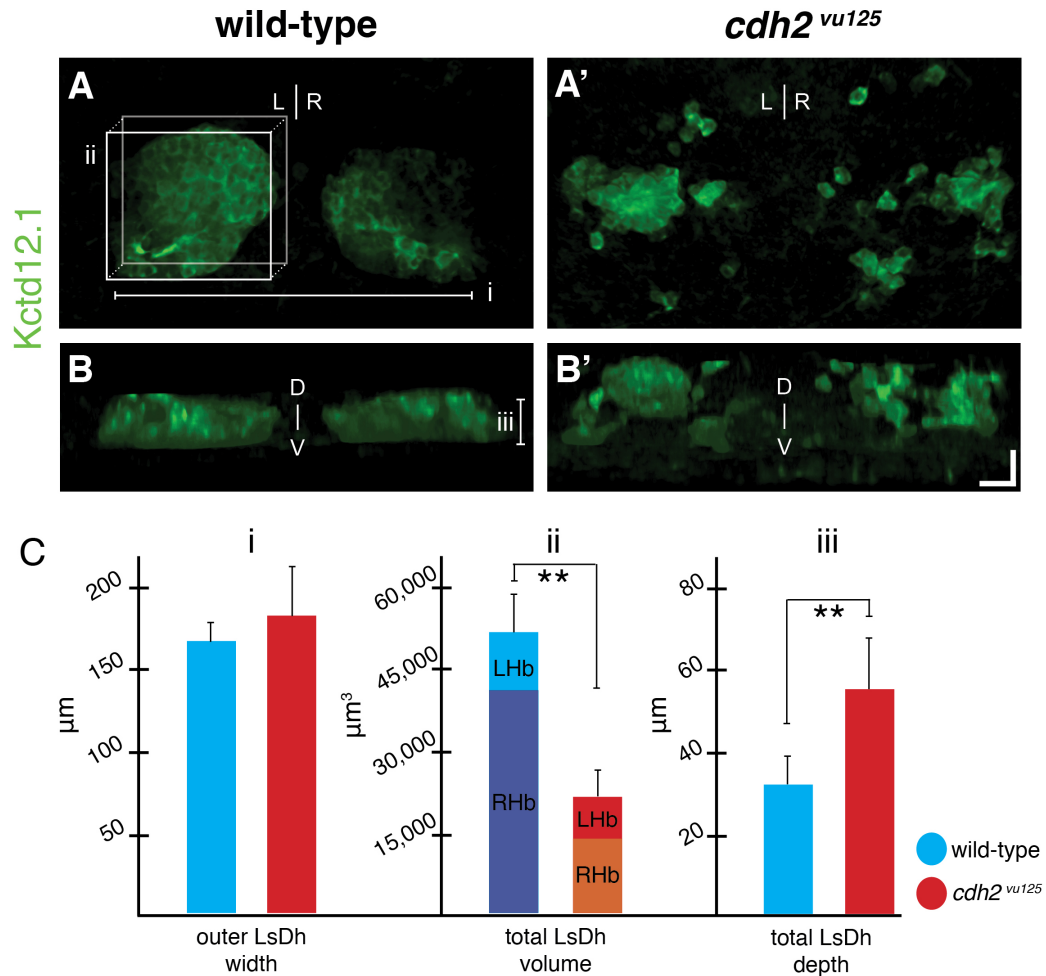
Figure 20. The LsDh of *cdh2*[vu125] mutants occupies less volume and more dorsoventral depth than wild-type siblings. Wild-type embryos contain two distinct, compact LsDh (A). In contrast, the LsDh of *cdh2*[vu125] mutants lack cohesion (A'). Along with obvious cohesion deficits, the LsDh of mutants occupy more dorsoventral depth (B';Ciii), and considerably less volume (Cii) than siblings, though the outer width of the LsDh does not differ significantly from wild-type. AI = asymmetry index. LHb, left habenula; RHb, right habenula. **p<0.01; n = 4. Scale in B' = 10 μm.

Rather, the total volume and the dorsoventral depth of the LsDh are altered. The volume of the Kctd12.1+ lateral subnucleus is significantly reduced in $cdh2^{vu125}$ mutants (Figure 20Cii), consistent with the reduced numbers of LsDh neurons (Figure 20). In addition, the scattered cells of the LsDh in $cdh2^{vu125}$ mutants occupy a greater dorsoventral depth (Figure 20Ciii). The more scattered distribution of LsDh neurons may indicate a deficit in migration from the ventral neuroepithelium to the dorsal habenulae. Indeed, ectopic Kctd12.1+ neurons are found ventral to the pineal complex, where late-born habenular neurons originate (Aizawa et al., 2007), in both mild and severe $cdh2^{vu125}$ mutants (Figure 20B',B'').

Pineal complex development is unaffected by the loss of N-cadherin

In zebrafish, lateralized development of the dorsal diencephalon is regulated by a signal(s) produced by the left-sided parapineal organ. Ablation of the parapineal results in lateral habenular nuclei that both resemble the right LsDh in wild-type controls (Gamse et al., 2003). Thus far, generation of two large, bilateral LsDh (both left and right LsDh resemble the wild-type left LsDh) has only been noted when larvae possess parapineal organs on both sides of the midline (Concha et al., 2000; Gamse et al., 2003), or in the absence of Sec61 translocon function (Doll et al., 2011). We therefore investigated pineal complex formation in $cdh2^{vu125}$ homozygous mutants.

We find that asymmetric features of the pineal complex still develop in $cdh2^{vu125}$ mutants. Expression of a pan-pineal gene, *otx5*, reveals that severely affected $cdh2^{vu125}$ mutants fail to close the dorsal neural tube as previously

described (Lele et al., 2002), as *otx5*+ cells are apparent in distinct clusters on either side of the midline (Figure 21B''). Mildly affected *cdh2*^{vu125} mutants exhibit a subtle neural tube closure phenotype revealed by a widening of the pineal organ. Both mild and severe *cdh2*^{vu125} homozygous mutants develop a single parapineal organ, and the parapineal migrates to the left side of the pineal organ in the vast majority of wild-type embryos, as marked by the expression of *gfi-1* (Figure 21A). In a small number of severe mutants, the parapineal organ remains in the center of the brain (Figure 21A',A''). Despite affecting neural tube closure, mutation of *cdh2* still results in formation of a single left-sided parapineal organ, indicating that symmetric development of the LsDh in mutants is not the result of bilateral parapineal signaling.

Depletion of *cdh2* leads to fewer dorsal habenula neurons but a higher percentage of neurons fated to the lateral subnucleus

Embryos depleted for *cdh2* generate fewer Kctd12.1$^+$ neurons of the LsDh at 72 hpf. This could indicate that the loss of N-cadherin leads to the production of fewer total habenular neurons, or alternatively that a smaller proportion of habenular neurons contribute to the LsDh. To distinguish these possibilities, we immunolabeled *cdh2*^{ATG-MO} morphants and non-injected control embryos (NIC) at 48 and 56 hpf with antibodies to detect the total number of neurons (HuC/D$^+$) and differentiated neurons of the lateral subnucleus (HuC$^+$Kctd12.1$^+$).

Non-injected control embryos develop more total neurons in the dorsal habenulae than N-cad morphants at 48 and 72 hpf. Control embryos have 50
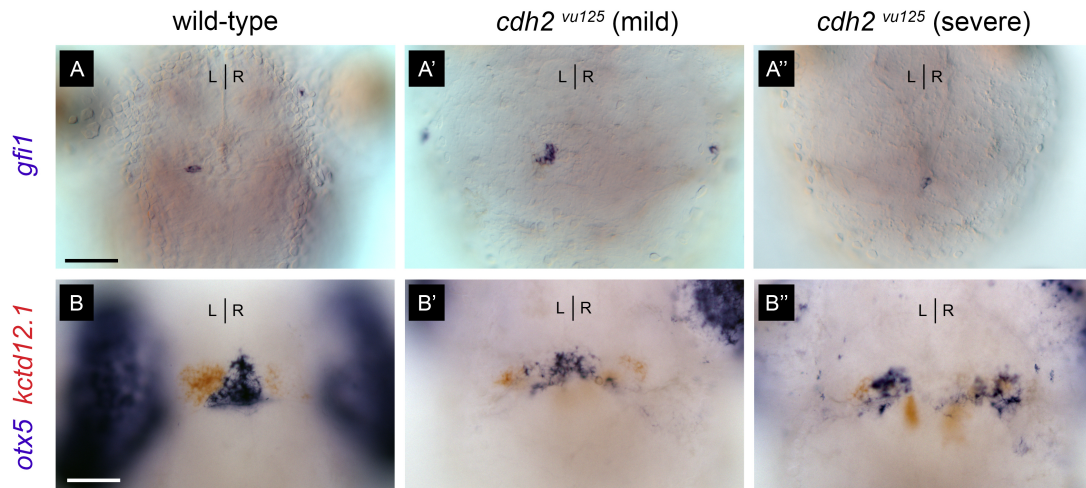
Figure 21. Despite incomplete neural tube closure, *cdh*[vu125] mutants generate lateralized parapineal organs. (A) The parapineal migrates to the left side of midline in wild-type embryos. Both mild (A') and severe (A'') *cdh*[vu125] mutants develop a single parapineal organ, though severe mutants do not always migrate away from the midline. (B) Pineal complex (*otx5*, blue) and lateral subnucleus neurons (*kctd12.1*, red) display L/R asymmetry and develop in the same dorsoventral plane. Severe *cdh*[vu125] mutants show incomplete neural tube closure (B'', *otx5*) and disrupted dorsal migration of LsDh neurons (B' and B'', *kctd12.1*). Scale bar = 10 μm. DIC images taken from dorsal aspect.

more total HuC$^+$ neurons at 48 hpf (Figure 22A''), and 100 more HuC$^+$ neurons than morphants at 72 hpf (Figure 22B''). Both morphants and controls displayed evidence of asymmetric neurogenesis during early phases of habenular development (48 hpf; AI^{NIC} = 0.11, AI^{cdh2MO} = 0.18) similar to previous studies (Roussigne et al., 2009).

Interestingly, at both 48 and 72 hpf, a higher proportion of morphant neurons in both habenulae co-express the HuC and Kctd12.1 than NIC (Figures 22A,A',B,B' insets; Figures 22A'',B'' green bars). This result suggests that loss of N-cadherin predisposes habenular precursor cells towards an LsDh fate. This result is especially striking in the RHb, where 64% of *cdh2* morphant habenular neurons are Kctd12.1$^+$, as compared to 44% in NIC at 48 hpf (Figure 22A'').

Sec61al1 and N-cadherin function in the same pathway for habenular development

To test the genetic relationship between Sec61al1 and N-cadherin on development of the lateral subnuclei of the dorsal habenulae, we generated larvae with depletion of both proteins simultaneously. If the two proteins function in the same pathway in habenular development, we would predict that the phenotype of doubly depleted larvae would resemble the phenotype when each protein is singly depleted. However, if an additive phenotype were observed in the doubly depleted larvae, this would indicate that the proteins act in separate pathways, each affecting habenular development. We find that asymmetry of the habenular nuclei in doubly depleted larvae is similar to singly depleted larvae
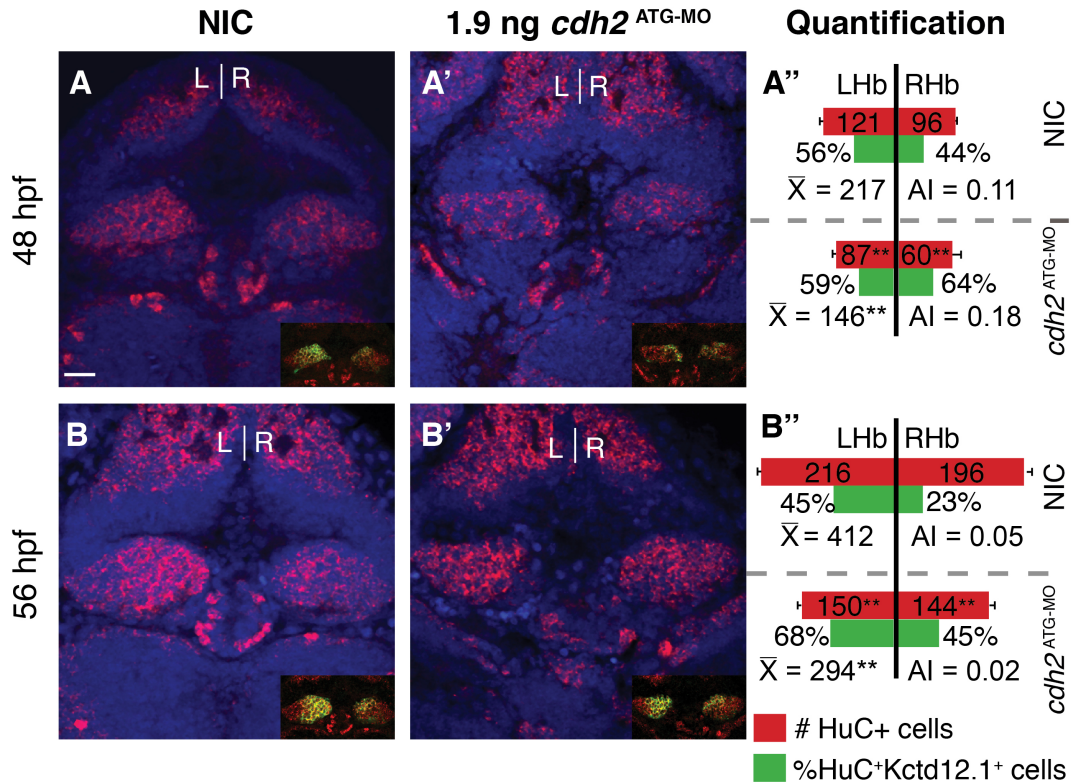
Figure 22. Progression of habenular neurogenesis upon depletion of *cdh2.* During early stages of habenular neurogenesis, non-injected control (NIC) embryos develop more HuC+ neurons on the left than the right (AI = 0.11; A,A''). Embryos depleted for N-cadherin retain habenular asymmetry at this stage (AI = 0.18), but do not produce as many neurons as wild-type. At 56 hpf, the right and left habenulae contain comparable numbers of neurons in NIC and morphants (B''), yet neurogenesis continues to lag in embryos depleted for *cdh2* (>100 fewer HuC+ cells than wild-type). Interestingly, a greater proportion of morphant habenular neurons express the LsDh marker Kctd12.1 than controls in each habenula at both time points (yellow bars). Inset images show expression of both HuC and Kctd12.1. **p<0.01. AI = asymmetry index. Scale = 10 μm.

(Figure 23). This suggests that function of one gene (*sec61al1*) is necessary for the expression, distribution, or transport of a second gene (*cdh2*).

We injected the progeny of a *cdh2*^{vu125} heterozygote cross with *sec61al1*$^{ATG-MO}$ and quantified the number of Kctd12.1+ neurons in the LsDh of both injected embryos and non-injected controls (NIC). This generates four classes of embryos: NIC wild-type (Figure 23A), NIC *cdh2*^{vu125} mutants (Figure 23B), wild-type + *sec61al1*$^{ATG-MO}$ (Figure 23A''), and *cdh2*^{vu125} + *sec61al1*$^{ATG-MO}$ (Figure 23B''). As expected, NIC wild-type embryos develop considerable LsDh asymmetry (AI = 0.49, average of 166 total Kctd12.1+ cells). Wild-type embryos injected with 500 pg *sec61al1*$^{ATG-MO}$ generate LsDh neurons, which are more symmetrically distributed, similar to our previous study (p<0.05 compared to NIC wild-type; AI = 0.11; average of 183 total Kctd12.1+ neurons)(Doll et al., 2011). NIC *cdh2*^{vu125} mutants also develop symmetrical habenula (AI = 0.14; p<0.05; 132 total Kctd12.1+ cells). Finally, asymmetry of the LsDh in larvae doubly depleted for *sec61al1* and *cdh2* resemble *cdh2*^{vu125} or *sec61al1*^{c163} single mutants (AI = 0.15; average of 123 cells; p<0.01 compared to NIC wild-type). Similar results were generated when *sec61al1* mutants were treated with *cdh2* morpholino (AI^{c163} = 0.17, AI^{cdh2ATGMO} = 0.08, AI$^{c163;cdh2ATGMO}$ = 0.12; Figure 23C). In summary, this test of genetic interaction indicates that the combined loss of both N-cadherin and Sec61al1 function has a similar effect on habenular asymmetry as loss of either protein alone.
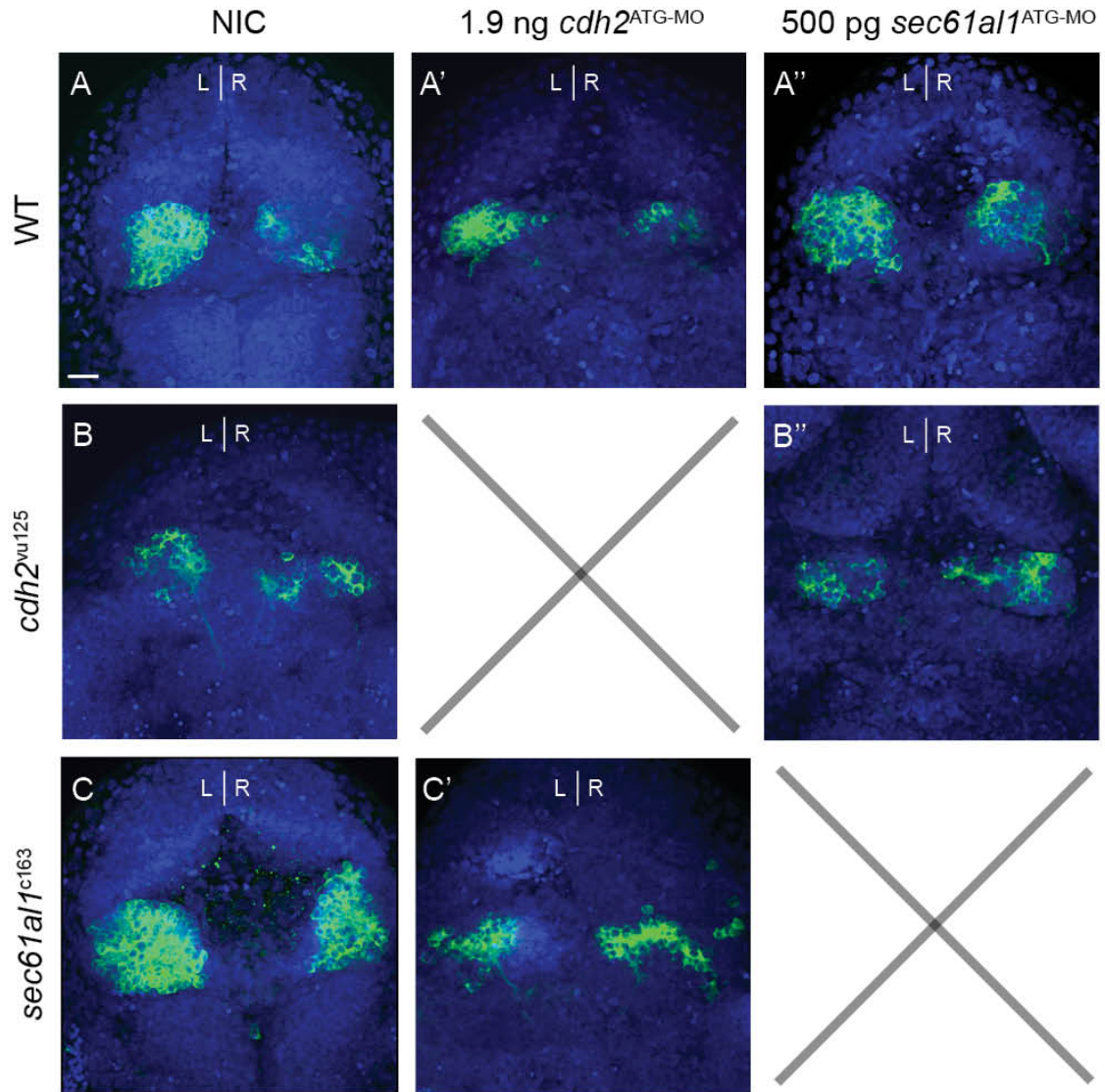
Figure 23. Genetic relationship between *sec61al1* and *cdh2* function on development of the LsDh. Morpholino-mediated depletion of both *cdh2* (A') and *sec61al1* (A'') in wild-type embryos leads to symmetric LsDh development, as compared to non-injected controls (A). The LsDh of *cdh2^vu125^* mutants depleted for *sec61al1* (B'') resemble single *cdh2^vu125^* mutants (B). Furthermore, morpholino depletion of *cdh2* in *sec61al1^c163^* mutants (C') leads to LsDh development reminiscent of *sec61al1^c163^* homozygous mutants (C). Scale bars = 10 μm. All images are 3D extended focus projections of confocal Z-stacks at 72 hpf.

Discussion

Our search for genes involved in L/R asymmetry generation in the dorsal diencephalon of zebrafish has led us to investigate a canonical member of the adherens junction, N-cadherin. This cell adhesion molecule modulates a variety of cellular activities, including proliferation of hindbrain neurons (Chalasani and Brewster, 2011), morphogenesis of chick brain (Detrick et al., 1990), neurulation (Hong and Brewster, 2006; Lele et al., 2002), cortical development (Kadowaki et al., 2007), orientation of multipolar neurons (Jossin and Cooper, 2011), sustained long-term potentiation (Bozdagi et al., 2000), and maintenance of neural progenitors (Rousso et al., 2012). With such important and diverse roles in neural development, we hypothesized that N-cadherin function may also be required for the control of asymmetric neurogenesis noted in the zebrafish habenulae (Aizawa et al., 2007). The present study is a continuation of previous work in which we noted the requirement for Sec61al1 in asymmetric development of the dorsal habenulae. As a transmembrane molecule, the N-cadherin protein represents a prime candidate to be trafficked through the Sec61 pore, as transmembrane proteins must be inserted into the ER membrane prior to transport to the cell surface.

Our previous study highlighted the fact that Sec61al1 function was necessary for both restricting the proliferation of habenular progenitors and promoting the differentiation of post-mitotic habenular neurons in the LsDh versus the MsDh. The present findings suggest a role for N-cadherin in

differentiation, but not proliferation. *cdh2* mutants and morphants generate fewer total dorsal habenular neurons than *sec61* mutants. However, *cdh2* morphants do develop symmetric LsDh, largely through a bilateral increase of Kctd12.1+ neurogenesis between 48 and 56 hpf as compared to wild-type. This symmetric neurogenesis is quite similar to the phenotype seen in *sec61al1* mutants (Doll et al., 2011). We infer that a protein(s) other than N-cad, trafficked via Sec61al1, restricts proliferation in habenular progenitor cells, despite the fact that previous studies have implicated N-cadherin in proliferation of other neuronal populations, including the zebrafish hindbrain (Chalasani Brewster). To address this directly, BrdU or EdU incorporation assays on *cdh2* mutants will help indicate whether loss of N-cadherin function affects Dh proliferation.

Importantly, a test of genetic interaction between *sec61al1* and *cdh2* indicates the two genes work in the same pathway toward LsDh development. Double morphants resemble individual single mutants, with bilaterally symmetric development of Kctd12.1+ neurons. We predict that N-cadherin does not impact the proliferation of habenular precursor cells. This can be further addressed through EdU-based proliferation assays at 32 and 48 hpf (similar to our *sec61al1* study). Interestingly, loss of N-cadherin increases proliferation of cells in the hindbrain of zebrafish (Chalasani and Brewster, 2011), though this increase did not appear to contribute to excess production of neurons.

Another interesting result concerns the high proportion of habenular neurons that adopt LsDh fate in embryos deficient for *cdh2* function. We are presently unable to address the development of the MsDh using Kctd12.2 as a

marker, because ectopic Kctd12.2 neurons from other regions of the brain are detected in the dorsal diencephalon of *cdh2* mutants. The identification of another marker specific to the MsDh may circumvent this issue. Nevertheless, the increased percentage of HuC+Kctd12.1+ neurons in *cdh2* morphants indicates that loss of N-cadherin influences the differentiation of habenular precursor cells. As a final note, although proliferation of hindbrain neurons is increased with loss of N-cadherin in zebrafish, this was not coupled with an increase in differentiation, as total HuC+ neurons appear reduced in the hindbrain of *cdh2* mutants (Chalasani and Brewster, 2011). N-cadherin and the adherens junction may interact with tissue-specific signaling pathways that control proliferation and/or differentiation of neurons, e.g. N-cadherin stabilization of beta-catenin in cortical precursors (Zhang et al., 2010).

CHAPTER IV

CONCLUSIONS AND FUTURE DIRECTIONS

ER Translocation and Zebrafish Development

Forward mutagenesis screens carry the profound capacity to implicate uncharacterized genes and to assign new functions to previously studied genes in a given developmental process. The zebrafish epithalamus has emerged as an excellent model of asymmetric brain development, though researchers continue to search for the molecular machinery that generates lateralized brain structures and gene expression. Our research on Sec61al1 adds to this genetic milieu, yet also serves as a starting point for further research. Sec61al1 impacts the production of hundreds of transmembrane and secreted proteins and could theoretically be used in enhancer screens to search for additional mediators of asymmetry. In short, much work remains to link the action of this ER translocon subunit toward production of the production of mature neurons from neuroepithelial progenitor cells.

Zebrafish development provides several crucial advantages over other vertebrate models when studying essential genes. Perhaps most important for this series of studies is the contribution of maternal transcripts in combination with a rapidly developing organism. Maternal loading provides embryos harboring lethal mutations the capacity to gastrulate and subsequently generate the nascent tissues of the body. *sec61* is an essential gene in yeast (Rapoport,

2007), and disruption of the endoplasmic reticular translocation machinery would most certainly prove lethal in other organisms. Maternal loading could in theory prove obstructive to research on early developmental processes, yet scientists can sidestep this by generating maternal-zygotic mutants to study the role of a given gene on early processes such as patterning and axis formation (Langdon and Mullins, 2011).

Our studies centered on neurodevelopment following neural tube closure in zebrafish, roughly between the hours of 24-72 post-fertilization. The maternal-to-zygotic transition (MTZ) - the point at which transcription of zygotic genes is enhanced and maternal transcripts begin to be degraded - occurs in zebrafish around 3.5 hpf (Tadros and Lipshitz, 2009). The ProtParam tool classifies the Sec61alpha protein channel as "Stable" (Instability Index = 28.27; values <40 are stable), and estimates a half-life of >20 hours *in vivo* in yeast, or 30 hours *in vitro* in human reticulocytes (yeastgenome.org)(Gasteiger E., 2005). Therefore, maternally loaded *sec61al1* transcript should facilitate development of zebrafish *sec61al1* mutants until at least 24 hours.

An alternative hypothesis to the maternal loading of Sec61al1 as mediator of early development is through compensatory activity of the closely related Sec61al2 (vertebrates possess 2 alpha subunit genes). Under this hypothesis, disrupted Sec61al1 function would spur the increase of *sec61al2* transcription and the Sec61al2 would mediate developmental processes. We have addressed this hypothesis in unpublished studies. Using RT-PCR we confirmed the presence of maternal *al1* and *al2* transcripts, as previously reported (Giraldez et

al., 2006). However, after the MTZ transition, transcription of *al2* decreases dramatically, and remains low throughout larval stages. In addition, there was no significant increase in *al2* transcription in *sec61al1^c163* mutants during larval stages (Table 1). Finally, depletion of *sec61al2* via injection of antisense morpholino did not affect LsDh development (Figure 24). In the zebrafish, the Sec61al1 subunit is likely to mediate most ER translocation, with limited contribution from the *sec61al2* gene.

At this point it is useful to envision the development of a mutant harboring a lethal mutation as a process of both development and degradation. We hypothesize that as maternal (wild-type) copies of the Sec61al1 translocon subunit degrade, the zygotic Sec61al1 is unable to provide the same translocation activity, as the mutant subunit lacks 6 of 10 transmembrane domains. We would thus anticipate production of truncated Sec61al1 protein (or degradation of incomplete *sec61al1* mRNA) between 24 and 30 hpf. Our data fit this model, as *sec61al1^c163* mutants can be distinguished by ~30 hpf by their characteristic retardation of jaw growth. Electron micrographs of Sec61al mutant jaws illustrate the lack of ER in highly secretory cell types and the impact on extracellular collagen deposition. This phenotype indicates that some cell types require additional translocation activity, though it is likely that in time all cell types would be affected. As a next step, it would be informative to perform Western blots from *sec61al* mutant and wild-type tissue for Sec61al1 over an extended developmental window; the presence of truncated protein bands would indicate

translation of an incomplete subunit, whereas a lack of band would suggest that truncated *sec61al1* mRNA was degraded.

Although *sec61al1* is an essential gene and would therefore be embryonic lethal when completely inactivated in humans, the broader protein secretion pathway has been associated with several malformations (perhaps due to a greater capacity to compensate with other gene isoforms). For example, mutations in the COPII coat proteins, which facilitate endoplasmic reticulum-to-Golgi protein transport, lead to craniofacial deformities in humans, a developmental defect also seen in zebrafish COPII mutations (Lang et al., 2006; Sarmah et al., 2010). As COPII components show cargo specificity (Melville et al., 2011), we sought to investigate the impact of two COPII gene isoforms on brain development, and therefore processed zebrafish *sec23a* mutants and *sec23b* morphants for LsDh development. The *sec23b* morphants developed symmetric LsDh, while *sec23a* mutant (*crusher*) LsDh developed asymmetric habenula similar to wild-type (Figure 24). Ultimately this suggests that secretory pathway components downstream of the ER translocon also impact Dh neurogenesis in an isoform-specific manner. The cargo-specific roles for individual isoforms could reveal a subset of *sec23b*-dependent proteins to narrow the search for LsDh asymmetry determinants.

The impact of ER translocation on the brain is not as immediately obvious as jaw chondrocytes through electron micrographs. Cells of the dorsal diencephalon and progenitor cells overlying the 3rd ventricle possess scant cytoplasm and we failed to detect the presence of a single endoplasmic reticulum
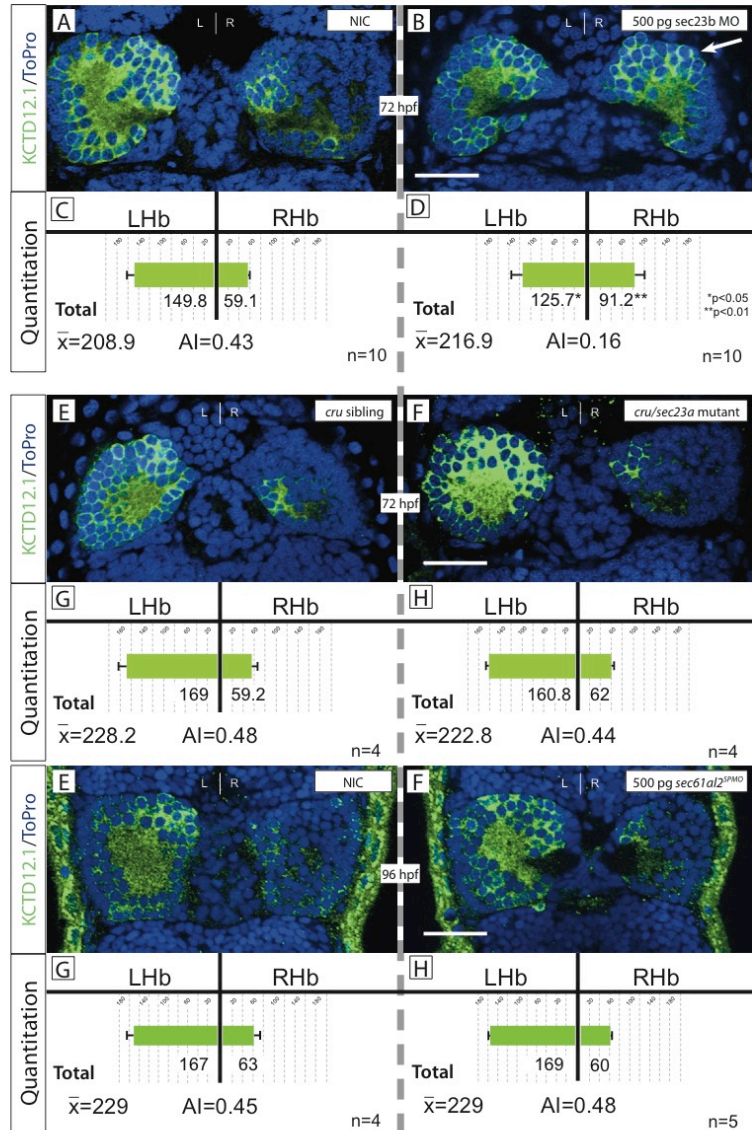
Figure 24. Specific paralogs of exocytic pathway genes are required for habenular asymmetry. Injection of 500 pg of $sec23b^{ATG\text{-}MO}$ is sufficient to disrupt asymmetry in the lateral subnucleus of the LdHb (B, white arrow), similar to the symmetry noted in *sec61al1* mutants at 72 hpf (Figure 3H, identical AI=0.16). However, mutation of the other *sec23* paralog: *sec23a/crusher* results in stereotypical asymmetric habenular development (F). In addition, disruption of the second *sec61alpha* paralog, using 500 pg $sec61al2^{SP\text{-}MO}$ also has no effect on lateral subnuclear development (J). Scale bars represent 33 uM. Significance determined by Student's T-Test.

in wild-type (30+ micrographs). Nevertheless, the impact of Sec61 disruption was fully evident at 54 hpf: the columnar cells of wild-type neuroepithelia were replaced by multilayered cells with apical blebbing in *sec61al1* mutants. Cell-cell junctions were reduced or wholly absent and ventricular cells (progenitors or former progenitors) resembled their dorsal periventricular neighbors (basal progenitors and precursors) in both morphology and nuclear composition. These ultrastructural views centered our focus on habenular neurogenesis and the proliferation of habenular precursor cells.

Impact of Sec61al1 depletion on habenular neurogenesis

Previous work has described the time course of neurogenesis in the lateral and medial subnuclei of the dorsal habenulae (Aizawa et al., 2007). Using incorporation of a BrdU as a marker of birth date, they demonstrated that LsDh neurons are first born soon after 24 hpf, and the peak of LsDh neurogenesis occurs at 32 hpf. The first MsDh neurons were not born until around 32 hpf, with the peak neurogenesis occurring at 48 hpf (Aizawa et al., 2007). The progenitors of the habenular neurons are bipotential, with single neuroepithelial cells able to give rise to both MsDh and LsDh neurons (Aizawa et al., 2007). We hypothesize that loss of Sec61al1 function in the neuroepithelium coincides with the onset of Dh neurogenesis. Furthermore, Sec61al1 is required to produce components of the adherens junction; in the absence of Sec61 function, cells of the neuroepithelium lose contact with one another, thereby losing their status as bipotential progenitor cells. This loss of progenitor status thereby limits the

capacity to generate neurons of the later-born MsDh class. Accordingly, Sec61al1 mutants produce an overabundance of LsDh neurons on both sides of the brain, and generate far fewer MsDh neurons.

We repeated LsDh birth dating experiments on *sec61al1* mutants and siblings and found that mutants produce LsDh neurons in the right habenula for longer period of time than wild-type, indicating an expansion of LsDh proliferation. There are two conceivable scenarios to explain this phenomenon: 1) loss of apical-basal polarity leads to equal inheritance of cell fate factors (Geldmacher-Voss et al., 2003; Wodarz and Huttner, 2003; Zhong and Chia, 2008), thereby fating all daughter cells toward the LsDh class. 2) the length of the cell cycle is altered in *sec61al1* habenular precursors, thereby leading to production of one class of neurons over another. We favor the former hypothesis, as disruption of another apical-basal polarity component, N-cadherin, leads to habenular development in which a significantly increased proportion of neurons contributing to the LsDh, although a contribution of cell cycle length has not been ruled out. Further study is necessary to investigate the presence and inheritance of factors contributing to dorsal subnucleus fate, although speculation will continue in the N-cadherin portion of this discussion.

Importantly, *sec61al1* mutants develop with early aspects of epithalamic asymmetry intact. A left-sided parapineal and left-sided Nodal signaling are necessary for the elaboration of LsDh in the left half of the brain (Concha et al., 2003; Gamse et al., 2005; Gamse et al., 2003). *sec61al1* mutants possess both of these lateralized features. In addition, neurogenesis initiates asymmetrically in

sec61al1 mutants (Figure 11A'). Despite all of these asymmetric cues, the subnuclei of mutants develop symmetrically. This can be explained through the dramatic increase in LsDh neurogenesis between 48 and 72 hpf in *sec61al1* mutants (Figure 5C',F'). These mutants continue to produce LsDh neurons after the characterized switch toward contribution to the MsDh, thereby generating subnuclei that resemble one another. We infer that the left-sided parapineal/left-sided Nodal normally induces a switch in habenular progenitor cells, instructing them to produce more MsDh and fewer LsDh neurons. Control of this switch is not yet understood but appears to involve activation of Notch signaling (Aizawa et al., 2007).

Translocation candidate, N-cadherin, mediates asymmetric neurogenesis in the dorsal habenula

cdh2 encodes N-cadherin, a canonical transmembrane cell adhesion molecule (Tepass et al., 2000). The importance of N-cadherin in neurodevelopment has been underlined repeatedly in this manuscript. As a transmembrane protein, it must be inserted into the ER membrane by activity of the Sec61 translocon channel. Accordingly, the loss of Sec61al1 activity results in a dramatic reduction of N-cadherin expression at the apical surface of neuroepithelial cells of the 3rd ventricle (Figure 18). In fact, embryos deficient for Sec61al1 function fail to apically traffic an assortment of canonical adherens junction proteins, including N-cadherin, β -catenin, aPKC, and F-actin. Collectively, the failure to deliver these components to the ventricular surface

suggests a failure of AJ formation. It is difficult to predict whether apical delivery of some AJ components is dependent on others, though the adhesive function of cadherins may be primarily essential, especially in the formation of epithelia (Green et al., 2010), and N-cadherin is the only one of these proteins that requires Sec61 activity for trafficking.

The symmetric LsDh development seen in *cdh2*[vu125] is quite reminiscent of Sec61al1 mutants. Like the latter mutants, *cdh2*[vu125] also develop asymmetric epithalamia, with single, left-sided parapineal organs (Figure 21). In addition, a neurogenesis timeline indicates that habenular neurogenesis initiates asymmetrically, as in wild-type (Figure 22)(Aizawa et al., 2007). It will be important to investigate the expression of Nodal genes in early stage *cdh2*[vu125] larvae to further confirm the presence of asymmetric cues. *cdh2*[vu125] mutants have neural tube closure defects, and it is unknown whether midline defects are also present ventrally at the floorplate, normally serves as a barrier to prevent left-sided Nodal expression from being activated on the right side as well (Sampath et al., 1998). Intriguingly, Nodal signaling is required for expression and localization of N-cadherin in the neural tube (Aquilina-Beck et al., 2007).

Though *cdh2*[vu125] mutants generate symmetric LsDh, these subnuclei do not contain as many neurons as in wild-type. This is a significant departure from the *sec61al1* mutant phenotype, which produces excess LsDh neurons as compared to wild-type. However, double morphant analysis indicates that Sec61al1 and N-cadherin function in the same pathway for LsDh asymmetry (Figure 23). In addition, *cdh2*[vu125] mutant habenulae have a higher proportion of

LsDh neurons in the dorsal habenula, also reminiscent of the Sec61al1 mutant phenotype. Therefore, we can conclude that N-cadherin, trafficked through Sec61al1, mediates asymmetric development of the dorsal habenulae, though the precise mechanism is not clear. We speculate that loss of N-cadherin leads to neuroepithelial delamination, loss of progenitor fate, and adoption of LsDh fate through a process of cell fate determinant inheritance.

In addition, Sec61al1 likely traffics another protein that affects proliferation of habenular precursor cells, as *sec61al1* mutants but not *cdh2* mutants exhibit excess proliferation. Components of the Notch/Delta, Wnt, and Fgf signaling pathways have all been implicated in proliferation of habenular neurons (Aizawa et al., 2007; Carl et al., 2007; Regan et al., 2009). Examining the trafficking of receptors and ligands in *sec61al1* mutants is an important future direction.

Another intriguing phenotype in *cdh2* mutants is the lack of cohesion of Kctd12.1+ cells in the dorsal habenula. From unpublished time lapse imaging of *Tg(HuC:Kaede)* embryos, it appears that habenular neurons migrate dorsally from the ventricular zone using chain migration (neurons remain in contact with one another). This process is similar to the cellular behaviors characterized in the rostral migratory stream (RMS) of mice. During chain migration of the RMS, neurons directly contact one another (Lois et al., 1996), in an N-cadherin dependent manner (Yagita et al., 2009). In addition, N-cadherin is abundantly expressed in murine neurospheres in culture (Lobo et al., 2003), and suppression of N-cadherin prevents neurosphere formation (Yagita et al., 2009). In an in vivo model, N-cadherin regulates the cortical organization of the mouse

cortex; upon conditional deletion of N-cadherin, intra-cortical structures were randomized with mitotic and post-mitotic cells scattered at random in the cortex (Kadowaki et al., 2007). Finally, N-cadherin expression is downregulated with the onset of neurosphere differentiation (Yagita et al., 2009). Collectively, this data indicates that both chain migration and cohesion of undifferentiated precursor cells requires N-cadherin in many contexts, and this may include habenular nucleus formation.

Several signaling pathways may mediate the mechanism of LsDh fate determination. We extensively investigated the role of Notch signaling on dorsal habenular development. Similar to previous studies, we found that constitutive expression of the Notch Intracellular Domain (NICD) specifically in the habenula results in a complete blockage of Dh neurogenesis. In addition, mib^{ta52b} mutants, (Mib is a ubiquitin protease necessary to cleave Delta protein on the signaling cell), which lack Notch signaling develop symmetric Dh (Figure 25A')(Aizawa et al., 2007). However, we found that symmetric Dh development is likely due to profound neural tube closure defects, as mib^{ta52b} mutants possess substantial populations of both LsDh and MsDh neurons at the midline, ventral to the dorsal surface (Figure 25A'). Conversely, constitutive Notch activity through Dh-specific expression of the Notch Intracellular Domain (NICD) leads to complete suppression of Kctd12.1 expression (Figure 25B'). Therefore, alteration of Notch signaling results in severe Dh phenotypes and thus Notch likely plays an essential role in habenular neurogenesis. As a juxtacrine signaling pathway, and a canonical mediator of progenitor cell fate in the nervous system (Louvi and
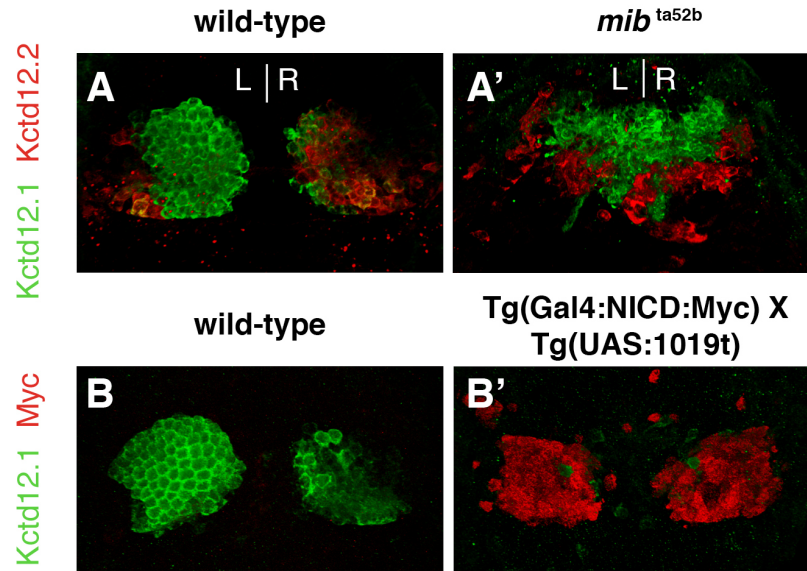
Figure 25. Effects of Notch pathway manipulation on dorsal habenula development. (A) *mib^{ta52b}* mutants generate excess neurons of both the LsDh and MsDh classes, with both subnuclei developing at the midline. (B) Specific overexpression of the Notch Intracellular Domain (NICD) via the UAS:1019t:Myc driver results in complete suppression of Kctd12.1 expression

Artavanis-Tsakonas, 2006) Notch signaling could theoretically be impacted by disruptions to the neuroepithelium. Loss of adherens junctions and columnar morphology could prevent Delta-Notch juxtacrine signaling and lead to the loss of progenitor fate. Hypomorphic *mib* alleles and more precise manipulation of Notch signaling in time and space could shed more light on the role and timing of Notch involvement in habenular development.

Recent studies implicate an interaction between N-cadherin and β-catenin signaling on development of the nervous system. In the spinal cord, activity of both N-cadherin and β/γ-catenins are necessary for correct motor neuron positioning and target specificity (Demireva et al., 2011). In addition, β-catenin signaling regulates precursor fate; knockdown of N-cadherin in vivo reduces β-catenin, leading to premature migration from the neural niche and increased differentiation (Zhang et al., 2010). In addition, excess Wnt signaling results in symmetric development of the habenular nuclei (Carl et al., 2007). Therefore, further investigation of β-catenin signaling and transcriptional response in both *sec61al1* and *cdh2* mutant zebrafish may reveal the molecular switch leading to premature differentiation of LsDh neurons.

In conclusion, the list of genes affecting asymmetric development in the zebrafish epithalamus continues to grow. We have characterized two genes that likely affect habenular neurogenesis by stabilizing neuroepithelial progenitor cells through adherens junctions. Sec61al1 and N-cadherin do not directly affect the initiation of asymmetric neurogenesis in habenular precursors, but rather promote asymmetric dorsal habenula by affecting differentiation of nascent post-

mitotic precursor cells. This work highlights the importance of adherens junctions in neurogenesis and facilitates further investigations into the cell fate determinants that influence the subnuclear differentiation of dorsal habenular neurons.

REFERENCES

Aaku-Saraste, E., Hellwig, A., Huttner, W.B., 1996. Loss of occludin and functional tight junctions, but not ZO-1, during neural tube closure--remodeling of the neuroepithelium prior to neurogenesis. Dev Biol 180, 664-679.

Adzick, N.S., 2010. Fetal myelomeningocele: natural history, pathophysiology, and in-utero intervention. Semin Fetal Neonatal Med 15, 9-14.

Agathon, A., Thisse, C., Thisse, B., 2003. The molecular nature of the zebrafish tail organizer. Nature 424, 448-452.

Agetsuma, M., Aizawa, H., Aoki, T., Nakayama, R., Takahoko, M., Goto, M., Sassa, T., Amo, R., Shiraki, T., Kawakami, K., Hosoya, T., Higashijima, S., Okamoto, H., 2010. The habenula is crucial for experience-dependent modification of fear responses in zebrafish. Nat Neurosci 13, 1354-1356.

Aizawa, H., Bianco, I.H., Hamaoka, T., Miyashita, T., Uemura, O., Concha, M.L., Russell, C., Wilson, S.W., Okamoto, H., 2005. Laterotopic representation of left-right information onto the dorso-ventral axis of a zebrafish midbrain target nucleus. Curr Biol 15, 238-243.

Aizawa, H., Goto, M., Sato, T., Okamoto, H., 2007. Temporally regulated asymmetric neurogenesis causes left-right difference in the zebrafish habenular structures. Dev Cell 12, 87-98.

Allwardt, B.A., Lall, A.B., Brockerhoff, S.E., Dowling, J.E., 2001. Synapse formation is arrested in retinal photoreceptors of the zebrafish nrc mutant. J Neurosci 21, 2330-2342.

Altman, J., Bayer, S.A., 1978. Development of the diencephalon in the rat. I. Autoradiographic study of the time of origin and settling patterns of neurons of the hypothalamus. J Comp Neurol 182, 945-971.

Alvarez-Medina, R., Cayuso, J., Okubo, T., Takada, S., Marti, E., 2008. Wnt canonical pathway restricts graded Shh/Gli patterning activity through the regulation of Gli3 expression. Development 135, 237-247.

Aquilina-Beck, A., Ilagan, K., Liu, Q., Liang, J.O., 2007. Nodal signaling is required for closure of the anterior neural tube in zebrafish. BMC Dev Biol 7, 126.

Araki, I., Nakamura, H., 1999. Engrailed defines the position of dorsal di-mesencephalic boundary by repressing diencephalic fate. Development 126, 5127-5135.

Argenton, F., Zecchin, E., Bortolussi, M., 1999. Early appearance of pancreatic hormone-expressing cells in the zebrafish embryo. Mech Dev 87, 217-221.

Arias-Carrion, O., Poppel, E., 2007. Dopamine, learning, and reward-seeking behavior. Acta Neurobiol Exp (Wars) 67, 481-488.

Arnold-Aldea, S.A., Cepko, C.L., 1996. Dispersion patterns of clonally related cells during development of the hypothalamus. Dev Biol 173, 148-161.

Aubert, J., Dunstan, H., Chambers, I., Smith, A., 2002. Functional gene screening in embryonic stem cells implicates Wnt antagonism in neural differentiation. Nat Biotechnol 20, 1240-1245.

Bach, A., Lallemand, Y., Nicola, M.A., Ramos, C., Mathis, L., Maufras, M., Robert, B., 2003. Msx1 is required for dorsal diencephalon patterning. Development 130, 4025-4036.

Bagatto, B., Francl, J., Liu, B., Liu, Q., 2006. Cadherin2 (N-cadherin) plays an essential role in zebrafish cardiovascular development. BMC Dev Biol 6, 23.

Bahary, N., Davidson, A., Ransom, D., Shepard, J., Stern, H., Trede, N., Zhou, Y., Barut, B., Zon, L.I., 2004. The Zon laboratory guide to positional cloning in zebrafish. Methods Cell Biol 77, 305-329.

Bang, A.G., Goulding, M.D., 1996. Regulation of vertebrate neural cell fate by transcription factors. Curr Opin Neurobiol 6, 25-32.

Beaumont, J.G., 2008. Introduction to neuropsychology, 2nd ed. Guilford Press, New York.

Bellaiche, Y., Radovic, A., Woods, D.F., Hough, C.D., Parmentier, M.L., O'Kane, C.J., Bryant, P.J., Schweisguth, F., 2001. The Partner of Inscuteable/Discs-large complex is required to establish planar polarity during asymmetric cell division in Drosophila. Cell 106, 355-366.

Bianco, I.H., Carl, M., Russell, C., Clarke, J.D., Wilson, S.W., 2008. Brain asymmetry is encoded at the level of axon terminal morphology. Neural Dev 3, 9.

Bisgrove, B.W., Essner, J.J., Yost, H.J., 2000. Multiple pathways in the midline regulate concordant brain, heart and gut left-right asymmetry. Development 127, 3567-3579.

Boller, F., 1988. Handbook of neuropsychology. Elsevier, Amsterdam ; New York.

Boorman, C.J., Shimeld, S.M., 2002a. The evolution of left-right asymmetry in chordates. Bioessays 24, 1004-1011.

Boorman, C.J., Shimeld, S.M., 2002b. Pitx homeobox genes in Ciona and amphioxus show left-right asymmetry is a conserved chordate character and define the ascidian adenohypophysis. Evol Dev 4, 354-365.

Borod, J.C., Bloom, R.L., Brickman, A.M., Nakhutina, L., Curko, E.A., 2002. Emotional processing deficits in individuals with unilateral brain damage. Appl Neuropsychol 9, 23-36.

Boyadjiev, S.A., Fromme, J.C., Ben, J., Chong, S.S., Nauta, C., Hur, D.J., Zhang, G., Hamamoto, S., Schekman, R., Ravazzola, M., Orci, L., Eyaid, W., 2006. Cranio-lenticulo-sutural dysplasia is caused by a SEC23A mutation leading to abnormal endoplasmic-reticulum-to-Golgi trafficking. Nat Genet 38, 1192-1197.

Bozdagi, O., Shan, W., Tanaka, H., Benson, D.L., Huntley, G.W., 2000. Increasing numbers of synaptic puncta during late-phase LTP: N-cadherin is synthesized, recruited to synaptic sites, and required for potentiation. Neuron 28, 245-259.

Braun, M.M., Etheridge, A., Bernard, A., Robertson, C.P., Roelink, H., 2003. Wnt signaling is required at distinct stages of development for the induction of the posterior forebrain. Development 130, 5579-5587.

Bronner-Fraser, M., Fraser, S., 1989. Developmental potential of avian trunk neural crest cells in situ. Neuron 3, 755-766.

Bronner-Fraser, M., Fraser, S.E., 1988. Cell lineage analysis reveals multipotency of some avian neural crest cells. Nature 335, 161-164.

Bronner-Fraser, M., Wolf, J.J., Murray, B.A., 1992. Effects of antibodies against N-cadherin and N-CAM on the cranial neural crest and neural tube. Dev Biol 153, 291-301.

Bronson, R.T., Lane, P.W., 1990. Hydrocephalus with hop gait (hyh): a new mutation on chromosome 7 in the mouse. Brain Res Dev Brain Res 54, 131-136.

Bultje, R.S., Castaneda-Castellanos, D.R., Jan, L.Y., Jan, Y.N., Kriegstein, A.R., Shi, S.H., 2009. Mammalian Par3 regulates progenitor cell asymmetric division via notch signaling in the developing neocortex. Neuron 63, 189-202.

Calegari, F., Haubensak, W., Haffner, C., Huttner, W.B., 2005. Selective lengthening of the cell cycle in the neurogenic subpopulation of neural progenitor cells during mouse brain development. J Neurosci 25, 6533-6538.

Calegari, F., Huttner, W.B., 2003. An inhibition of cyclin-dependent kinases that lengthens, but does not arrest, neuroepithelial cell cycle induces premature neurogenesis. J Cell Sci 116, 4947-4955.

Campione, M., Steinbeisser, H., Schweickert, A., Deissler, K., van Bebber, F., Lowe, L.A., Nowotschin, S., Viebahn, C., Haffter, P., Kuehn, M.R., Blum, M., 1999. The homeobox gene Pitx2: mediator of asymmetric left-right signaling in vertebrate heart and gut looping. Development 126, 1225-1234.

Cantalupo, C., Hopkins, W.D., 2001. Asymmetric Broca's area in great apes. Nature 414, 505.

Capdevila, J., Vogan, K.J., Tabin, C.J., Izpisua Belmonte, J.C., 2000. Mechanisms of left-right determination in vertebrates. Cell 101, 9-21.

Cappello, S., Attardo, A., Wu, X., Iwasato, T., Itohara, S., Wilsch-Brauninger, M., Eilken, H.M., Rieger, M.A., Schroeder, T.T., Huttner, W.B., Brakebusch, C., Gotz, M., 2006. The Rho-GTPase cdc42 regulates neural progenitor fate at the apical surface. Nat Neurosci 9, 1099-1107.

Carl, M., Bianco, I.H., Bajoghli, B., Aghaallaei, N., Czerny, T., Wilson, S.W., 2007. Wnt/Axin1/beta-catenin signaling regulates asymmetric nodal activation, elaboration, and concordance of CNS asymmetries. Neuron 55, 393-405.

Caviness, V.S., Jr., Takahashi, T., Nowakowski, R.S., 2000. Neocortical malformation as consequence of nonadaptive regulation of neuronogenetic sequence. Ment Retard Dev Disabil Res Rev 6, 22-33.

Cayouette, M., Raff, M., 2002. Asymmetric segregation of Numb: a mechanism for neural specification from Drosophila to mammals. Nat Neurosci 5, 1265-1269.

Chae, T.H., Kim, S., Marz, K.E., Hanson, P.I., Walsh, C.A., 2004. The hyh mutation uncovers roles for alpha Snap in apical protein localization and control of neural cell fate. Nat Genet 36, 264-270.

Chalasani, K., Brewster, R.M., 2011. N-cadherin-mediated cell adhesion restricts cell proliferation in the dorsal neural tube. Mol Biol Cell 22, 1505-1515.

Changeux, J.-P., 1997. Neuronal man : the biology of mind. Princeton University Press, Princeton, N.J.

Chatterjee, M., Li, J.Y., 2012. Patterning and compartment formation in the diencephalon. Front Neurosci 6, 66.

Cheng, A.M., Thisse, B., Thisse, C., Wright, C.V., 2000. The lefty-related factor Xatv acts as a feedback inhibitor of nodal signaling in mesoderm induction and L-R axis development in xenopus. Development 127, 1049-1061.

Chenn, A., McConnell, S.K., 1995. Cleavage orientation and the asymmetric inheritance of Notch1 immunoreactivity in mammalian neurogenesis. Cell 82, 631-641.

Chenn, A., Walsh, C.A., 2002. Regulation of cerebral cortical size by control of cell cycle exit in neural precursors. Science 297, 365-369.

Chenn, A., Zhang, Y.A., Chang, B.T., McConnell, S.K., 1998. Intrinsic polarity of mammalian neuroepithelial cells. Mol Cell Neurosci 11, 183-193.

Chiang, C., Litingtung, Y., Lee, E., Young, K.E., Corden, J.L., Westphal, H., Beachy, P.A., 1996. Cyclopia and defective axial patterning in mice lacking Sonic hedgehog gene function. Nature 383, 407-413.

Chizhikov, V.V., Millen, K.J., 2004. Control of roof plate formation by Lmx1a in the developing spinal cord. Development 131, 2693-2705.

Cho, K.W., De Robertis, E.M., 1990. Differential activation of Xenopus homeo box genes by mesoderm-inducing growth factors and retinoic acid. Genes Dev 4, 1910-1916.

Clary, D.O., Griff, I.C., Rothman, J.E., 1990. SNAPs, a family of NSF attachment proteins involved in intracellular membrane fusion in animals and yeast. Cell 61, 709-721.

Colas, J.F., Schoenwolf, G.C., 2000. Subtractive hybridization identifies chick-cripto, a novel EGF-CFC ortholog expressed during gastrulation, neurulation and early cardiogenesis. Gene 255, 205-217.

Collignon, J., Varlet, I., Robertson, E.J., 1996. Relationship between asymmetric nodal expression and the direction of embryonic turning. Nature 381, 155-158.

Collin, J.P., Voisin, P., Falcon, J., Faure, J.P., Brisson, P., Defaye, J.R., 1989. Pineal transducers in the course of evolution: molecular organization, rhythmic metabolic activity and role. Arch Histol Cytol 52 Suppl, 441-449.

Concha, M.L., Burdine, R.D., Russell, C., Schier, A.F., Wilson, S.W., 2000. A nodal signaling pathway regulates the laterality of neuroanatomical asymmetries in the zebrafish forebrain. Neuron 28, 399-409.

Concha, M.L., Russell, C., Regan, J.C., Tawk, M., Sidi, S., Gilmour, D.T., Kapsimali, M., Sumoy, L., Goldstone, K., Amaya, E., Kimelman, D., Nicolson, T., Grunder, S., Gomperts, M., Clarke, J.D., Wilson, S.W., 2003. Local tissue interactions across the dorsal midline of the forebrain establish CNS laterality. Neuron 39, 423-438.

Concha, M.L., Wilson, S.W., 2001. Asymmetry in the epithalamus of vertebrates. J Anat 199, 63-84.

Cooke, J., 2004. The evolutionary origins and significance of vertebrate left-right organisation. Bioessays 26, 413-421.

Corballis, M.C., 2009. The evolution and genetics of cerebral asymmetry. Philos Trans R Soc Lond B Biol Sci 364, 867-879.

Costa, M.R., Wen, G., Lepier, A., Schroeder, T., Gotz, M., 2008. Par-complex proteins promote proliferative progenitor divisions in the developing mouse cerebral cortex. Development 135, 11-22.

Courchesne, E., Pierce, K., Schumann, C.M., Redcay, E., Buckwalter, J.A., Kennedy, D.P., Morgan, J., 2007. Mapping early brain development in autism. Neuron 56, 399-413.

D'Souza-Schorey, C., 2005. Disassembling adherens junctions: breaking up is hard to do. Trends Cell Biol 15, 19-26.

Dale, L., Wardle, F.C., 1999. A gradient of BMP activity specifies dorsal-ventral fates in early Xenopus embryos. Semin Cell Dev Biol 10, 319-326.

Damasio, A.R., Geschwind, N., 1984. The neural basis of language. Annu Rev Neurosci 7, 127-147.

Dantzig, A.H., Hoskins, J.A., Tabas, L.B., Bright, S., Shepard, R.L., Jenkins, I.L., Duckworth, D.C., Sportsman, J.R., Mackensen, D., Rosteck, P.R., Jr., et al., 1994. Association of intestinal peptide transport with a protein related to the cadherin superfamily. Science 264, 430-433.

Delaune, E., Lemaire, P., Kodjabachian, L., 2005. Neural induction in Xenopus requires early FGF signalling in addition to BMP inhibition. Development 132, 299-310.

Demireva, E.Y., Shapiro, L.S., Jessell, T.M., Zampieri, N., 2011. Motor neuron position and topographic order imposed by beta- and gamma-catenin activities. Cell 147, 641-652.

Deng, C., Rogers, L.J., 1997. Differential contributions of the two visual pathways to functional lateralization in chicks. Behav Brain Res 87, 173-182.

Desmond, M.E., Levitan, M.L., 2002. Brain expansion in the chick embryo initiated by experimentally produced occlusion of the spinal neurocoel. Anat Rec 268, 147-159.

Desmond, M.E., Schoenwolf, G.C., 1985. Timing and positioning of occlusion of the spinal neurocele in the chick embryo. J Comp Neurol 235, 479-487.

Detrait, E.R., George, T.M., Etchevers, H.C., Gilbert, J.R., Vekemans, M., Speer, M.C., 2005. Human neural tube defects: developmental biology, epidemiology, and genetics. Neurotoxicol Teratol 27, 515-524.

Detrick, R.J., Dickey, D., Kintner, C.R., 1990. The effects of N-cadherin misexpression on morphogenesis in Xenopus embryos. Neuron 4, 493-506.

Dharmaretnam, M., Rogers, L.J., 2005. Hemispheric specialization and dual processing in strongly versus weakly lateralized chicks. Behav Brain Res 162, 62-70.

Diaz, E., Bravo, D., Rojas, X., Concha, M.L., 2011. Morphologic and immunohistochemical organization of the human habenular complex. J Comp Neurol 519, 3727-3747.

Doll, C.A., Burkart, J.T., Hope, K.D., Halpern, M.E., Gamse, J.T., 2011. Subnuclear development of the zebrafish habenular nuclei requires ER translocon function. Dev Biol 360, 44-57.

Doyle, S., Menaker, M., 2007. Circadian photoreception in vertebrates. Cold Spring Harb Symp Quant Biol 72, 499-508.

Dufourcq, P., Rastegar, S., Strahle, U., Blader, P., 2004. Parapineal specific expression of gfi1 in the zebrafish epithalamus. Gene Expr Patterns 4, 53-57.

Echelard, Y., Epstein, D.J., St-Jacques, B., Shen, L., Mohler, J., McMahon, J.A., McMahon, A.P., 1993. Sonic hedgehog, a member of a family of putative signaling molecules, is implicated in the regulation of CNS polarity. Cell 75, 1417-1430.

Emery, J.L., 1963. Functional Asymmetry of the Liver. Ann N Y Acad Sci 111, 37-44.

Engelhardt, B., Sorokin, L., 2009. The blood-brain and the blood-cerebrospinal fluid barriers: function and dysfunction. Semin Immunopathol 31, 497-511.

Epstein, D.J., Vekemans, M., Gros, P., 1991. Splotch (Sp2H), a mutation affecting development of the mouse neural tube, shows a deletion within the paired homeodomain of Pax-3. Cell 67, 767-774.

Ericson, J., Briscoe, J., Rashbass, P., van Heyningen, V., Jessell, T.M., 1997. Graded sonic hedgehog signaling and the specification of cell fate in the ventral neural tube. Cold Spring Harb Symp Quant Biol 62, 451-466.

Ericson, J., Morton, S., Kawakami, A., Roelink, H., Jessell, T.M., 1996. Two critical periods of Sonic Hedgehog signaling required for the specification of motor neuron identity. Cell 87, 661-673.

Essner, J.J., Vogan, K.J., Wagner, M.K., Tabin, C.J., Yost, H.J., Brueckner, M., 2002. Conserved function for embryonic nodal cilia. Nature 418, 37-38.

Facchin, L., Burgess, H.A., Siddiqi, M., Granato, M., Halpern, M.E., 2009. Determining the function of zebrafish epithalamic asymmetry. Philos Trans R Soc Lond B Biol Sci 364, 1021-1032.

Fadok, J.P., Dickerson, T.M., Palmiter, R.D., 2009. Dopamine is necessary for cue-dependent fear conditioning. J Neurosci 29, 11089-11097.

Fainsod, A., Deissler, K., Yelin, R., Marom, K., Epstein, M., Pillemer, G., Steinbeisser, H., Blum, M., 1997. The dorsalizing and neural inducing gene follistatin is an antagonist of BMP-4. Mech Dev 63, 39-50.

Fainsod, A., Steinbeisser, H., De Robertis, E.M., 1994. On the function of BMP-4 in patterning the marginal zone of the Xenopus embryo. Embo J 13, 5015-5025.

Falcon, J., 1999. Cellular circadian clocks in the pineal. Prog Neurobiol 58, 121-162.

Falcon, J., Besseau, L., Fuentes, M., Sauzet, S., Magnanou, E., Boeuf, G., 2009. Structural and functional evolution of the pineal melatonin system in vertebrates. Ann N Y Acad Sci 1163, 101-111.

Farkas, L.M., Huttner, W.B., 2008. The cell biology of neural stem and progenitor cells and its significance for their proliferation versus differentiation during mammalian brain development. Curr Opin Cell Biol 20, 707-715.

Fehon, R.G., McClatchey, A.I., Bretscher, A., 2010. Organizing the cell cortex: the role of ERM proteins. Nat Rev Mol Cell Biol 11, 276-287.

Fero, M.L., Rivkin, M., Tasch, M., Porter, P., Carow, C.E., Firpo, E., Polyak, K., Tsai, L.H., Broudy, V., Perlmutter, R.M., Kaushansky, K., Roberts, J.M., 1996. A syndrome of multiorgan hyperplasia with features of gigantism, tumorigenesis, and female sterility in p27(Kip1)-deficient mice. Cell 85, 733-744.

Fishell, G., Kriegstein, A.R., 2003. Neurons from radial glia: the consequences of asymmetric inheritance. Curr Opin Neurobiol 13, 34-41.

Fishman, M.C., Chien, K.R., 1997. Fashioning the vertebrate heart: earliest embryonic decisions. Development 124, 2099-2117.

Fraser, S., Keynes, R., Lumsden, A., 1990. Segmentation in the chick embryo hindbrain is defined by cell lineage restrictions. Nature 344, 431-435.

Fuchs, E., Tumbar, T., Guasch, G., 2004. Socializing with the neighbors: stem cells and their niche. Cell 116, 769-778.

Fuentealba, L.C., Eivers, E., Ikeda, A., Hurtado, C., Kuroda, H., Pera, E.M., De Robertis, E.M., 2007. Integrating patterning signals: Wnt/GSK3 regulates the duration of the BMP/Smad1 signal. Cell 131, 980-993.

Fujimori, T., Miyatani, S., Takeichi, M., 1990. Ectopic expression of N-cadherin perturbs histogenesis in Xenopus embryos. Development 110, 97-104.

Furuta, Y., Piston, D.W., Hogan, B.L., 1997. Bone morphogenetic proteins (BMPs) as regulators of dorsal forebrain development. Development 124, 2203-2212.

Gage, P.J., Suh, H., Camper, S.A., 1999. Dosage requirement of Pitx2 for development of multiple organs. Development 126, 4643-4651.

Galaburda, A.M., LeMay, M., Kemper, T.L., Geschwind, N., 1978a. Right-left asymmetrics in the brain. Science 199, 852-856.

Galaburda, A.M., Sanides, F., Geschwind, N., 1978b. Human brain. Cytoarchitectonic left-right asymmetries in the temporal speech region. Arch Neurol 35, 812-817.

Gamse, J.T., Kuan, Y.S., Macurak, M., Brosamle, C., Thisse, B., Thisse, C., Halpern, M.E., 2005. Directional asymmetry of the zebrafish epithalamus guides dorsoventral innervation of the midbrain target. Development 132, 4869-4881.

Gamse, J.T., Shen, Y.C., Thisse, C., Thisse, B., Raymond, P.A., Halpern, M.E., Liang, J.O., 2002. Otx5 regulates genes that show circadian expression in the zebrafish pineal complex. Nat Genet 30, 117-121.

Gamse, J.T., Thisse, C., Thisse, B., Halpern, M.E., 2003. The parapineal mediates left-right asymmetry in the zebrafish diencephalon. Development 130, 1059-1068.

Gannon, P.J., Holloway, R.L., Broadfield, D.C., Braun, A.R., 1998. Asymmetry of chimpanzee planum temporale: humanlike pattern of Wernicke's brain language area homolog. Science 279, 220-222.

Ganzler-Odenthal, S.I., Redies, C., 1998. Blocking N-cadherin function disrupts the epithelial structure of differentiating neural tissue in the embryonic chicken brain. J Neurosci 18, 5415-5425.

Gasteiger E., H.C., Gattiker A., Duvaud S., Wilkins M.R., Appel R.D., Bairoch A., 2005. The Proteomics Protocols Handbook. Humana Press.

Gazzaniga, M.S., 2005. Forty-five years of split-brain research and still going strong. Nat Rev Neurosci 6, 653-659.

Geldmacher-Voss, B., Reugels, A.M., Pauls, S., Campos-Ortega, J.A., 2003. A 90-degree rotation of the mitotic spindle changes the orientation of mitoses of zebrafish neuroepithelial cells. Development 130, 3767-3780.

Geschwind, N., Levitsky, W., 1968. Human brain: left-right asymmetries in temporal speech region. Science 161, 186-187.

Ghosh, S., Marquardt, T., Thaler, J.P., Carter, N., Andrews, S.E., Pfaff, S.L., Hunter, T., 2008. Instructive role of aPKCzeta subcellular localization in the assembly of adherens junctions in neural progenitors. Proc Natl Acad Sci U S A 105, 335-340.

Gilbert, S.F., 2000. Developmental biology, 6th ed. Sinauer Associates, Sunderland, Mass.

Giraldez, A.J., Mishima, Y., Rihel, J., Grocock, R.J., Van Dongen, S., Inoue, K., Enright, A.J., Schier, A.F., 2006. Zebrafish MiR-430 promotes deadenylation and clearance of maternal mRNAs. Science 312, 75-79.

Godsave, S.F., Slack, J.M., 1989. Clonal analysis of mesoderm induction in Xenopus laevis. Dev Biol 134, 486-490.

Golden, J.A., Chernoff, G.F., 1993. Intermittent pattern of neural tube closure in two strains of mice. Teratology 47, 73-80.

Golling, G., Amsterdam, A., Sun, Z., Antonelli, M., Maldonado, E., Chen, W., Burgess, S., Haldi, M., Artzt, K., Farrington, S., Lin, S.Y., Nissen, R.M., Hopkins, N., 2002. Insertional mutagenesis in zebrafish rapidly identifies genes essential for early vertebrate development. Nat Genet 31, 135-140.

Gothilf, Y., Coon, S.L., Toyama, R., Chitnis, A., Namboodiri, M.A., Klein, D.C., 1999. Zebrafish serotonin N-acetyltransferase-2: marker for development of pineal photoreceptors and circadian clock function. Endocrinology 140, 4895-4903.

Grande, C., Patel, N.H., 2009. Nodal signalling is involved in left-right asymmetry in snails. Nature 457, 1007-1011.

Green, K.J., Getsios, S., Troyanovsky, S., Godsel, L.M., 2010. Intercellular junction assembly, dynamics, and homeostasis. Cold Spring Harb Perspect Biol 2, a000125.

Gross, J.M., Dowling, J.E., 2005. Tbx2b is essential for neuronal differentiation along the dorsal/ventral axis of the zebrafish retina. Proc Natl Acad Sci U S A 102, 4371-4376.

Grunz, H., Tacke, L., 1989. Neural differentiation of Xenopus laevis ectoderm takes place after disaggregation and delayed reaggregation without inducer. Cell Differ Dev 28, 211-217.

Grunz, H., Tacke, L., 1990. Extracellular matrix components prevent neural differentiation of disaggregated Xenopus ectoderm cells. Cell Differ Dev 32, 117-123.

Gumbiner, B., Stevenson, B., Grimaldi, A., 1988. The role of the cell adhesion molecule uvomorulin in the formation and maintenance of the epithelial junctional complex. J Cell Biol 107, 1575-1587.

Halpern, M.E., Gunturkun, O., Hopkins, W.D., Rogers, L.J., 2005. Lateralization of the vertebrate brain: taking the side of model systems. J Neurosci 25, 10351-10357.

Halpern, M.E., Liang, J.O., Gamse, J.T., 2003. Leaning to the left: laterality in the zebrafish forebrain. Trends Neurosci 26, 308-313.

Hansen, D.V., Lui, J.H., Parker, P.R., Kriegstein, A.R., 2010. Neurogenic radial glia in the outer subventricular zone of human neocortex. Nature 464, 554-561.

Harrington, M.J., Hong, E., Brewster, R., 2009. Comparative analysis of neurulation: first impressions do not count. Mol Reprod Dev 76, 954-965.

Harris, T.J., Tepass, U., 2010. Adherens junctions: from molecules to morphogenesis. Nat Rev Mol Cell Biol 11, 502-514.

Hashimoto-Torii, K., Motoyama, J., Hui, C.C., Kuroiwa, A., Nakafuku, M., Shimamura, K., 2003. Differential activities of Sonic hedgehog mediated by Gli transcription factors define distinct neuronal subtypes in the dorsal thalamus. Mech Dev 120, 1097-1111.

Hatta, K., Takeichi, M., 1986. Expression of N-cadherin adhesion molecules associated with early morphogenetic events in chick development. Nature 320, 447-449.

Haydar, T.F., Ang, E., Jr., Rakic, P., 2003. Mitotic spindle rotation and mode of cell division in the developing telencephalon. Proc Natl Acad Sci U S A 100, 2890-2895.

Heinrich, S.U., Mothes, W., Brunner, J., Rapoport, T.A., 2000. The Sec61p complex mediates the integration of a membrane protein by allowing lipid partitioning of the transmembrane domain. Cell 102, 233-244.

Heldt, S.A., Ressler, K.J., 2006. Lesions of the habenula produce stress- and dopamine-dependent alterations in prepulse inhibition and locomotion. Brain Res 1073-1074, 229-239.

Hemmati-Brivanlou, A., Kelly, O.G., Melton, D.A., 1994. Follistatin, an antagonist of activin, is expressed in the Spemann organizer and displays direct neuralizing activity. Cell 77, 283-295.

Hemmati-Brivanlou, A., Thomsen, G.H., 1995. Ventral mesodermal patterning in Xenopus embryos: expression patterns and activities of BMP-2 and BMP-4. Dev Genet 17, 78-89.

Herbert, M.R., Ziegler, D.A., Deutsch, C.K., O'Brien, L.M., Kennedy, D.N., Filipek, P.A., Bakardjiev, A.I., Hodgson, J., Takeoka, M., Makris, N., Caviness, V.S., Jr., 2005. Brain asymmetries in autism and developmental language disorder: a nested whole-brain analysis. Brain 128, 213-226.

Hikosaka, O., Sesack, S.R., Lecourtier, L., Shepard, P.D., 2008. Habenula: crossroad between the basal ganglia and the limbic system. J Neurosci 28, 11825-11829.

Hodge, R.D., D'Ercole, A.J., O'Kusky, J.R., 2004. Insulin-like growth factor-I accelerates the cell cycle by decreasing G1 phase length and increases cell cycle reentry in the embryonic cerebral cortex. J Neurosci 24, 10201-10210.

Hong, E., Brewster, R., 2006. N-cadherin is required for the polarized cell behaviors that drive neurulation in the zebrafish. Development 133, 3895-3905.

Hong, H.K., Chakravarti, A., Takahashi, J.S., 2004. The gene for soluble N-ethylmaleimide sensitive factor attachment protein alpha is mutated in hydrocephaly with hop gait (hyh) mice. Proc Natl Acad Sci U S A 101, 1748-1753.

Horsfield, K., Cumming, G., 1968. Morphology of the bronchial tree in man. J Appl Physiol 24, 373-383.

Hoyle, C., Brown, N.A., Wolpert, L., 1992. Development of left/right handedness in the chick heart. Development 115, 1071-1078.

Hubbard, T.J., Aken, B.L., Ayling, S., Ballester, B., Beal, K., Bragin, E., Brent, S., Chen, Y., Clapham, P., Clarke, L., Coates, G., Fairley, S., Fitzgerald, S., Fernandez-Banet, J., Gordon, L., Graf, S., Haider, S., Hammond, M., Holland, R., Howe, K., Jenkinson, A., Johnson, N., Kahari, A., Keefe, D., Keenan, S., Kinsella, R., Kokocinski, F., Kulesha, E., Lawson, D., Longden, I., Megy, K., Meidl, P., Overduin, B., Parker, A., Pritchard, B., Rios, D., Schuster, M., Slater, G., Smedley, D., Spooner, W., Spudich, G., Trevanion, S., Vilella, A., Vogel, J., White, S., Wilder, S., Zadissa, A., Birney, E., Cunningham, F., Curwen, V., Durbin, R., Fernandez-Suarez, X.M., Herrero, J., Kasprzyk, A., Proctor, G., Smith, J., Searle, S., Flicek, P., 2009. Ensembl 2009. Nucleic Acids Res 37, D690-697.

Huttner, W.B., Brand, M., 1997. Asymmetric division and polarity of neuroepithelial cells. Curr Opin Neurobiol 7, 29-39.

Iemura, S., Yamamoto, T.S., Takagi, C., Uchiyama, H., Natsume, T., Shimasaki, S., Sugino, H., Ueno, N., 1998. Direct binding of follistatin to a complex of bone-morphogenetic protein and its receptor inhibits ventral and epidermal cell fates in early Xenopus embryo. Proc Natl Acad Sci U S A 95, 9337-9342.

Imai, F., Hirai, S., Akimoto, K., Koyama, H., Miyata, T., Ogawa, M., Noguchi, S., Sasaoka, T., Noda, T., Ohno, S., 2006. Inactivation of aPKClambda results in the loss of adherens junctions in neuroepithelial cells without

affecting neurogenesis in mouse neocortex. Development 133, 1735-1744.

Ishibashi, M., McMahon, A.P., 2002. A sonic hedgehog-dependent signaling relay regulates growth of diencephalic and mesencephalic primordia in the early mouse embryo. Development 129, 4807-4819.

Ishimaru, Y., Yoshioka, H., Tao, H., Thisse, B., Thisse, C., C, V.E.W., Hamada, H., Ohuchi, H., Noji, S., 2000. Asymmetric expression of antivin/lefty1 in the early chick embryo. Mech Dev 90, 115-118.

Jan, Y.N., Jan, L.Y., 2001. Asymmetric cell division in the Drosophila nervous system. Nat Rev Neurosci 2, 772-779.

Jessell, T.M., 2000. Neuronal specification in the spinal cord: inductive signals and transcriptional codes. Nat Rev Genet 1, 20-29.

Jossin, Y., Cooper, J.A., 2011. Reelin, Rap1 and N-cadherin orient the migration of multipolar neurons in the developing neocortex. Nat Neurosci 14, 697-703.

Kadowaki, M., Nakamura, S., Machon, O., Krauss, S., Radice, G.L., Takeichi, M., 2007. N-cadherin mediates cortical organization in the mouse brain. Dev Biol 304, 22-33.

Karabagli, H., Karabagli, P., Ladher, R.K., Schoenwolf, G.C., 2002. Comparison of the expression patterns of several fibroblast growth factors during chick gastrulation and neurulation. Anat Embryol (Berl) 205, 365-370.

Karfunkel, P., 1972. The activity of microtubules and microfilaments in neurulation in the chick. J Exp Zool 181, 289-301.

Katayama, K., Melendez, J., Baumann, J.M., Leslie, J.R., Chauhan, B.K., Nemkul, N., Lang, R.A., Kuan, C.Y., Zheng, Y., Yoshida, Y., 2011. Loss of RhoA in neural progenitor cells causes the disruption of adherens junctions and hyperproliferation. Proc Natl Acad Sci U S A 108, 7607-7612.

Kazimi, N., Cahill, G.M., 1999. Development of a circadian melatonin rhythm in embryonic zebrafish. Brain Res Dev Brain Res 117, 47-52.

Keller, R., Shih, J., Sater, A., 1992. The cellular basis of the convergence and extension of the Xenopus neural plate. Dev Dyn 193, 199-217.

Kengaku, M., Okamoto, H., 1993. Basic fibroblast growth factor induces differentiation of neural tube and neural crest lineages of cultured ectoderm cells from Xenopus gastrula. Development 119, 1067-1078.

Kengaku, M., Okamoto, H., 1995. bFGF as a possible morphogen for the anteroposterior axis of the central nervous system in Xenopus. Development 121, 3121-3130.

Kimmel, C.B., Ballard, W.W., Kimmel, S.R., Ullmann, B., Schilling, T.F., 1995. Stages of embryonic development of the zebrafish. Dev Dyn 203, 253-310.

Kimura, D., 1983. Speech representation in an unbiased sample of left-handers. Hum Neurobiol 2, 147-154.

Kitamura, K., Miura, H., Miyagawa-Tomita, S., Yanazawa, M., Katoh-Fukui, Y., Suzuki, R., Ohuchi, H., Suehiro, A., Motegi, Y., Nakahara, Y., Kondo, S., Yokoyama, M., 1999. Mouse Pitx2 deficiency leads to anomalies of the

ventral body wall, heart, extra- and periocular mesoderm and right pulmonary isomerism. Development 126, 5749-5758.

Knoblich, J.A., 2001. Asymmetric cell division during animal development. Nat Rev Mol Cell Biol 2, 11-20.

Kosaki, K., Bassi, M.T., Kosaki, R., Lewin, M., Belmont, J., Schauer, G., Casey, B., 1999. Characterization and mutation analysis of human LEFTY A and LEFTY B, homologues of murine genes implicated in left-right axis development. Am J Hum Genet 64, 712-721.

Kuan, Y.S., Gamse, J.T., Schreiber, A.M., Halpern, M.E., 2007a. Selective asymmetry in a conserved forebrain to midbrain projection. J Exp Zool B Mol Dev Evol 308, 669-678.

Kuan, Y.S., Yu, H.H., Moens, C.B., Halpern, M.E., 2007b. Neuropilin asymmetry mediates a left-right difference in habenular connectivity. Development 134, 857-865.

Kuo, C.T., Mirzadeh, Z., Soriano-Navarro, M., Rasin, M., Wang, D., Shen, J., Sestan, N., Garcia-Verdugo, J., Alvarez-Buylla, A., Jan, L.Y., Jan, Y.N., 2006. Postnatal deletion of Numb/Numblike reveals repair and remodeling capacity in the subventricular neurogenic niche. Cell 127, 1253-1264.

Lamb, T.M., Harland, R.M., 1995. Fibroblast growth factor is a direct neural inducer, which combined with noggin generates anterior-posterior neural pattern. Development 121, 3627-3636.

Lang, M.R., Lapierre, L.A., Frotscher, M., Goldenring, J.R., Knapik, E.W., 2006. Secretory COPII coat component Sec23a is essential for craniofacial chondrocyte maturation. Nat Genet 38, 1198-1203.

Langdon, Y.G., Mullins, M.C., 2011. Maternal and zygotic control of zebrafish dorsoventral axial patterning. Annu Rev Genet 45, 357-377.

Launay, C., Fromentoux, V., Shi, D.L., Boucaut, J.C., 1996. A truncated FGF receptor blocks neural induction by endogenous Xenopus inducers. Development 122, 869-880.

Lee, K.J., Dietrich, P., Jessell, T.M., 2000. Genetic ablation reveals that the roof plate is essential for dorsal interneuron specification. Nature 403, 734-740.

Lee, K.J., Mendelsohn, M., Jessell, T.M., 1998. Neuronal patterning by BMPs: a requirement for GDF7 in the generation of a discrete class of commissural interneurons in the mouse spinal cord. Genes Dev 12, 3394-3407.

Lele, Z., Folchert, A., Concha, M., Rauch, G.J., Geisler, R., Rosa, F., Wilson, S.W., Hammerschmidt, M., Bally-Cuif, L., 2002. parachute/n-cadherin is required for morphogenesis and maintained integrity of the zebrafish neural tube. Development 129, 3281-3294.

Leonard, C.M., Eckert, M.A., 2008. Asymmetry and dyslexia. Dev Neuropsychol 33, 663-681.

Levin, M., 2004. The embryonic origins of left-right asymmetry. Crit Rev Oral Biol Med 15, 197-206.

Levin, M., Johnson, R.L., Stern, C.D., Kuehn, M., Tabin, C., 1995. A molecular pathway determining left-right asymmetry in chick embryogenesis. Cell 82, 803-814.

Liang, J.O., Etheridge, A., Hantsoo, L., Rubinstein, A.L., Nowak, S.J., Izpisua Belmonte, J.C., Halpern, M.E., 2000. Asymmetric nodal signaling in the zebrafish diencephalon positions the pineal organ. Development 127, 5101-5112.

Liem, K.F., Jr., Tremml, G., Jessell, T.M., 1997. A role for the roof plate and its resident TGFbeta-related proteins in neuronal patterning in the dorsal spinal cord. Cell 91, 127-138.

Lien, W.H., Klezovitch, O., Fernandez, T.E., Delrow, J., Vasioukhin, V., 2006. alphaE-catenin controls cerebral cortical size by regulating the hedgehog signaling pathway. Science 311, 1609-1612.

Lim, Y., Golden, J.A., 2007. Patterning the developing diencephalon. Brain Res Rev 53, 17-26.

Lin, C.R., Kioussi, C., O'Connell, S., Briata, P., Szeto, D., Liu, F., Izpisua-Belmonte, J.C., Rosenfeld, M.G., 1999. Pitx2 regulates lung asymmetry, cardiac positioning and pituitary and tooth morphogenesis. Nature 401, 279-282.

Linker, C., De Almeida, I., Papanayotou, C., Stower, M., Sabado, V., Ghorani, E., Streit, A., Mayor, R., Stern, C.D., 2009. Cell communication with the neural plate is required for induction of neural markers by BMP inhibition:

evidence for homeogenetic induction and implications for Xenopus animal cap and chick explant assays. Dev Biol 327, 478-486.

Lippolis, G., Bisazza, A., Rogers, L.J., Vallortigara, G., 2002. Lateralisation of predator avoidance responses in three species of toads. Laterality 7, 163-183.

Litingtung, Y., Chiang, C., 2000. Specification of ventral neuron types is mediated by an antagonistic interaction between Shh and Gli3. Nat Neurosci 3, 979-985.

Liu, Q.R., Hattar, S., Endo, S., MacPhee, K., Zhang, H., Cleary, L.J., Byrne, J.H., Eskin, A., 1997. A developmental gene (Tolloid/BMP-1) is regulated in Aplysia neurons by treatments that induce long-term sensitization. J Neurosci 17, 755-764.

Lobo, M.V., Alonso, F.J., Redondo, C., Lopez-Toledano, M.A., Caso, E., Herranz, A.S., Paino, C.L., Reimers, D., Bazan, E., 2003. Cellular characterization of epidermal growth factor-expanded free-floating neurospheres. J Histochem Cytochem 51, 89-103.

Logan, M., Pagan-Westphal, S.M., Smith, D.M., Paganessi, L., Tabin, C.J., 1998. The transcription factor Pitx2 mediates situs-specific morphogenesis in response to left-right asymmetric signals. Cell 94, 307-317.

Lois, C., Garcia-Verdugo, J.M., Alvarez-Buylla, A., 1996. Chain migration of neuronal precursors. Science 271, 978-981.

Londin, E.R., Niemiec, J., Sirotkin, H.I., 2005. Chordin, FGF signaling, and mesodermal factors cooperate in zebrafish neural induction. Dev Biol 279, 1-19.

Long, S., Ahmad, N., Rebagliati, M., 2003. The zebrafish nodal-related gene southpaw is required for visceral and diencephalic left-right asymmetry. Development 130, 2303-2316.

Louvi, A., Artavanis-Tsakonas, S., 2006. Notch signalling in vertebrate neural development. Nat Rev Neurosci 7, 93-102.

Lowe, L.A., Supp, D.M., Sampath, K., Yokoyama, T., Wright, C.V., Potter, S.S., Overbeek, P., Kuehn, M.R., 1996. Conserved left-right asymmetry of nodal expression and alterations in murine situs inversus. Nature 381, 158-161.

Lowery, L.A., Sive, H., 2004. Strategies of vertebrate neurulation and a re-evaluation of teleost neural tube formation. Mech Dev 121, 1189-1197.

Lu, M.F., Pressman, C., Dyer, R., Johnson, R.L., Martin, J.F., 1999. Function of Rieger syndrome gene in left-right asymmetry and craniofacial development. Nature 401, 276-278.

Lustig, K.D., Kroll, K., Sun, E., Ramos, R., Elmendorf, H., Kirschner, M.W., 1996. A Xenopus nodal-related gene that acts in synergy with noggin to induce complete secondary axis and notochord formation. Development 122, 3275-3282.

Manabe, N., Hirai, S., Imai, F., Nakanishi, H., Takai, Y., Ohno, S., 2002. Association of ASIP/mPAR-3 with adherens junctions of mouse neuroepithelial cells. Dev Dyn 225, 61-69.

Marieb, E.N., Hoehn, K., 2007. Human anatomy & physiology, 7th ed. Pearson Benjamin Cummings, San Francisco.

Marusich, M.F., Furneaux, H.M., Henion, P.D., Weston, J.A., 1994. Hu neuronal proteins are expressed in proliferating neurogenic cells. J Neurobiol 25, 143-155.

Mastick, G.S., Davis, N.M., Andrew, G.L., Easter, S.S., Jr., 1997. Pax-6 functions in boundary formation and axon guidance in the embryonic mouse forebrain. Development 124, 1985-1997.

Matsunaga, E., Araki, I., Nakamura, H., 2000. Pax6 defines the di-mesencephalic boundary by repressing En1 and Pax2. Development 127, 2357-2365.

McConnell, S.K., 1995. Constructing the cerebral cortex: neurogenesis and fate determination. Neuron 15, 761-768.

Megason, S.G., McMahon, A.P., 2002. A mitogen gradient of dorsal midline Wnts organizes growth in the CNS. Development 129, 2087-2098.

Melville, D.B., Montero-Balaguer, M., Levic, D.S., Bradley, K., Smith, J.R., Hatzopoulos, A.K., Knapik, E.W., 2011. The feelgood mutation in zebrafish dysregulates COPII-dependent secretion of select extracellular matrix proteins in skeletal morphogenesis. Dis Model Mech 4, 763-776.

Meng, W., Takeichi, M., 2009. Adherens junction: molecular architecture and regulation. Cold Spring Harb Perspect Biol 1, a002899.

Meno, C., Gritsman, K., Ohishi, S., Ohfuji, Y., Heckscher, E., Mochida, K., Shimono, A., Kondoh, H., Talbot, W.S., Robertson, E.J., Schier, A.F., Hamada, H., 1999. Mouse Lefty2 and zebrafish antivin are feedback inhibitors of nodal signaling during vertebrate gastrulation. Mol Cell 4, 287-298.

Meno, C., Ito, Y., Saijoh, Y., Matsuda, Y., Tashiro, K., Kuhara, S., Hamada, H., 1997. Two closely-related left-right asymmetrically expressed genes, lefty-1 and lefty-2: their distinct expression domains, chromosomal linkage and direct neuralizing activity in Xenopus embryos. Genes Cells 2, 513-524.

Meno, C., Saijoh, Y., Fujii, H., Ikeda, M., Yokoyama, T., Yokoyama, M., Toyoda, Y., Hamada, H., 1996. Left-right asymmetric expression of the TGF beta-family member lefty in mouse embryos. Nature 381, 151-155.

Miklosi, A., Andrew, R.J., 2006. The zebrafish as a model for behavioral studies. Zebrafish 3, 227-234.

Miklosi, A., Andrew, R.J., Gasparini, S., 2001. Role of right hemifield in visual control of approach to target in zebrafish. Behav Brain Res 122, 57-65.

Miklosi, A., Andrew, R.J., Savage, H., 1997. Behavioural lateralisation of the tetrapod type in the zebrafish (Brachydanio rerio). Physiol Behav 63, 127-135.

Millonig, J.H., Millen, K.J., Hatten, M.E., 2000. The mouse Dreher gene Lmx1a controls formation of the roof plate in the vertebrate CNS. Nature 403, 764-769.

Miyata, T., Kawaguchi, A., Saito, K., Kawano, M., Muto, T., Ogawa, M., 2004. Asymmetric production of surface-dividing and non-surface-dividing cortical progenitor cells. Development 131, 3133-3145.

Moens, C.B., Prince, V.E., 2002. Constructing the hindbrain: insights from the zebrafish. Dev Dyn 224, 1-17.

Moffat, S.D., Hampson, E., Lee, D.H., 1998. Morphology of the planum temporale and corpus callosum in left handers with evidence of left and right hemisphere speech representation. Brain 121 (Pt 12), 2369-2379.

Molloy, A.M., Kirke, P.N., Troendle, J.F., Burke, H., Sutton, M., Brody, L.C., Scott, J.M., Mills, J.L., 2009. Maternal vitamin B12 status and risk of neural tube defects in a population with high neural tube defect prevalence and no folic Acid fortification. Pediatrics 123, 917-923.

Mori, N., Kuwamura, M., Tanaka, N., Hirano, R., Nabe, M., Ibuki, M., Yamate, J., 2012. Ccdc85c encoding a protein at apical junctions of radial glia is disrupted in hemorrhagic hydrocephalus (hhy) mice. Am J Pathol 180, 314-327.

Morissette, M.C., Boye, S.M., 2008. Electrolytic lesions of the habenula attenuate brain stimulation reward. Behav Brain Res 187, 17-26.

Mueller, T., Wullimann, M.F., 2005. Atlas of early zebrafish brain development : a tool for molecular neurogenetics, 1st ed. Elsevier, Amsterdam ; Boston, Mass.

Mukouyama, Y.S., Deneen, B., Lukaszewicz, A., Novitch, B.G., Wichterle, H., Jessell, T.M., Anderson, D.J., 2006. Olig2+ neuroepithelial motoneuron

progenitors are not multipotent stem cells in vivo. Proc Natl Acad Sci U S A 103, 1551-1556.

Murciano, A., Zamora, J., Lopez-Sanchez, J., Frade, J.M., 2002. Interkinetic nuclear movement may provide spatial clues to the regulation of neurogenesis. Mol Cell Neurosci 21, 285-300.

Muroyama, Y., Fujihara, M., Ikeya, M., Kondoh, H., Takada, S., 2002. Wnt signaling plays an essential role in neuronal specification of the dorsal spinal cord. Genes Dev 16, 548-553.

Nagele, R.G., Lee, H.Y., 1987. Studies on the mechanisms of neurulation in the chick: morphometric analysis of the relationship between regional variations in cell shape and sites of motive force generation. J Exp Zool 241, 197-205.

Nakagawa, S., Takeichi, M., 1995. Neural crest cell-cell adhesion controlled by sequential and subpopulation-specific expression of novel cadherins. Development 121, 1321-1332.

Nakamura, T., Takio, K., Eto, Y., Shibai, H., Titani, K., Sugino, H., 1990. Activin-binding protein from rat ovary is follistatin. Science 247, 836-838.

Nakayama, K., Ishida, N., Shirane, M., Inomata, A., Inoue, T., Shishido, N., Horii, I., Loh, D.Y., 1996. Mice lacking p27(Kip1) display increased body size, multiple organ hyperplasia, retinal dysplasia, and pituitary tumors. Cell 85, 707-720.

Niehrs, C., 2004. Regionally specific induction by the Spemann-Mangold organizer. Nat Rev Genet 5, 425-434.

Niessen, C.M., Gottardi, C.J., 2008. Molecular components of the adherens junction. Biochim Biophys Acta 1778, 562-571.

Nissen, R.M., Amsterdam, A., Hopkins, N., 2006. A zebrafish screen for craniofacial mutants identifies wdr68 as a highly conserved gene required for endothelin-1 expression. BMC Dev Biol 6, 28.

Noctor, S.C., Martinez-Cerdeno, V., Ivic, L., Kriegstein, A.R., 2004. Cortical neurons arise in symmetric and asymmetric division zones and migrate through specific phases. Nat Neurosci 7, 136-144.

Nonaka, S., Tanaka, Y., Okada, Y., Takeda, S., Harada, A., Kanai, Y., Kido, M., Hirokawa, N., 1998. Randomization of left-right asymmetry due to loss of nodal cilia generating leftward flow of extraembryonic fluid in mice lacking KIF3B motor protein. Cell 95, 829-837.

Ohi, Y., Wright, C.V., 2007. Anteriorward shifting of asymmetric Xnr1 expression and contralateral communication in left-right specification in Xenopus. Dev Biol 301, 447-463.

Olson, E.N., 2006. Gene regulatory networks in the evolution and development of the heart. Science 313, 1922-1927.

Orentas, D.M., Hayes, J.E., Dyer, K.L., Miller, R.H., 1999. Sonic hedgehog signaling is required during the appearance of spinal cord oligodendrocyte precursors. Development 126, 2419-2429.

Pang, T., Atefy, R., Sheen, V., 2008. Malformations of cortical development. Neurologist 14, 181-191.

Papan, C., Campos-Ortega, J.A., 1999. Region-specific cell clones in the developing spinal cord of the zebrafish. Dev Genes Evol 209, 135-144.

Park, H.C., Hong, S.K., Kim, H.S., Kim, S.H., Yoon, E.J., Kim, C.H., Miki, N., Huh, T.L., 2000. Structural comparison of zebrafish Elav/Hu and their differential expressions during neurogenesis. Neurosci Lett 279, 81-84.

Patel, K., Isaac, A., Cooke, J., 1999. Nodal signalling and the roles of the transcription factors SnR and Pitx2 in vertebrate left-right asymmetry. Curr Biol 9, 609-612.

Pauls, S., Geldmacher-Voss, B., Campos-Ortega, J.A., 2001. A zebrafish histone variant H2A.F/Z and a transgenic H2A.F/Z:GFP fusion protein for in vivo studies of embryonic development. Dev Genes Evol 211, 603-610.

Piccolo, S., Sasai, Y., Lu, B., De Robertis, E.M., 1996. Dorsoventral patterning in Xenopus: inhibition of ventral signals by direct binding of chordin to BMP-4. Cell 86, 589-598.

Piedra, M.E., Icardo, J.M., Albajar, M., Rodriguez-Rey, J.C., Ros, M.A., 1998. Pitx2 participates in the late phase of the pathway controlling left-right asymmetry. Cell 94, 319-324.

Portch, P.A., Barson, A.J., 1974. Scanning electron microscopy of neurulation in the chick. J Anat 117, 341-350.

Puschel, A.W., Westerfield, M., Dressler, G.R., 1992. Comparative analysis of Pax-2 protein distributions during neurulation in mice and zebrafish. Mech Dev 38, 197-208.

Raden, D., Song, W., Gilmore, R., 2000. Role of the cytoplasmic segments of Sec61alpha in the ribosome-binding and translocation-promoting activities of the Sec61 complex. J Cell Biol 150, 53-64.

Radice, G.L., Rayburn, H., Matsunami, H., Knudsen, K.A., Takeichi, M., Hynes, R.O., 1997. Developmental defects in mouse embryos lacking N-cadherin. Dev Biol 181, 64-78.

Rakic, P., 1988. Specification of cerebral cortical areas. Science 241, 170-176.

Rapoport, T.A., 2007. Protein translocation across the eukaryotic endoplasmic reticulum and bacterial plasma membranes. Nature 450, 663-669.

Rapoport, T.A., Goder, V., Heinrich, S.U., Matlack, K.E., 2004. Membrane-protein integration and the role of the translocation channel. Trends Cell Biol 14, 568-575.

Rasin, M.R., Gazula, V.R., Breunig, J.J., Kwan, K.Y., Johnson, M.B., Liu-Chen, S., Li, H.S., Jan, L.Y., Jan, Y.N., Rakic, P., Sestan, N., 2007. Numb and Numbl are required for maintenance of cadherin-based adhesion and polarity of neural progenitors. Nat Neurosci 10, 819-827.

Rasmussen, T., Milner, B., 1977. The role of early left-brain injury in determining lateralization of cerebral speech functions. Ann N Y Acad Sci 299, 355-369.

Rauch, G.J., Granato, M., Haffter, P., 1997. A polymorphic zebrafish line for genetic mapping using SSLPs on high-percentage agarose gels Tech. Tips Online.

Regan, J.C., Concha, M.L., Roussigne, M., Russell, C., Wilson, S.W., 2009. An Fgf8-dependent bistable cell migratory event establishes CNS asymmetry. Neuron 61, 27-34.

Reynolds, A.B., Daniel, J., McCrea, P.D., Wheelock, M.J., Wu, J., Zhang, Z., 1994. Identification of a new catenin: the tyrosine kinase substrate p120cas associates with E-cadherin complexes. Mol Cell Biol 14, 8333-8342.

Roberts, R.K., Appel, B., 2009. Apical polarity protein PrkCi is necessary for maintenance of spinal cord precursors in zebrafish. Dev Dyn 238, 1638-1648.

Rodriguez Esteban, C., Capdevila, J., Economides, A.N., Pascual, J., Ortiz, A., Izpisua Belmonte, J.C., 1999. The novel Cer-like protein Caronte mediates the establishment of embryonic left-right asymmetry. Nature 401, 243-251.

Rogers, L.J., 2000. Evolution of hemispheric specialization: advantages and disadvantages. Brain Lang 73, 236-253.

Rogers, L.J., Andrew, R.J., 2002. Comparative vertebrate lateralization. Cambridge University Press, Cambridge ; New York.

Rogers, L.J., Workman, L., 1989. Light Exposure during Incubation Affects Competitive Behavior in Domestic Chicks. Appl Anim Behav Sci 23, 187-198.

Rogers, L.J., Zucca, P., Vallortigara, G., 2004. Advantages of having a lateralized brain. Proc Biol Sci 271 Suppl 6, S420-422.

Rossi, A., Stratta, P., Di Michele, V., Gallucci, M., Splendiani, A., de Cataldo, S., Casacchia, M., 1991. Temporal lobe structure by magnetic resonance in bipolar affective disorders and schizophrenia. J Affect Disord 21, 19-22.

Roussigne, M., Bianco, I.H., Wilson, S.W., Blader, P., 2009. Nodal signalling imposes left-right asymmetry upon neurogenesis in the habenular nuclei. Development 136, 1549-1557.

Rousso, D.L., Pearson, C.A., Gaber, Z.B., Miquelajauregui, A., Li, S., Portera-Cailliau, C., Morrisey, E.E., Novitch, B.G., 2012. Foxp-mediated suppression of N-cadherin regulates neuroepithelial character and progenitor maintenance in the CNS. Neuron 74, 314-330.

Rubenstein, J.L., Martinez, S., Shimamura, K., Puelles, L., 1994. The embryonic vertebrate forebrain: the prosomeric model. Science 266, 578-580.

Ryan, A.K., Blumberg, B., Rodriguez-Esteban, C., Yonei-Tamura, S., Tamura, K., Tsukui, T., de la Pena, J., Sabbagh, W., Greenwald, J., Choe, S., Norris, D.P., Robertson, E.J., Evans, R.M., Rosenfeld, M.G., Izpisua Belmonte, J.C., 1998. Pitx2 determines left-right asymmetry of internal organs in vertebrates. Nature 394, 545-551.

Sampath, K., Cheng, A.M., Frisch, A., Wright, C.V., 1997. Functional differences among Xenopus nodal-related genes in left-right axis determination. Development 124, 3293-3302.

Sampath, K., Rubinstein, A.L., Cheng, A.M., Liang, J.O., Fekany, K., Solnica-Krezel, L., Korzh, V., Halpern, M.E., Wright, C.V., 1998. Induction of the

zebrafish ventral brain and floorplate requires cyclops/nodal signalling. Nature 395, 185-189.

Sano, K., Tanihara, H., Heimark, R.L., Obata, S., Davidson, M., St John, T., Taketani, S., Suzuki, S., 1993. Protocadherins: a large family of cadherin-related molecules in central nervous system. Embo J 12, 2249-2256.

Sarkisian, M.R., Bartley, C.M., Rakic, P., 2008. Trouble making the first move: interpreting arrested neuronal migration in the cerebral cortex. Trends Neurosci 31, 54-61.

Sarmah, S., Barrallo-Gimeno, A., Melville, D.B., Topczewski, J., Solnica-Krezel, L., Knapik, E.W., 2010. Sec24D-dependent transport of extracellular matrix proteins is required for zebrafish skeletal morphogenesis. PLoS One 5, e10367.

Sasai, Y., Lu, B., Steinbeisser, H., Geissert, D., Gont, L.K., De Robertis, E.M., 1994. Xenopus chordin: a novel dorsalizing factor activated by organizer-specific homeobox genes. Cell 79, 779-790.

Sato, S.M., Sargent, T.D., 1989. Development of neural inducing capacity in dissociated Xenopus embryos. Dev Biol 134, 263-266.

Saude, L., Woolley, K., Martin, P., Driever, W., Stemple, D.L., 2000. Axis-inducing activities and cell fates of the zebrafish organizer. Development 127, 3407-3417.

Sausedo, R.A., Smith, J.L., Schoenwolf, G.C., 1997. Role of nonrandomly oriented cell division in shaping and bending of the neural plate. J Comp Neurol 381, 473-488.

Schier, A.F., Shen, M.M., 2000. Nodal signalling in vertebrate development. Nature 403, 385-389.

Schier, A.F., Talbot, W.S., 2005. Molecular genetics of axis formation in zebrafish. Annu Rev Genet 39, 561-613.

Schilling, T.F., 2008. Anterior-posterior patterning and segmentation of the vertebrate head. Integr Comp Biol 48, 658-667.

Schmid, R.S., Anton, E.S., 2003. Role of integrins in the development of the cerebral cortex. Cereb Cortex 13, 219-224.

Schnell, D.J., Hebert, D.N., 2003. Protein translocons: multifunctional mediators of protein translocation across membranes. Cell 112, 491-505.

Schoenwolf, G.C., Alvarez, I.S., 1989. Roles of neuroepithelial cell rearrangement and division in shaping of the avian neural plate. Development 106, 427-439.

Schoenwolf, G.C., Franks, M.V., 1984. Quantitative analyses of changes in cell shapes during bending of the avian neural plate. Dev Biol 105, 257-272.

Scholpp, S., Lohs, C., Brand, M., 2003. Engrailed and Fgf8 act synergistically to maintain the boundary between diencephalon and mesencephalon. Development 130, 4881-4893.

Schweickert, A., Campione, M., Steinbeisser, H., Blum, M., 2000. Pitx2 isoforms: involvement of Pitx2c but not Pitx2a or Pitx2b in vertebrate left-right asymmetry. Mech Dev 90, 41-51.

Selleck, M.A., Bronner-Fraser, M., 1995. Origins of the avian neural crest: the role of neural plate-epidermal interactions. Development 121, 525-538.

Sheen, V.L., Ganesh, V.S., Topcu, M., Sebire, G., Bodell, A., Hill, R.S., Grant, P.E., Shugart, Y.Y., Imitola, J., Khoury, S.J., Guerrini, R., Walsh, C.A., 2004. Mutations in ARFGEF2 implicate vesicle trafficking in neural progenitor proliferation and migration in the human cerebral cortex. Nat Genet 36, 69-76.

Shinotsuka, C., Waguri, S., Wakasugi, M., Uchiyama, Y., Nakayama, K., 2002a. Dominant-negative mutant of BIG2, an ARF-guanine nucleotide exchange factor, specifically affects membrane trafficking from the trans-Golgi network through inhibiting membrane association of AP-1 and GGA coat proteins. Biochem Biophys Res Commun 294, 254-260.

Shinotsuka, C., Yoshida, Y., Kawamoto, K., Takatsu, H., Nakayama, K., 2002b. Overexpression of an ADP-ribosylation factor-guanine nucleotide exchange factor, BIG2, uncouples brefeldin A-induced adaptor protein-1 coat dissociation and membrane tubulation. J Biol Chem 277, 9468-9473.

Shiratori, H., Hamada, H., 2006. The left-right axis in the mouse: from origin to morphology. Development 133, 2095-2104.

Sive, H.L., Draper, B.W., Harland, R.M., Weintraub, H., 1990. Identification of a retinoic acid-sensitive period during primary axis formation in Xenopus laevis. Genes Dev 4, 932-942.

Smith, J.L., Schoenwolf, G.C., 1987. Cell cycle and neuroepithelial cell shape during bending of the chick neural plate. Anat Rec 218, 196-206.

Smith, J.L., Schoenwolf, G.C., 1989. Notochordal induction of cell wedging in the chick neural plate and its role in neural tube formation. J Exp Zool 250, 49-62.

Smith, J.L., Schoenwolf, G.C., 1991. Further evidence of extrinsic forces in bending of the neural plate. J Comp Neurol 307, 225-236.

Smith, W.C., Harland, R.M., 1992. Expression cloning of noggin, a new dorsalizing factor localized to the Spemann organizer in Xenopus embryos. Cell 70, 829-840.

Smukler, S.R., Runciman, S.B., Xu, S., van der Kooy, D., 2006. Embryonic stem cells assume a primitive neural stem cell fate in the absence of extrinsic influences. J Cell Biol 172, 79-90.

Snelson, C.D., Santhakumar, K., Halpern, M.E., Gamse, J.T., 2008. Tbx2b is required for the development of the parapineal organ. Development 135, 1693-1702.

Soroldoni, D., Bajoghli, B., Aghaallaei, N., Czerny, T., 2007. Dynamic expression pattern of Nodal-related genes during left-right development in medaka. Gene Expr Patterns 7, 93-101.

Spemann, H., Mangold, H., 2001. Induction of embryonic primordia by implantation of organizers from a different species. 1923. Int J Dev Biol 45, 13-38.

Stepniak, E., Radice, G.L., Vasioukhin, V., 2009. Adhesive and signaling functions of cadherins and catenins in vertebrate development. Cold Spring Harb Perspect Biol 1, a002949.

Streit, A., Lee, K.J., Woo, I., Roberts, C., Jessell, T.M., Stern, C.D., 1998. Chordin regulates primitive streak development and the stability of induced neural cells, but is not sufficient for neural induction in the chick embryo. Development 125, 507-519.

Stuckmann, I., Weigmann, A., Shevchenko, A., Mann, M., Huttner, W.B., 2001. Ephrin B1 is expressed on neuroepithelial cells in correlation with neocortical neurogenesis. J Neurosci 21, 2726-2737.

Sun, T., Walsh, C.A., 2006. Molecular approaches to brain asymmetry and handedness. Nat Rev Neurosci 7, 655-662.

Sutherland, R.J., 1982. The dorsal diencephalic conduction system: a review of the anatomy and functions of the habenular complex. Neurosci Biobehav Rev 6, 1-13.

Szeto, D.P., Kimelman, D., 2006. The regulation of mesodermal progenitor cell commitment to somitogenesis subdivides the zebrafish body musculature into distinct domains. Genes Dev 20, 1923-1932.

Tadros, W., Lipshitz, H.D., 2009. The maternal-to-zygotic transition: a play in two acts. Development 136, 3033-3042.

Taraschenko, O.D., Rubbinaccio, H.Y., Shulan, J.M., Glick, S.D., Maisonneuve, I.M., 2007a. Morphine-induced changes in acetylcholine release in the interpeduncular nucleus and relationship to changes in motor behavior in rats. Neuropharmacology 53, 18-26.

Taraschenko, O.D., Shulan, J.M., Maisonneuve, I.M., Glick, S.D., 2007b. 18-MC acts in the medial habenula and interpeduncular nucleus to attenuate

dopamine sensitization to morphine in the nucleus accumbens. Synapse 61, 547-560.

Taylor, R.W., Hsieh, Y.W., Gamse, J.T., Chuang, C.F., 2010. Making a difference together: reciprocal interactions in C. elegans and zebrafish asymmetric neural development. Development 137, 681-691.

Taylor, R.W., Qi, J.Y., Talaga, A.K., Ma, T.P., Pan, L., Bartholomew, C.R., Klionsky, D.J., Moens, C.B., Gamse, J.T., 2011. Asymmetric inhibition of Ulk2 causes left-right differences in habenular neuropil formation. J Neurosci 31, 9869-9878.

Tepass, U., Truong, K., Godt, D., Ikura, M., Peifer, M., 2000. Cadherins in embryonic and neural morphogenesis. Nat Rev Mol Cell Biol 1, 91-100.

Tessier-Lavigne, M., Goodman, C.S., 1996. The molecular biology of axon guidance. Science 274, 1123-1133.

Thisse, B., Wright, C.V., Thisse, C., 2000. Activin- and Nodal-related factors control antero-posterior patterning of the zebrafish embryo. Nature 403, 425-428.

Thisse, C., Thisse, B., 2008. High-resolution in situ hybridization to whole-mount zebrafish embryos. Nat Protoc 3, 59-69.

Thouvenot, E., Lafon-Cazal, M., Demettre, E., Jouin, P., Bockaert, J., Marin, P., 2006. The proteomic analysis of mouse choroid plexus secretome reveals a high protein secretion capacity of choroidal epithelial cells. Proteomics 6, 5941-5952.

Timmer, J.R., Wang, C., Niswander, L., 2002. BMP signaling patterns the dorsal and intermediate neural tube via regulation of homeobox and helix-loop-helix transcription factors. Development 129, 2459-2472.

Trujillo, C.M., Alonso, A., Delgado, A.C., Damas, C., 2005. The rostral and caudal boundaries of the diencephalon. Brain Res Brain Res Rev 49, 202-210.

Ulloa, F., Itasaki, N., Briscoe, J., 2007. Inhibitory Gli3 activity negatively regulates Wnt/beta-catenin signaling. Curr Biol 17, 545-550.

Van den Berg, B., Clemons, W.M., Jr., Collinson, I., Modis, Y., Hartmann, E., Harrison, S.C., Rapoport, T.A., 2004. X-ray structure of a protein-conducting channel. Nature 427, 36-44.

Vestweber, D., Kemler, R., 1985. Identification of a putative cell adhesion domain of uvomorulin. Embo J 4, 3393-3398.

von der Hardt, S., Bakkers, J., Inbal, A., Carvalho, L., Solnica-Krezel, L., Heisenberg, C.P., Hammerschmidt, M., 2007. The Bmp gradient of the zebrafish gastrula guides migrating lateral cells by regulating cell-cell adhesion. Curr Biol 17, 475-487.

Walker, C., 1999. Haploid screens and gamma-ray mutagenesis. Methods Cell Biol 60, 43-70.

Warren, N., Price, D.J., 1997. Roles of Pax-6 in murine diencephalic development. Development 124, 1573-1582.

Weigmann, A., Corbeil, D., Hellwig, A., Huttner, W.B., 1997. Prominin, a novel microvilli-specific polytopic membrane protein of the apical surface of

epithelial cells, is targeted to plasmalemmal protrusions of non-epithelial cells. Proc Natl Acad Sci U S A 94, 12425-12430.

Weinstein, D.C., Hemmati-Brivanlou, A., 1999. Neural induction. Annu Rev Cell Dev Biol 15, 411-433.

Whitaker, H., 2010. Concise encyclopedia of brain and language. Elsevier, Boston, MA.

Wianny, F., Real, F.X., Mummery, C.L., Van Rooijen, M., Lahti, J., Samarut, J., Savatier, P., 1998. G1-phase regulators, cyclin D1, cyclin D2, and cyclin D3: up-regulation at gastrulation and dynamic expression during neurulation. Dev Dyn 212, 49-62.

Wilson, P.A., Hemmati-Brivanlou, A., 1995. Induction of epidermis and inhibition of neural fate by Bmp-4. Nature 376, 331-333.

Wilson, S.I., Graziano, E., Harland, R., Jessell, T.M., Edlund, T., 2000. An early requirement for FGF signalling in the acquisition of neural cell fate in the chick embryo. Curr Biol 10, 421-429.

Wodarz, A., Huttner, W.B., 2003. Asymmetric cell division during neurogenesis in Drosophila and vertebrates. Mech Dev 120, 1297-1309.

Wodarz, A., Nathke, I., 2007. Cell polarity in development and cancer. Nat Cell Biol 9, 1016-1024.

Yagita, Y., Sakurai, T., Tanaka, H., Kitagawa, K., Colman, D.R., Shan, W., 2009. N-cadherin mediates interaction between precursor cells in the subventricular zone and regulates further differentiation. J Neurosci Res 87, 3331-3342.

Yoshioka, H., Meno, C., Koshiba, K., Sugihara, M., Itoh, H., Ishimaru, Y., Inoue, T., Ohuchi, H., Semina, E.V., Murray, J.C., Hamada, H., Noji, S., 1998. Pitx2, a bicoid-type homeobox gene, is involved in a lefty-signaling pathway in determination of left-right asymmetry. Cell 94, 299-305.

Yurgelun-Todd, D.A., Waternaux, C.M., Cohen, B.M., Gruber, S.A., English, C.D., Renshaw, P.F., 1996. Functional magnetic resonance imaging of schizophrenic patients and comparison subjects during word production. Am J Psychiatry 153, 200-205.

Zechner, D., Fujita, Y., Hulsken, J., Muller, T., Walther, I., Taketo, M.M., Crenshaw, E.B., 3rd, Birchmeier, W., Birchmeier, C., 2003. beta-Catenin signals regulate cell growth and the balance between progenitor cell expansion and differentiation in the nervous system. Dev Biol 258, 406-418.

Zeltser, L.M., Larsen, C.W., Lumsden, A., 2001. A new developmental compartment in the forebrain regulated by Lunatic fringe. Nat Neurosci 4, 683-684.

Zhadanov, A.B., Provance, D.W., Jr., Speer, C.A., Coffin, J.D., Goss, D., Blixt, J.A., Reichert, C.M., Mercer, J.A., 1999. Absence of the tight junctional protein AF-6 disrupts epithelial cell-cell junctions and cell polarity during mouse development. Curr Biol 9, 880-888.

Zhang, J., Woodhead, G.J., Swaminathan, S.K., Noles, S.R., McQuinn, E.R., Pisarek, A.J., Stocker, A.M., Mutch, C.A., Funatsu, N., Chenn, A., 2010.

Cortical neural precursors inhibit their own differentiation via N-cadherin maintenance of beta-catenin signaling. Dev Cell 18, 472-479.

Zhong, W., Chia, W., 2008. Neurogenesis and asymmetric cell division. Curr Opin Neurobiol 18, 4-11.

Zhou, X., Babu, J.R., da Silva, S., Shu, Q., Graef, I.A., Oliver, T., Tomoda, T., Tani, T., Wooten, M.W., Wang, F., 2007. Unc-51-like kinase 1/2-mediated endocytic processes regulate filopodia extension and branching of sensory axons. Proc Natl Acad Sci U S A 104, 5842-5847.

Zimmerman, L.B., De Jesus-Escobar, J.M., Harland, R.M., 1996. The Spemann organizer signal noggin binds and inactivates bone morphogenetic protein 4. Cell 86, 599-606.